

DTIC FILE COPY

4

CHEMICAL
RESEARCH,
DEVELOPMENT &
ENGINEERING
CENTER

CRDEC-TR-88163

AD-A200 285

MILITARILY-SIGNIFICANT PROPERTIES OF
ATMOSPHERIC WATER VAPOR AND ITS
ADSORBED SURFACE LAYERS

by Hugh R. Carlon, U.S. Army Fellow
RESEARCH DIRECTORATE

August 1988

DTIC
ELECTE
OCT 28 1988
S E



U.S. ARMY
ARMAMENT
MUNITIONS
CHEMICAL COMMAND

Aberdeen Proving Ground, Maryland 21010-5423

88 10 28 07E

Disclaimer

The findings in this report are not to be construed as an official Department of the Army position unless so designated by other authorizing documents.

Distribution Statement

Approved for public release; distribution is unlimited.

REPORT DOCUMENTATION PAGE

1a. REPORT SECURITY CLASSIFICATION UNCLASSIFIED			1b. RESTRICTIVE MARKINGS	
2a. SECURITY CLASSIFICATION AUTHORITY			3. DISTRIBUTION/AVAILABILITY OF REPORT Approved for public release; distribution is unlimited.	
2b. DECLASSIFICATION/DOWNGRADING SCHEDULE				
4. PERFORMING ORGANIZATION REPORT NUMBER(S) CRDEC-TR-88163			5. MONITORING ORGANIZATION REPORT NUMBER(S)	
6a. NAME OF PERFORMING ORGANIZATION CRDEC		6b. OFFICE SYMBOL (if applicable) SMCCR-RSP-P		7a. NAME OF MONITORING ORGANIZATION
6c. ADDRESS (City, State, and ZIP Code) Aberdeen Proving Ground, MD 21010-5423			7b. ADDRESS (City, State, and ZIP Code)	
8a. NAME OF FUNDING/SPONSORING ORGANIZATION CRDEC		8b. OFFICE SYMBOL (if applicable) SMCCR-RSP-P		9. PROCUREMENT INSTRUMENT IDENTIFICATION NUMBER
8c. ADDRESS (City, State, and ZIP Code) Aberdeen Proving Ground, MD 21010-5423			10. SOURCE OF FUNDING NUMBERS	
			PROGRAM ELEMENT NO. 1L161101	TASK NO. A91A
11. TITLE (Include Security Classification) Militarily-Significant Properties of Atmospheric Water Vapor and its Adsorbed Surface Layers				
12. PERSONAL AUTHOR(S) Carlton, Hugh R., U.S. Army Fellow				
13a. TYPE OF REPORT Technical		13b. TIME COVERED FROM 1979 TO 87 May		14. DATE OF REPORT (Year, Month, Day) 1988 August
15. PAGE COUNT 85				
16. SUPPLEMENTARY NOTATION				
17. COSATI CODES			18. SUBJECT TERMS (Continue on reverse if necessary and identify by block number)	
FIELD	GROUP	SUB-GROUP	CAM Ionization detectors, Infrared)	
04	02		Remote sensing, Atmospheric absorption, Surface layers. (mgm)	
20	05		Monolayers, Adhesion, (continued on reverse)	
19. ABSTRACT (Continue on reverse if necessary and identify by block number)				
<p>In the development of new military hardware, devices that work well under controlled experimental conditions often fail to be type-classified because they do not work in the battlefield environment. New technology continues to produce increasingly sensitive devices which are, in turn, more vulnerable to unknown factors in the atmospheric environment. Atmospheric humidity effects need to be understood to the extent that they do not cause hardware development programs to fail. Water and its vapor are far more complex than we might realize. Molecular aggregates or "clusters" comprise liquid water, and water vapor can also be extensively clustered. The liquid/vapor interface of water and interfaces between air and surfaces with adsorbed water layers are not understood at all, but many new scientific clues may soon alter this situation. Adsorbed water surface layers exhibit "hysteresis" phenomena in adhesion forces and electrical conductivity. In high-voltage fields, water is evaporated at greatly-accelerated rates, and in corona discharges the vapor pressure of water vapor increases significantly even though the vapor temperature does not increase. <u>Water surface</u></p> <p>(continued on reverse)</p>				
20. DISTRIBUTION/AVAILABILITY OF ABSTRACT <input checked="" type="checkbox"/> UNCLASSIFIED/UNLIMITED <input type="checkbox"/> SAME AS RPT. <input type="checkbox"/> DTIC USERS			21. ABSTRACT SECURITY CLASSIFICATION UNCLASSIFIED	
22a. NAME OF RESPONSIBLE INDIVIDUAL SANDRA J. JOHNSON			22b. TELEPHONE (Include Area Code) (301) 671-2914	22c. OFFICE SYMBOL SMCCR-SPS-T

18. SUBJECT TERMS (continued)

Water clusters
Water ions
Water vapor
High voltage
Corona discharge

Accelerated evaporation
Relative humidity
Vapor electrical conductivity
Mass spectra
Hysteresis

Survivability
Adsorption
Nucleation phenomena
Surface effects
Electrical leakage

19. ABSTRACT (continued)

layer thicknesses are strongly dependent upon vapor relative humidity (RH). Ions are apparently produced in the vapor separating two conductive surfaces having adsorbed water layers when an electrical potential is applied between the two surfaces. These phenomena are shown to have a direct bearing upon several problems in CB* defense, including C-agent detection using ionization detectors, infrared remote sensing, surface CB decontamination, vapor decontamination, air filtration, and overall survivability of hardware systems. Recommendations are given for new basic research studies with the potential for significant payoffs in CB defense.

*Chemical and Biological

PREFACE

The work described in this report was authorized under Project No. 1L161101A91A, In-House Laboratory Independent Research (ILIR) from 1979 through 1982 and from May 1986 through May 1987 under a U.S. Secretary of the Army Science and Engineering Fellowship. The Fellowship research was performed at the University of Manchester Institute of Science and Technology (UMIST), Manchester, England, UK.

The use of trade names or manufacturers' names in this report does not constitute an official endorsement of any commercial products. This report may not be cited for purposes of advertisement.

Reproduction of this document in whole or in part is prohibited except with permission of the Commander, U.S. Army Chemical Research, Development and Engineering Center, ATTN: SMCCR-SPS-T, Aberdeen Proving Ground, Maryland 21010-5423. However, the Defense Technical Information Center and the National Technical Information Service are authorized to reproduce the document for U.S. Government purposes.

This document has been approved for release to the public.

Accession For	
NTIS GRA&I	<input checked="checked" type="checkbox"/>
DTIC TAB	<input checked="checked" type="checkbox"/>
Unannounced	<input type="checkbox"/>
Justification	
By _____	
Distribution/	
Availability Codes	
Dist	Avail and/or Special
A-1	



Blank

CONTENTS

	Page
1. INTRODUCTION.....	11
2. THE NATURE OF WATER-SUBSTANCE.....	12
2.1 Liquid Water.....	12
2.2 Water Vapor.....	12
2.3 The Liquid Surface.....	12
2.4 Evidence for Cluster Activity in Water Vapor and Moist Air.....	13
3. WATER CLUSTERS.....	14
3.1 Ion (Charged) vs. Neutral (Uncharged) Clusters.....	14
3.2 Cluster Equilibria in the Vapor.....	15
3.3 Cluster Formation in Water Vapor.....	17
4. VAPOR MEASUREMENTS.....	17
4.1 Mass Spectral Data.....	17
4.2 Infrared (IR) Data.....	20
4.3 Electrical Conductivity (Ion Population) Data.....	23
5. ADSORBED WATER SURFACE LAYERS.....	26
5.1 Proportionality of Layer Thickness to Relative Humidity (RH).....	26
5.2 Surface Phenomena and Hysteresis Effects.....	26
5.3 Sources of Atmospheric Ions.....	27
6. HIGH VOLTAGE PHENOMENA.....	28
6.1 Hysteresis and Corona Discharges.....	28
6.2 Accelerated Drying.....	29
6.3 The Vapor Pressure of Water.....	30
7. DISCUSSION.....	31
8. CONCLUSIONS AND RECOMMENDATIONS.....	33
LITERATURE CITED.....	35

LIST OF FIGURES

	Page
1. Examples of Water Clusters.....	37
2. Water Molecules (Monomers) Clustering About Ions.....	38
3. Model of a Water Ion (Center) "Swarmed" by Water Monomers.....	39
4. An Open-Chain Water Cluster of "Size" $c = 13$, e.g., $H^+(H_2O)_c...$	40
5. A Closed-Chain Water Cluster of Size 13.....	41
6. Models of a Closed-Structure, Clathrate-Like Large Water Cluster, With Monomers at the Apexes and Hydrogen Bonds Represented by the Edges.....	42
7. The Thomson/Kelvin Equation, With Explanation.....	43
8. Water Cluster and Droplet Equilibrium Curves.....	44
9. C.T.R. Wilson's Reasoning That the Known (Correct) Water Molecule Radius Was Too Small by a Factor of Three.....	45
10. Cluster Equilibrium Curves Deduced by Including Hydrogen Bonding Effects in the Thomson/Kelvin Equation.....	46
11. Basic Premises if Water Clusters Are Assumed to Form by Evaporation of Liquid Water or Droplets.....	47
12. Examples of Ion Mechanisms Leading to Ion-Induced, Neutral Cluster Formation in Water Vapor.....	48
13. Further Example of Ion-Induced, Neutral Cluster Formation.....	49
14. Other Examples of Cluster-Forming Mechanisms.....	50
15. Conceptualization of Water Cluster Equilibria in Water Vapor...	51
16. Ion Mass Spectra at 100°C for Several Saturation Ratios.....	52
17. Ion Mass Spectra at 99°C for Several Saturation Ratios.....	53
18. Ion Mass Spectrum of "Clean Air" at 23°C and 75% RH.....	54

19. Effect of Heating Water Vapor Sample at Constant Partial Pressure from Saturation ($s = 1.0$) at 28°C to $s = 0.042$ at 96°C ; Corresponding Mean Size of the Cluster Distribution Falls from $c_{\mu} = 24$ to $c_{\mu} = 11$	55
20. Mean Cluster Size, c_{μ} , of Water Ion Clusters $\text{H}^+(\text{H}_2\text{O})_c$ in Moist Atmospheric Air, Based on Available Data Points Shown.....	56
21. Droplet Nucleation Experiment in Which Nucleation Rate is Estimated by Light Scattered from He:Ne Laser Beam in Perfectly Clean, Saturated Atmospheric Air, as a Function of Temperature (Ref. 19)...	57
22. Schematic Diagram Showing How a Single "Critical" Water Cluster Size of $c = 45$ Can Account for All Droplet Nucleation in Water Vapor Over a Wide Range of Temperature and Saturation Ratio.....	58
23. Infrared (IR) Transmission Spectrum of the Atmosphere for Two Different Optical Path Lengths.....	59
24. Infrared (IR) Transmission Spectrum of Water Vapor.....	60
25. Infrared (IR) Transmission Spectrum of Water Film $10\mu\text{m}$ Thick...	61
26. Ratio of Liquid Water to Vapor Absorption Coefficients vs. Wavelength from Infrared to Centimeter-Wavelengths; also Shown on Ordinate is Ratio of "Anomalous" or Continuum Absorption, Due to Water Clusters, to Absorption of All Water Monomers, Based on 10^{-3} Fraction of Cluster in Vapor at 20°C and $s = 0.43$ (43% RH); Ratios Are Much Larger for Very Humid Conditions, Especially if Droplets Are Present in the Vapor.....	62
27. Infrared (IR) Spectra of Individual Neutral Water Clusters, by Size (Ref. 17); as Cluster Size Increases from $c = 3$ to 6, Cluster Spectra Increasingly Resemble the Liquid Water Spectrum Shown at G..	63
28. Experimental Set-Up for Simultaneous Measurement of IR Absorption and Ion Content (Electrical Conductivity) of Moist Atmospheric Air; Long-Path Optical Cell ("White cell") is Shown Connected by Hoses for Air Recirculation to Cabinet Containing Vapor Electrical Conductivity Cells.....	64
29. Close-Up of White cell, Showing Precision Optical Bench and IR Radiometer.....	65
30. Mobility of Singly-Charged Water Ions vs. Size, for Atmospheric Conditions.....	66
31. An Early Pair of Vapor Electrical Conductivity Cells, Identical in Plate Spacing, Number (40), and Insulator Configuration; They Differ Only in Plate Area Thus Allowing Air Conductivity to be Discerned Regardless of Any Leakage Currents Across the Insulators..	67

32. Improved Cell Design, Using Only Two Insulators and Lightweight (Aluminum) Plates; Also See Figure 33.....	68
33. Improved Cell Design; Cell Differs From That in Figure 32 Only in Plate Area and Thus in Vapor Conductivity Sensitivity; Otherwise Cell Plate Spacing, Number (40), and Insulator Configurations Are Identical.....	69
34. Family of Improved Cells Differing Only in Plate Area, in Cabinet Also Shown in Experimental Set-Up in Figure 28.....	70
35. Oblique View of Family of Cells Shown in Test Cabinet in Figures 28 and 34.....	71
36. State-of-Art Cell Design With Insulators in Heated Chamber.....	72
37. State-of-Art Cell Design Showing Detail of Insulators in Separate, Heated Chamber.....	73
38. Schematic of State-of-Art Cell Shown in Figures 36 and 37; Heated Air Duct Containing Insulators is Shown, With Small Holes to Inner Test Chamber Through Which Pass Steel Rods Supporting Cell Plates Inside Chamber.....	74
39. Data From State-of-Art Cell (Figures 36-38) Showing s^{13} Dependency of Cell (Vapor) Current vs. Saturation Ratio, for Humidification by Ultrasonic Nebulizer (Solid Points) and Drying Down (Hollow Points); Voltage Applied to Cell was 400 VDC.....	75
40. Data as in Figure 39 for Slightly Different Test Conditions....	76
41. Data as in Figure 39, Except for 1000 VDC Voltage Applied to Cell, Showing s^7 and s^{13} Dependencies of Cell (Vapor) Current on Saturation Ratio During Humidification (Solid Points) and "Hysteresis" Effects During Drying-Down (Hollow Points).....	77
42. More Data From New cell (Figures 36-38), for a Range of DC Voltages (E_p) Applied to Cell at Average Temperature of 27°C; Saturation Ratios as Marked on the Curves; Note "Knee" in Top Curve.....	78
43. Accumulation of Water Monolayers on Surfaces, vs. Saturation Ratio, $s = (\%RH/100)$	79
44. Hysteresis Effects in Surface Adhesion Force Due to Changes in Adsorbed Water Surface Layer With Relative Humidity.....	80
45. Evaporation Rates of Water at 50°C From Metal Beaker, With and Without 15 kVAC Electric Field Applied to Assist Evaporation.....	81
46. Drying Rates of Cotton Toweling With and Without 10 kVDC Electric Field Applied to Assist Operation.....	82

47. Author's Device to Demonstrate 10^3 - 10^4 Increase in Evaporation Rate From Linen and Other Wetted Substrates in High-Voltage Electric Fields.....	83
48. Data from Author's Device (Figure 47) Using Linen Substrates on One or Both Disc Electrodes; Substrates Wetted with Water.....	84
49. Data from Author's Device (Figure 47) Using Linen Substrates on One or Both Disc Electrodes; Substrates Wetted with Oil, Turpentine, or Water Solutions of Ethanol or Acetone.....	85

Blank

MILITARILY-SIGNIFICANT PROPERTIES OF ATMOSPHERIC WATER VAPOR AND ITS ADSORBED SURFACE LAYERS

1. INTRODUCTION

During development of new military hardware, we often find that sensitive devices which work well under controlled experimental conditions fail to be type-classified because they do not work in the battlefield environment. As devices become ever more sensitive, involving concepts like surface chemistry and physics, and molecular engineering, they become more vulnerable to unknown factors in the atmospheric environment. Atmospheric humidity effects need to be understood to the extent that they do not cause our hardware development programs to fail.

Water vapor and its atmospheric manifestations are so familiar to us that we simply do not realize how complex this substance really is. It dictates our weather through processes that still defy scientific explanation. Humidity makes impermeable protective clothing uncomfortable; it fouls and spoils our supplies; it affects static electricity, and thus filtration and other processes; it exhibits complex behavior when adsorbed on surfaces; it interacts with chemicals and chemical agents; it affects infrared remote detection, and aerosol nucleation and obscuration; water ions "dance" in the vapor sampled by ionization detectors like CAM, greatly complicating C-agent detection. Its effects in tropical climates are especially severe. Yet most of us continue to regard water vapor as a simple gas of H_2O molecules.

The author became interested in the structure of atmospheric water vapor nearly 30 years ago, while developing infrared (IR) remote sensors that were the forerunners of our XM21 and LIDAR detectors. Humidity alters atmospheric IR propagation very unpredictably, and often very significantly, due to absorption that is unrelated to optical scattering by conventional aerosols such as hazes, smokes and fogs.

Its absorption of IR is not simply determined by water vapor partial pressure, but arises from aggregates of water molecules (called "water clusters") that are held together by intermolecular hydrogen bonds and are formed either by the clustering of single water molecules ("monomers") about atmospheric ions, or by evaporation of water droplets to a size such that they contain fewer than about 45 monomers. The mean cluster sizes in the vapor are strongly dependent upon relative humidity, and to a lesser extent upon temperature.

Much of the research which will be described here was supported by U.S. Army Chemical Research, Development and Engineering Center In-House Laboratory Independent Research (CRDEC ILIR) funds. The work led to the award of a U.S. Secretary of the Army Science and Engineering Fellowship, which was performed at the University of Manchester in England during the period from May, 1986 to May, 1987. Many new discoveries made during the fellowship research remain to be exploited, pending availability of new ILIR funds.

2. THE NATURE OF WATER-SUBSTANCE

2.1 Liquid Water.

For many decades it has been known that liquid water is extensively structured due to hydrogen bonding. The bonds form molecular aggregates or "clusters" which comprise the liquid.¹ Luck² has deduced that at 25°C, for example, 85% of liquid water is clustered at any instant of time. Water exhibits a much smaller (10^{-6} to 10^{-5} times) rate of evaporation than would be expected from kinetic theory; yet this theory works very well for unassociated substances such as mercury.³ The heat of vaporization and surface tension of water are much larger than those of other substances. All of this behavior is consistent with the extensive clustering due to hydrogen bonding in the liquid, and thus it is generally explained on these grounds.

2.2 Water Vapor.

Water vapor, on the other hand, has been almost universally assumed to consist of an overwhelming majority of single molecules (monomers) and perhaps traces of Boltzmann-distributed dimers, trimers, etc. Our present view of homogeneous nucleation theory⁴ is based on this interpretation. Yet C.T.R. Wilson, in his classical cloud chamber studies^{5,6} which were carried out before hydrogen bonding was known to exist, could only wonder at the vast numbers (greater than 10^8 per cc of vapor) of large uncharged clusters he observed in his experiments which served as nuclei for the condensation of his "cloud-like" water droplets. Since these clusters had radii three times larger than the accepted radius for the water monomer, and since monomer collision and momentary "sticking" was the only clustering mechanism that could be accommodated by classical kinetic theory, Wilson could only suggest that perhaps the known molecular (monomer) radius was in error by a factor of three! He wrote⁵ "...it is difficult to account for the immense number of these nuclei, otherwise than on the view that they actually are simply small aggregates of water molecules, such as may come into existence momentarily through encounters of the molecules. On this view the dimensions of the molecules cannot be small compared with 6×10^{-8} centim.". The radius of the water molecule is, of course, 2×10^{-8} cm.

In retrospect Wilson seems to have understood these phenomena better than the cloud microphysicists who succeeded him and produced elaborate theories to explain observed behavior in water vapor.⁷ These theories could be hypothesized but never proven, because the droplets grown large enough for optical detection and studied in the cleanest vapor contained 10^7 more monomers than the molecular aggregates or "water clusters" from which they had nucleated. Seven orders of magnitude could scarcely be accommodated without introducing serious questions in the interpretation of experimental data, however carefully taken.

2.3 The Liquid Surface.

It is not surprising, therefore, that the physical interface between liquid water and its vapor, through which pass the species that determine fundamental physical properties of water such as saturation vapor pressure

and surface tension, also is poorly understood. DeBoer³ has stated that if this surface behavior was as expected from classical theory many lakes and seas would evaporate in a few hours, and the oceans would be dry in a few days. Croxton⁸ devotes a short chapter to the subject, after stating in a prologue that any statistical mechanical theoretical treatment of the water surface presents particularly formidable problems and, indeed, that such a discussion of these interfacial properties might well be "premature".

But through all of this no one has seriously proposed that water vapor, particularly when saturated, might be extensively structured by populations of liquid-like molecular water clusters having size distributions corresponding to equilibria established for particular temperature and partial pressure conditions. Theory, if unchallenged, eventually becomes accepted. And, once accepted, it becomes unchallengeable. Perhaps that has happened in our evolution of such theories stemming from C.T.R. Wilson's original, brilliant experimental work.^{5,6} While Wilson went on to further accomplishments, the heirs to his discoveries were gradually leading us further astray.

2.4 Evidence for Cluster Activity in Water Vapor and Moist Air.

There is formidable evidence in the literature that cluster activity exists in water vapor and moist air. In infrared water vapor absorption measurements Bignell⁹ extended the work of Varanasi, et al.¹⁰, to show anomalous or excessive absorption which had a quadratic partial pressure and an inverse temperature dependence and could be attributed to molecular structure in the vapor. Quite naturally, the water dimer was suggested as the possible cause. This led to a long and continuing series of investigations of this infrared "continuum absorption", which is observed in wavelength intervals where the water monomer has little or no absorption. Gebbie¹¹ and his co-workers, who organized a concerted attack on this problem, reported that anomalous absorption in the atmosphere at ambient temperatures could not be attributed to equilibrium water dimers. It was proposed in 1978 that the infrared water vapor continuum absorption could have a "molecular interpretation" based on hydrogen bonding in the vapor.¹² but no specific mechanisms were postulated. Completely unexpected behavior of steam-generated, cooling water fogs was reported¹³ in 1979 in infrared radiometric spectral emission studies, which was explicable only on the grounds that large clusters must exist in large numbers in warm water vapor. It was also reported in 1979 that the observed temperature dependency of the infrared continuum absorption could be, inexplicably, calculated almost precisely from the square root of the dissociative ion product of liquid water, and that simple molecular oscillator models could be used to calculate the infrared continuum absorption by assuming that distributions of large water clusters could exist in the atmosphere.¹⁴ It was the ability to model the continuum absorption of the water vapor from the dissociative ion product of liquid water that suggested many of the investigations that are described in this report.

Millimeter-wave absorption by fogs shows intense activity by species that are presently unknown.¹⁵ Commenting on these observations and their variability, Gebbie¹⁶ proposed a metastable cluster of about 50 monomers to explain the absorption and yet to conform to accepted kinetic and nucleation theories. He did not, however, investigate the possible existence of large, stable equilibrium populations of hydrogen-bonded clusters in the vapor which easily could have explained these data.

At what "size", or number of monomers comprising it, does a water cluster in the vapor begin to exhibit the thermodynamic properties of liquid water? Studies of water clusters using crossed-beam techniques¹⁷ have shown that when a cluster comprises about 6 or more monomers its near-infrared absorption spectrum closely resembles that of liquid water. Castleman and his co-workers,¹⁸ in extensive measurements of entropy and other thermodynamic properties of water ion clusters of the structure $H^+(H_2O)_n$, have found that clusters of size $n = 4$ to 6 or more are, thermodynamically, liquid water. Thus water clusters nearly ten times smaller than the critical size needed for droplet nucleation already behave like liquid water "droplets" in the vapor, and can impart to the vapor liquid-like behavior including infrared and mm-wave spectral absorption, and electrical properties described later in this report. It is also known that when liquid water and saturated moist air at atmospheric pressure, however clean, exist together at temperatures above about 50°C, water droplets will begin to appear spontaneously in the vapor.¹⁹ These droplets are nucleated in the absence of foreign nuclei in the vapor, and their numbers steadily increase as the atmospheric boiling point is approached. This means that even in the most careful measurement of such fundamental physical properties of water as its saturation vapor pressure at temperatures above 50°C, droplets and evaporatively-produced clusters like $(H_2O)_n$ must always be present, and that their populations increase with increasing temperature. Thus, the saturated vapor is to some extent clustered and this clustering will, according to kinetic theory, proportionately reduce the measured equilibrium vapor pressure.

Some questions of obvious interest include (1) to what extent clustering also occurs in the saturated vapor at temperatures below 50°C in the absence of droplets large enough for critical detection, and (2) how this clustering can be described as a function of temperature and saturation ratio (fractional relative humidity) in water vapor; i.e., what fraction of all monomers in the vapor is involved in clustering at any instant of time?

3. WATER CLUSTERS

3.1 Ion (Charged) vs. Neutral (Uncharged) Clusters.

Although water clusters are three orders of magnitude smaller than the wavelengths of visible light, a great deal is known about them from direct measurements that confirm theoretical considerations. Some examples of water cluster configurations are shown in Figure 1. Clusters can be ions, typically carrying a single electronic charge, or they can be electrically neutral (uncharged), depending upon how they form. Possible configurations can include open chains or closed rings or "solids", the latter being favored because they represent low-energy configurations for a given clus-

ter "size", i.e., the number of water molecules (monomers) that comprise it. The cluster of size 20, whose faces form a pentagonal dodecahedron as shown at the bottom of Figure 1, is often observed experimentally as will be shown later. Often, a single monomer is "caged" in the center of this clathrate-like structure, indicating that this central monomer was originally an ion that attracted other monomers which swarmed about it. These other monomers then became cross-linked by a network of hydrogen bonds, as represented in Figure 1. The binding energy of a hydrogen bond is on the order of 0.1 to 0.2 electronvolts (eV), while that of a single ionic charge is on the order of 1.0 eV. Thus, even if an ion attracts other water monomers to form a cluster and then loses its charge, the combined hydrogen bond energy is sufficient to hold the cluster together for a significant time if the cluster contains more than a few monomers. In this way, the populations of neutral clusters in water vapor far exceed the populations of water ion clusters at any instant of time, since the ion charge lifetimes are on the order of a microsecond or less,²⁰ while neutral clusters can survive for lifetimes ranging from milliseconds or longer for small clusters to seconds or longer for larger clusters.

Clusters can form by ion clustering or by the evaporation of water droplets. As Figure 2 shows, clustering of water monomers about positively-charged ions is an orderly process, since the oxygen atom of each monomer is oriented inwardly with the smaller hydrogen atoms oriented toward the cluster surface where they can, in turn, bond with other oxygen atoms in other monomers. Clustering about negative ions, by contrast, is not so orderly. Hydrogen atoms are oriented inwardly, with other hydrogen and oxygen atoms oriented outwardly where they can bond with each other or, with some difficulty, with other monomers. Thus clusters formed about positive ions tend to be larger, and more predictable, than those formed about negative ions; as a consequence, positive water ions are usually studied experimentally in preference to negative ones.

Visualization of water cluster ion formation is aided by molecular ball-and-stick models wherein water monomers are represented by spheres and hydrogen bonds are represented by sticks. Some examples are shown in Figures 3 to 6. In Figure 3, the central ion is surrounded by closely-packed monomers, while in Figure 4 an open-chained cluster of size 13 is shown for comparison with one of the same size, but with closed rings, in Figure 5. Figure 6 shows a conceptualization of a larger clathrate-like cluster having water monomers at the apexes of the geometric solid shown with it. As clusters become very large and approach the critical size for droplet nucleation (about 45 monomers), they assume near-spherical, lowest-energy configurations which, themselves, resemble tiny droplets. Liquid-phase properties, such as surface tension, begin to be manifested by the hydrogen-bonded clusters. The unusually high surface tension of liquid water itself is due to extensive hydrogen bonding at its surface.

3.2 Cluster Equilibria in the Vapor.

Equilibria between water ions, or other condensation nuclei, and water droplets in the vapor are described by the Thomson/Kelvin equation⁷ (Figure 7). This equation does not account for hydrogen bonding, as occurs in

water clusters and droplets, since this phenomenon was unknown when the equation was derived and later used by C.T.R. Wilson in his classical cloud chamber investigations.^{5,6} However, because hydrogen bonding increases the surface tension (T , in Figure 7) of water, it is possible that some compensation results due to its inclusion. The term $f(H)$ in Figure 7 cannot be evaluated. When the equation is plotted without $f(H)$ the curves shown in Figure 8 result. The domain of water ion clusters in the real atmosphere is shown by the near-vertical curve labeled "ION" for saturation ratios of $s \approx 1.0$ or less ($s = \%RH/100$, where RH is the relative humidity). At larger radii are shown other types of atmospheric nuclei including Aitken nuclei, and combustion (continental) and salt (maritime) nuclei. While the latter are capable of growing into hazes or fogs by sorption of water vapor at RHs below or slightly above 100%, the curves show that water ion nuclei must attain "supersaturations" on the order of about $s = 4.2$ for droplets to be nucleated. The dashed curve shows that uncharged clusters are not supposed to exist in the real atmosphere since they require supersaturations of about $s = 7.4$ or more to form and nucleate droplets.

When C.T.R. conducted his experiments, he gradually increased the extent of supersaturation in his cloud chamber in a series of steps in which a piston was suddenly released to cause adiabatic expansion of the water vapor sample in the chamber. Thus, the salt nuclei were first activated to form water droplets which precipitated into a pool of water on the floor of the chamber. The combustion and Aitken nuclei were similarly consumed at somewhat higher saturation ratios. Wilson, at $s = 4.2$, then reached the supersaturation where his "rain-like" condensation on ions produced about 100 water droplets per cc. Continuing to still higher supersaturations, Wilson encountered the "cloud-like" condensation which completely baffled him, and which led him to theorize that the molecular radius of the water molecule (monomer) must be three times larger than the then-accepted (and correct) value. Wilson worked with experimental clouds that were so beautifully controlled that he knew from their color tints⁶ almost precisely what their mean radii were. Thus he was able to calculate almost exactly the starting mean radii of his neutral (uncharged) nuclei. But because he knew nothing about hydrogen bonding, he had to conclude that the enormous neutral (cluster) nuclei populations he observed (greater than 10^8 per cc, his limit of optical resolution with focused gaslight) were simply aggregates of a few colliding monomers (see Figure 9).

The undefined term $f(H)$ in the Thomson/Kelvin equation (Figure 7) probably is the key to understanding what Wilson saw. This hydrogen bonding term, whatever its form, must account for the presence of another curve representing the real atmosphere to the left of the "ION" curve in Figure 8. This added curve, as is shown in Figure 10, must lie just above the ION curve, but below the dashed theoretical uncharged monomer curve which does not take into account hydrogen bonding. Thus the new curve represents equilibria of neutral water clusters, produced on ions with subsequent loss of charge, or by droplet evaporation, or perhaps by still other mechanisms. This curve gives a physical basis for the enormous populations of water nuclei and droplets Wilson observed in his cloud chamber, which he incorrectly attributed to momentary encounters of water molecules (Figure 9). The mean sizes of the neutral clusters he observed would have been about 20 to 30.

Thus their diameters or radii were about three times larger than those of single water molecules. This led Wilson to propose that the water molecules must themselves be larger than the accepted (and correct) value, by a factor of three.

3.3 Cluster Formation in Water Vapor.

We can now consider specific formation mechanisms for water clusters, and the dynamic equilibria that must exist between ion clusters and neutral clusters in water vapor. While the neutral cluster populations have been shown to be much larger than the water ion cluster populations, the two species appear to exist in proportional numbers. Thus, as will be shown, for given conditions the ratio of ion clusters, measured by vapor electrical conductivity, to neutral clusters, measured by infrared absorption of the vapor, will be reasonably constant. If, for example, neutral clusters are produced by droplet evaporation, they will ionize to a small extent. The ions thus produced will capture more monomers to produce larger clusters which, when their charge is lost, will repeat the process. In cloud or fog conditions, water droplets and clusters are present in large numbers. There will be a continuing interchange between droplets evaporating, on the one hand, and droplets nucleating and growing, on the other hand.

Consider first the hypothesis that neutral water clusters are produced by evaporation of water droplets, or even by the simple evaporation of water from its liquid surface (since the nature of water surface evaporation is completely unknown).^{3,8} The basic premises are then those shown in Figure 11. Here, water ions are produced constantly by the slight dissociation of neutral clusters, which is enhanced by natural radiation, or by radiation sources deliberately introduced into the system.

Alternatively, neutral clusters can be formed from ions as shown in Figures 12 and 13. These are sometimes referred to as "ion-induced" neutral water clusters. It is even possible, as shown in Figure 14, that neutral clusters might be formed from monomers which ionize slightly and attract other monomers to their extremities. Figure 15 indicates that water cluster equilibria can be far more complex than would be indicated by considering water vapor as a simple gas of single molecules. Some of the mechanisms shown in this figure will be considered in more detail in the remaining sections of this report.

4. VAPOR MEASUREMENTS

4.1 Mass Spectral Data.

Carlson and Harden²¹ presented mass spectra of water ion clusters $H^+(H_2O)_c$, where c is the cluster size. They showed that these clusters exist in near-Gaussian size distributions for which the mean size is statistically significant, and that this mean size increases very rapidly with increasing relative humidity. Temperature also affects mean cluster size, although not as significantly as does humidity. They also showed that the changes in mean cluster size with humidity and temperature could explain most precisely the dependence of the infrared "continuum" absorption of

water vapor, which is attributable to clusters in the vapor, upon these same parameters. Thus, their results indicated quite clearly that neutral clusters in water vapor or moist air are the cause of this anomalous or excessive infrared absorption, which had been unexplained previously.

Some of their data are shown in Figures 16 to 20. In Figures 16 and 17, cluster distributions are shown for 99-100°C for saturation ratios of $s = 0.056, 0.15, 0.31, 0.38, 0.47$ and 0.55 , corresponding to relative humidity values of 5.6%, 15%, 31%, 38%, 47% and 55%, respectively. In Figure 16 (top), the enhanced population of clusters of size $c = 21$ can be seen clearly. This cluster structure would correspond to that shown at the bottom of Figure 1, but with an H_3O^+ ion caged in the center. Such favored cluster sizes are sometimes referred to as "magic numbers", and they tell something of how a given cluster was formed.¹⁸ In Figure 17, another magic number configuration is indicated at cluster size $c = 28$, although its geometry is a matter of conjecture.

Mass spectra like those shown in Figures 16 and 17 for constant temperature at 99-100°C, showing a strong dependence of the mean cluster size upon humidity, are also observed at ambient temperatures. For example, Figure 18 shows a spectrum for "clean air" at 23°C and 75% RH ($s = 0.75$). Note that the mean of this distribution is near $c = 8$, far smaller than the value $c = 33$ shown in Figure 17 for an RH of only 55% ($s = 0.55$). This behavior reflects the fact that water vapor exhibits a rapidly-increasing vapor pressure with increasing temperature; thus clusters grow in mean size with increasing temperature if humidity is held constant or is not permitted to fall rapidly during heating. However, if a condition of constant partial pressure is maintained during heating, the resulting relative humidity or saturation ratio will fall rapidly causing the mean cluster size (c)_μ to decrease with temperature. This is shown in Figure 19, for a sample with a water vapor partial pressure of 28.4 mm Hg at one atmosphere, heated from 28°C to 96°C, resulting in a reduction in mean cluster size from about $c = 24$ near saturation to $c = 11$ at the highest temperature (which produced a relative humidity of only 4.2% ($s = 0.042$)).

When all available data of this kind are evaluated for the water ion species $H^+(H_2O)_c$ in moist atmospheric air, it is possible to roughly estimate the effects of temperature and saturation ratio on mean cluster size as is done in Figure 20. It is arguable whether the water ion distributions measured by a mass spectrometer are like those sampled into the spectrometer from the atmosphere. Samples undergo free-jet expansion and cooling, with irradiation, to yield the spectra shown here.²¹ It is possible that the measured ion clusters are very representative of neutral cluster populations in the sampled moist air; these would simply be ionized by irradiation and rapidly "frozen" to preserve their integrity. Or, it can be argued that the ion clusters are actually formed in the free-jet expansion on ions that are produced by irradiation, and that these ions are swarmed by water monomers. These arguments are academic, however. We know that the water ion distributions measured in a mass spectrometer must be closely related to the neutral cluster distributions in the sampled moist air, particularly as regards their temperature and humidity dependencies (Figure 20). Otherwise, it would not be possible to model the temperature and humidity

dependencies of the atmospheric infrared water vapor continuum absorption, which arises from neutral cluster absorption, by using these dependencies as deduced from water ions in a mass spectrometer (Figures 16-19).²¹

Other experiments strongly suggest the existence of huge populations of neutral water clusters in water vapor and moist air. Figure 21 shows a simple apparatus with which nucleation rates of water droplets in very clean moist air at atmospheric pressure were be estimated for various vapor temperatures.¹⁹ Observations showed that droplet nucleation apparently can occur spontaneously with warming, beginning at about 50°C, even in purified saturated air at atmospheric pressure that is free of nuclei other than water clusters. When the mass spectra of Figure 17 were measured²¹, it was found that if the saturation ratio exceeded $s = 0.55$ at 99-100°C the cluster distributions remained smooth to the left of the mean but began to deteriorate very badly to the right of the mean for cluster sizes greater than $c = 45$. One interpretation of these results was that clusters reaching a size of about $c = 45$ were able to "spontaneously" nucleate droplets in moist atmospheric air that was approaching saturation ($s = 1$); i.e., to nucleate or condense droplets upon themselves without the need for large, conventional condensation nuclei to be present (Figure 8). Common atmospheric observations of nucleation, such as the steaming of water that begins at about 50°C as the liquid is heated, have been presumed by most observers to be explicable as droplet condensation on impurity nuclei that are always present in atmospheric air. But the apparatus in Figure 21 allowed this behavior to be observed even in the absence of impurity nuclei.

The interested reader is referred to Ref. 19 for full details. Briefly, these experimental results suggested that a single, critical cluster size of about $c = 45$ could explain nucleation in water vapor over a wide range of temperatures and partial pressures. Thus a specific, clathrate-like, near-spherical structure would be associated with this critical size, and that structure would embody incipient liquid water. Figure 22, from Ref. 19, can be used to demonstrate this. The figure shows schematically how water cluster distributions would respond to changes in temperature or water vapor partial pressure. The ordinate indicates the fraction of water vapor that is clustered, and the abscissa shows the saturation ratio. The measured cluster distribution from the top of Figure 17, for $s = 0.55$, is shown in Figure 22 atop the 100°C temperature curve.

The critical cluster size for droplet nucleation is shown by the heavy curve labeled $c = 45$. Thus if the saturation ratio were raised above $s = 0.55$ (55% RH), the distribution would "slide" to the right along the 100°C line, and clusters exceeding size $c = 45$ would produce droplets in the vapor. Similarly, if the temperature were reduced below 100°C under constant partial pressure conditions, the distribution would move to the right along the dashed line, producing droplets. At a temperature of about 50°C in saturated vapor ($s = 1$, the vertical line), a solid point indicates the position upon which the cluster distribution for these conditions would be centered. The right-hand "tail" of this distribution would just reach the $c = 45$ curve under these conditions, and droplet nucleation in the vapor would cease as the distribution descended the vertical $s = 1$ line to still

lower temperatures. These were exactly the experimental observations. Much more detailed analyses are presented in Ref. 19.

4.2 Infrared (IR) Data.

The IR transmission of the atmosphere is limited by absorption of atmospheric gases and by optical scattering of suspended particulates. Atmospheric spectra for two different path lengths are shown in Figure 23. "Window" regions exist where interatomic absorption by gases is minimal; these are commonly used for remote-sensing and other instrumentation. Two windows, one at 3-5 μm wavelengths (excluding the CO_2 band at 4.2 μm), and another extending from 7 to 13 μm , are most popular for the operation of a wide variety of instrumentation. The 7-13 μm window (partially shown in Figure 23) is especially important because its wavelengths correspond to those of the peak blackbody emission of the earth's mantle, and thus it is heavily involved in the "greenhouse" effect. The high-powered CO_2 laser operates at 10.6 μm in this window.

Aside from its obvious role in producing hazes and fogs on atmospheric nuclei at higher humidities which attenuate radiation, water vapor also attenuates in the IR by two kinds of absorption: atomic and molecular. Atomic absorption arises from single water molecules (monomers), due to vibrations of interatomic O-H bonds, and rotation of molecules. Molecular absorption arises from hydrogen-bonded water clusters in the vapor, which have liquid-like spectral absorption to which is usually attributed the IR "continuum absorption" of water vapor.

TABLE 1.

WAVELENGTHS (λ) OF PRIMARY INTERATOMIC AND ROTATIONAL INFRARED
ABSORPTION BANDS IN THE VAPOR AND LIQUID PHASES OF WATER

Band Designation	$\lambda_{\mu\text{m}}$, in Vapor	$\lambda_{\mu\text{m}}$, in Liquid
ν_1	2.76	2.90
ν_2	6.27	6.10
ν_3	2.66	2.77

The three primary atomic absorption bands of water are remarkably similar regardless of whether they are measured in the vapor or liquid phases. Table 1 summarizes the absorption wavelengths of these bands. Only small differences exist between the peak absorption wavelengths of water vapor and liquid water; these can be attributed to molecular interactions in the much denser liquid phase compared to the vapor phase. But measurements show that the absorption intensities of each of the three bands are very similar for equal sample quantities of water vapor or liquid. That is, the absorptivities or absorption coefficients of the three bands are about the same regardless of whether the water samples are liquid or vapor.

But the situation is decidedly different in the window regions between water's atomic absorption bands. In these windows, where the IR continuum absorption is troublesome, liquid water has far larger absorption coefficients than does water vapor consisting primarily of single molecules (monomers). These are the spectral regions of molecular absorption; similar absorption is also seen at longer wavelengths extending into the millimeter and centimeter-waves, i.e., the radar region. This molecular absorption results from hydrogen-bonded clusters floating in the vapor phase. Figure 24 shows the IR spectrum of water vapor consisting almost entirely of monomers. Note that there is much fine structure due to interatomic modes of the water molecules; this is also apparent in Figure 23. The window regions at 3-5 μm and 7-13 μm are clearly defined. In the centers of these windows, water vapor has virtually no spectral absorption. For comparison, Figure 25 shows the IR spectrum of liquid water. Note that there is no fine structure because of intermolecular forces in liquid water, which is almost completely hydrogen-bonded.² The three absorption bands shown in Table 1 are present in Figure 25, but the ν_1 and ν_3 bands are smeared together due to the intense absorption of this liquid sample, which was a water film only 10 μm thick.

If we go wavelength-by-wavelength through the IR and radar regions and we take the ratio of the absorption coefficient of liquid water to the absorption coefficient of pure water vapor (a gas of monomers), the result is shown in Figure 26. The height of the peaks in Figure 26 indicates how troublesome the absorption by liquid-like water clusters will be in various wavelength regions. For example, in the 7-13 μm IR window region, the peak exceeds 10^4 . This indicates, for example, that if a cluster fraction of only about 10^{-4} were present in water vapor, the clusters would account for as much spectral absorption themselves as the absorption by all of the vast majority of single water molecules combined. Typical atmospheric water vapor actually contains a cluster fraction of about 10^{-3} . Thus the continuum or "anomalous" absorption due to clusters exceeds that due to all of the vapor by a factor of 10. In other spectral regions the cluster absorption is less dramatic, but it is still troublesome. When the cluster fraction in water vapor increases, e.g. at higher humidities and especially in clouds and fogs, the cluster absorption completely dominates monomer absorption in determining atmospheric radiative transfer. At higher humidities hazes and droplets also attenuate visible and IR wavelengths due to their optical scattering, but this must not be confused with or used to explain away the very substantial spectral absorption due to water clusters, which are far too small to scatter radiation at these

wavelengths; thus, they are pure absorbers. Cluster absorption, for example in steam, can account for much greater extinction of radiation than that due to scattering by droplets that also are suspended with the clusters in the vapor.

The liquid-like absorption of neutral water clusters can be appreciated if we compare IR spectra, obtained by new crossed-beam techniques,¹⁷ for clusters of different sizes with the spectrum of liquid water. Figure 27 shows near-infrared spectra of neutral water clusters ranging from size $c = 3$ to size $c = 6$. The liquid water spectrum is shown at G. in this figure. The spectrum of the cluster of size three has little resemblance to that of liquid water. But as cluster size increases the finer spectral structure of smaller clusters is gradually blurred and, for the cluster of size $c = 6$, the spectral envelope has attained a shape approaching that of the liquid. In other words, neutral clusters of size six or more behave very much like liquid water as regards their IR absorption. This tends to confirm thermodynamic observations¹⁸ which show that by the time water clusters reach a size of six they are, for all practical purposes, liquid water. Thus we can understand why neutral clusters, when suspended in water vapor, give rise to absorption that is indistinguishable from that due to an equal mass of liquid water in a vapor sample, with the exception that the clusters are so tiny that they behave as pure absorbers, while liquid water would also attenuate by optical scattering if it were present in larger droplets. We can see that the ratio of absorption coefficients (Figure 26) of liquid water to its vapor does give a good indication of the extent of cluster or "continuum" absorption to be expected in a given spectral region.

Large populations of neutral water clusters exist, in water vapor and in moist atmospheric air, in equilibrium with much smaller populations of water ions (Figures 11 to 15). C.T.R. Wilson's cloud chamber data^{5,6} gave the first indication that their populations are on the order of hundreds of ion clusters per cc, and greater than 10^8 neutral clusters per cm^3 (his experimental limit of resolution). Thus the population ratio of neutral to ion clusters in water vapor is greater than 10^6 , but because equilibria exist between the two species they are present in proportional populations even though their absolute numbers may vary widely depending upon ambient conditions. Experiment confirms²² that the infrared absorption (due to neutral clusters) and the ion content of moist atmospheric air are proportional to each other. Simultaneous measurements have been made of the electrical conductivity of moist air and its infrared absorption under typical room conditions. A multi-pass optical cell ("White cell") giving path lengths up to 94 meters was used to monitor IR absorption of recirculating moist air which also passed through a chamber in which sensitive vapor electrical conductivity cells were located (Figure 28). Temperature and humidity were monitored over a wide range of values. A precision optical bench was used with a sensitive IR radiometer (Figure 29); a He:Ne laser was co-aligned with the radiometer to monitor droplet scattering in the visible region at the $0.63 \mu\text{m}$ at higher humidities, over the same optical path. Experiments like these showed that the ion content of moist air could be monitored to learn how both water ion clusters and neutral clusters behave under various temperature and humidity conditions in moist air.

Thus, electrical measurements of moist air became important and were carried out extensively between 1979 and 1987.

4.3 Electrical Conductivity (Ion Population) Data.

The mobility of a water ion moving in an electric field under atmospheric conditions depends strongly upon the cluster size (Figure 30). Mobilities are given in the units $\text{cm}^2/\text{volt-second}$. Thus, the velocity of a water ion cluster of a given size, in cm/sec , can be related to the strength of an electric field, in volts/cm . If conductivity cell dimensions are known, it is possible not only to determine the total ion content between cell plates or electrodes immersed in moist atmospheric air, but also to separate ions according to their sizes if this is desired.

Because water vapor is thousands of times less dense than liquid water, vapor electrical conductivity cells are larger than their liquid cell counterparts. In the CRDEC work, a long evolution of cell design has taken place²³ but the objective has always been the same: to separate electrical leakage currents through thin water layers on cell insulators from currents due to ions in the vapor between cell plates or electrodes. The latter currents are, of course, the ones that one wishes to study as functions of temperature and humidity.

Figure 31 shows an early vapor conductivity cell design¹⁴ in which 40 steel plates were supported in parallel stacks by five fiberglass rod insulators passing through the corners and centers of the stacks. The plates in these cells, and in all subsequent cells, were interleaved in the fashion of an automotive electric storage battery except that moist air, rather than an electrolyte, occupied the spaces between the cell plates. In this way the alternate plates could be mechanically supported by metal rods which stiffened the interleaved stacks, and also provided electrical connection between every other plate. Thus when an electrical potential (DC voltage) was applied to a given cell, each plate would have the opposite polarity of its neighbors, and all plates of a given polarity would be electrically and mechanically connected together. The insulators supported the plates so that a uniform air gap was maintained between the two interleaved sets of 20 plates each. The gap spacing was usually 0.66 cm. As shown in Figure 31, it was common practice to use cells of at least two different plate areas. This gave the cells vastly different sensitivities to ions in the moist air between the cell plates, because a great many more ions (and thus a much higher ion current) would exist in the large cell than in the small one. But the total number of cell plates, and their gap spacing, were always the same and their insulators were always identical. Thus the moist air (water ion) currents measured between the plates could always be distinguished from insulator leakage currents and other experimental artifacts.

The cell designs became more sophisticated. Aluminum replaced steel as the plate material, allowing fewer insulators to support the reduced weight. Teflon insulators were found to have less electrical leakage than fiberglass ones, and replaced the latter. Figures 32 and 33 show construction details of two teflon-and-aluminum cells having two identical

insulators. Later, entire families of cells of different plate areas and vapor ion sensitivities, but with identical insulators and insulator leakage characteristics, were fabricated (Figures 34 and 35). The cells shown here in their cabinet were the ones used in this configuration to measure the ion content of moist room air as it was recirculated through an optical cell for simultaneous measurements of IR absorption (Figure 28).

Despite the sophistication of these cell designs, it was decided that the results of the measurements were of sufficient importance to warrant a new cell design that would, in effect, completely eliminate insulator electrical leakage as an experimental consideration. It was decided to build a single, large cell of interleaved aluminum plates that would be supported by special insulators located outside the moist air test chamber. Furthermore, the environment of the insulators would be controlled to keep all surfaces very dry, and thus to eliminate water surface films and their attendant electrical leakage currents. This was accomplished by passing the steel rods supporting the cell plates through small holes in the chamber walls, and supporting them with teflon insulators in an outer ducted chamber to which very hot air could be continuously delivered by a hot air blower. Photographs of the apparatus are shown in Figures 36 and 37, and it is shown schematically in Figure 38. A close observation of Figures 36 and 37 will show the cell plates in the inner test chamber and the steel rods passing through the chamber walls to the teflon insulators, with pointed bases, in the hot air duct surrounding the outside of the chamber. Temperature and humidity indicators can be seen in the top of the hot air duct.

The hot air blower atop the duct is clearly visible in Figure 37. Each set of 20 interleaved cell plates was supported by its own set of four insulators. Thus, as indicated by Figure 38, if electrical leakage were to occur at all the current would have to pass from a cell plate of a given polarity, along a steel supporting rod to its insulator, down the insulator and through its sharply-pointed base, across a teflon surface upon which the point rested to another insulator, up that insulator point to a steel rod and along the rod to a cell plate of opposite polarity. Repeated experiments showed that no leakage current whatsoever could be measured in normal operation, during which the insulators were maintained in a continuous flow of hot air at temperatures of 70°C or more and relative humidities (RHs) below 20%. It will be shown in the next section of this report that at these RHs water monolayers cannot form even on active surfaces like glass, much less on hydrophobic surfaces like teflon. Since insulator surface (leakage) currents are directly proportional to water layer thickness, no current can flow when not even a single continuous monolayer is permitted to form on the insulators. Thus the vapor conductivity and ion population data measured using this cell of new design should be unequivocal; this is important because of the controversial nature of cluster structure in water vapor and its dependence upon RH and temperature.¹²

A year's research was carried out using this new cell in studies funded by a U.S. Army research fellowship.²⁴ The results confirmed and greatly expanded the data base obtained using earlier cells (Figures 31 to 35). Some typical data are shown in Figure 39, where the cell current due to ions in moist air is plotted vs. the saturation ratio, s ($\%RH/100$),

starting at an air temperature of 24°C at 60% RH ($s = 0.6$). The solid points indicate the increase in cell current (vapor ion content) during humidification with an ultrasonic nebulizer. At saturation ($s = 1.0$), the ion population has increased from about 100 per cc at $s = 0.6$ to about 10^5 per cm^3 . The nebulizer was then shut off, and the humidity was allowed to fall (hollow points) as the chamber temperature rose to 35°C in response to continuous heating of the chamber walls by the hot air blower in the outside duct which was used to keep the insulators dry. Separate experiments established that neither the blower nor a fan sometimes used in the chamber to recirculate the moist air sample were, themselves, significant sources of ions. Other data (Figure 40) show similar trends over a somewhat narrower temperature range. The data show less scatter than do those in Figure 39. All data of this kind indicated that the dependence of cell current and water vapor ion content upon humidity was approximately s^{13} , i.e., the thirteenth power of the saturation ratio when a potential of 400 VDC was applied to the cell plates, resulting in an electric field of 600 volts/cm. The behavior was ohmic down to potentials of only a few VDC, i.e., Ohm's law was obeyed and the cell current was linearly dependent upon the voltage applied to the cell.

In other experiments, higher cell potentials were used. Figure 41 shows data for a potential of 1000 VDC, resulting in an electric field of 1500 volts/cm. During the dry-down phase here (hollow points), "hysteresis" effects are noted. That is, as drying was begun the cell current fell more rapidly than expected, but at lower humidities ($s = 0.8$ to 0.95) the current stabilized and rose above values observed during the humidification phase. Finally, below $s = 0.8$ the cell currents returned to values at the start of the experiment. Also note that for this electric field strength the current follows the function s^{13} only at higher humidities; it is nearer s^7 or s^8 at humidities below about $s = 0.85$.

Cell currents also can be represented vs. applied voltage, E_p , for various humidities as shown in Figure 42. These plots clearly show the linear or ohmic nature of the data at lower potentials, and the orderly reduction of cell current at lower humidities. But a "knee" is observed when the cell potential exceeds 1000 VDC. This probably indicates that the water ions being measured, which invariably carry a single electronic charge in smaller electric fields, begin to carry two or more charges in stronger fields. Since the ions are limited in number, each must carry more than one charge when the electric field strength exceeds some threshold value corresponding to the conditions of temperature and humidity in a given experiment.

Data like these confirm the observation that the populations of water ions in moist atmospheric air, and of neutral clusters in equilibrium with them, increase with humidity and, especially under conditions of energetic humidification with droplets present, can reach numbers much larger than those in typical ambient atmospheres. Under energetic conditions at high humidities, the data suggest that water vapor can become extensively clustered if it is not, in fact, almost completely clustered.

5. ADSORBED WATER SURFACE LAYERS

5.1 Proportionality of Layer Thickness to Relative Humidity (RH).

Many kinds of experimental data show clearly that thin layers of water molecules attach themselves to surfaces at higher RHs, and that the layer thicknesses are directly proportional to RH. The nature of the surface determines the RH at which the first molecular monolayer is deposited. In experiments during which water films are deliberately made to form on electrical insulators so that the resulting electrical leakage currents across the surfaces can be measured, it is found (1) that the current at a given potential is directly proportional to the film or layer thickness, and (2) that the layer thickness is usually directly proportional to RH during the humidification phase, but can vary widely about proportionality during the dehumidification or drying phase. The latter is usually referred to as "hysteresis" behavior.

Figure 43 shows data relating the equivalent number of water monolayers that are adsorbed on surfaces of two kinds, glass and platinum, as functions of RH. On glass the first monolayer forms at about 60% RH, and the adsorbed water layer can reach a thickness of 100 monolayers or more as saturation humidity is approached. Dissolved salts and impurities in glass interact with surface water; thus monolayer formation begins at modest levels of RH. But the first monolayer is not formed on a platinum surface until the RH reaches about 90%, and the maximum adsorbed layer thickness approaches only about 20 monolayers at saturation humidity. Platinum, like teflon, is a quite hydrophobic surface. Also shown in Figure 43 are the humidity dependencies observed (Figures 39 to 41) for the water ion content and electrical conductivity of moist atmospheric air. Thus the data tend to suggest that the populations of water clusters, including water ions, on surfaces mimic the populations of water clusters in moist air, as functions of humidity. This would indicate that equilibria exist between water clusters in the vapor and those on surfaces; perhaps insights can be gained from such observations into the nature of the liquid water surface and the unknown mechanisms that govern this liquid/vapor interface.^{3,8}

5.2 Surface Phenomena and Hysteresis Effects.

Hysteresis effects were noted in the ion content and electrical conductivity of moist air as a function of atmospheric humidity (Figure 41). We have mentioned that surface hysteresis effects are observed in measurements of surface water layers on teflon insulators by electrical conductivity. There are other practical examples of hysteresis behavior on surfaces. For example, Figure 44 shows how the adhesive forces holding dusts to surfaces are affected by ambient relative humidity (RH). One of the strongest binding forces governing adhesion of dusts to surfaces is capillary condensation. As the figure indicates (also see Figure 43), when RH is increased there is a delayed (i.e., nonlinear) increase in the adhesion number, which relates adhesion force as a percentage to the maximum value reached at 100% RH. The adsorbed surface water layer thickness increases rapidly with humidification above 50% RH, reaching a maximum at 100% RH. But when drying occurs (upper curve), the "evaporation" of the

surface layer is not immediate. Again there is hysteresis. Together, the curves form an almost classical "hysteresis loop" such as is observed, e.g., in the inductance of electrical coils with voltage changes. The data indicate that if it were required to remove, e.g., biological or radiological dust contamination from surfaces, this is more difficult to accomplish once the surfaces have become moist and are subsequently dried, than if decontamination were performed before water layers formed on the surfaces. Thus daytime decontamination, before the evening drop of air temperature with subsequent increase in RH, might be advisable in a BR defense scenario even though delay was otherwise considered to be unimportant.

5.3 Sources of Atmospheric Ions.

Experimental data like these raise fundamental questions concerning not only the nature of water-substance itself, but our understanding of the electrochemistry of liquid water and water vapor. At low humidities in water vapor, layers of water molecules do not form on surfaces (Figure 43). Under these same conditions, the water ion content of the vapor is at its minimum (Figures 39 to 41). At higher humidities the plates or electrodes of vapor electrical conductivity cells become moist as molecular layers accumulate on them, while proportionally larger ion populations are found in the vapor. What has completely escaped notice until very recently is that there may be a causal relationship here, i.e., the ions in the vapor may be generated from moist surfaces in electric fields. Thus moist surfaces, between which existed even small electric fields typical of the earth's atmosphere in fair weather (a few volts/cm), might be the sources of atmospheric water ions. In effect this would mean that electric currents produce ions in moist air, rather than ions producing electric currents in moist air, in the presence of even small electric fields. It would also explain why conventional atmospheric ion counters, such as Gerdien tubes,²⁵ whose electrodes are kept dry even as humid air samples are passed through them, would fail to count increasing ion populations with increasing RH: the source of the ions (the electrodes) would not carry the surface water layers necessary to generate water ions to pass through the vapor gap between them under the given potential (voltage) difference between the electrodes.²³ These questions can only be resolved by a continuation of the research begun in the author's fellowship studies.^{23,24}

Although molecular layers of water on surfaces in electric fields appear to be sources of atmospheric water ions between surfaces at different electrical potentials, the surface of liquid water is an extremely poor source of atmospheric ions. In the author's electrical conductivity studies of moist air,^{23,24} if finely-structured molecular layers of water on the electrodes (cell plates) coalesced into liquid water films or droplets, the electric current between electrodes dropped precipitously, often by orders of magnitude. This behavior would be consistent with the view that so long as water molecules in adsorbed layers on surfaces maintain their integrity they are free to leave the surfaces in an electric field, as charge carriers (water ions), either individually or (more likely) as clusters of molecules that pass into the vapor and move under the influence of the electric field. But once the surface molecules coalesce into bulk liquid

water, they become much more firmly bound to their neighbors in the condensed phase and they cannot leave the surface except under the influence of very large electric fields.

6. HIGH VOLTAGE PHENOMENA

6.1 Hysteresis and Corona Discharges.

As electric fields reach levels exceeding one to two thousand volts/cm (1-2 kV/cm), atmospheric water ions that move under their influence begin to carry more than one electronic charge²⁵ (Figure 42). In very large fields corona discharges occur, involving not only water but air molecules, and highly-conductive plasmas exist until the electrical resistance of the vapor finally breaks down and electric arcs, like miniature lightning discharges, are struck through the vapor. As corona and breakdown conditions are approached in increasing electric fields, adsorbed water surface layers on insulators and walls become increasingly important. Insulators which work very well at lower voltages and/or lower humidities are degraded and, under extreme conditions, electric arcs will be struck across their surfaces producing carbonization (charring) and permanent damage. Thus insulators must be excellent, and preferably should be kept dry, in high-voltage applications.

For possible CB defense (air filtration) applications, research has been carried out using corona glow discharges to decontaminate airstreams. Invariably in such research the question of decontamination efficiency arises, and this depends on how effectively cell current flows through electrodes (typically needles) and thus through flowing air, as opposed to its alternative route through surface water layers on cell insulators and/or walls. The total current drawn will be the sum of both the vapor and leakage currents, and this will dictate the power required for operation. At high air humidities, the problem becomes worse. Design considerations are very similar to those for the vapor conductivity cells shown in Figures 36 to 38.

Hysteresis behavior due to adsorbed surface water layers is often observed in high-voltage air filtration studies employing corona discharges. It is important to distinguish between these surface effects, and other water ion vapor phenomena that might in fact be real, in such studies. But this is not always easy, because the data can be very difficult to interpret, and can often seem to be explicable on the wrong grounds. In electric fields on the order of 15-20 kV/cm, air filtration cell currents can vary by a factor of ten over a range of 20 to 70% RH, and hysteresis effects can be very pronounced. Since agent simulant destruction efficiencies by corona are on the order of only ten percent, a clear understanding of whether air filtration by this means is or is not feasible depends on an understanding of how the factor of ten in cell current vs. humidity arises. Typically, experimentalists working with corona air purification systems will find that RH affects current-voltage behavior of the corona more than any other parameter. Critical levels are RH are found where currents increase dramatically. Some type of "inertia" is said to exist in the systems, and system response to changes in RH is not

immediate. A clear understanding will only be gained through further research employing the guidelines discussed in this report.

6.2 Accelerated Drying.

Asakawa²⁶ has shown that simply by applying a high-voltage electric field to the surface of liquid water, one can increase the evaporation rate by an order of magnitude. Figure 45 shows the experimental set-up schematically, for water at 50°C in a metal beaker in the center of which, above the liquid surface, is suspended a wire electrode. In this case an alternating current potential of 15 kVAC was applied between the water in the beaker and the wire electrode, but DC can be used as well. The curves show the water evaporation rate for natural evaporation (bottom) and electrically assisted evaporation (top). The mechanisms involved are not understood, but clearly they can or even must involve water ion clusters. It is perhaps significant that at 50°C spontaneous nucleation of droplets begins above the liquid water surface, and that this can be explained by water cluster theory (Ref. 19, and Section 4.1 of the present report). Perhaps clusters of "critical" size for droplet nucleation ($c = 45$) are the species that leave the liquid water surface intact and thus greatly increase the surface evaporation rate in the electric field. The time scale of the alternating current would be very slow compared to that of the water clusters leaving the water surface and diffusing away through the vapor. Asakawa does not indicate whether 50°C and higher temperatures are best to achieve accelerated evaporation.

Even very simple experiments show quite dramatically that the drying of fabrics can be accelerated by electric fields. Figure 46 shows the effect of drying wet cotton toweling on an electrically-conductive rod with or without a potential of 10 kV applied between the rod and earthed ground. The effect of the field is significant, and would increase with increasing applied voltage.

Figure 47 shows an apparatus used by the author to investigate a new phenomenon which he discovered recently.²⁴ A large polystyrene insulator is shaped to support two horizontal disc electrodes with high-voltage connections. Heater wires on the insulator prevent the surface water layer adsorption and electrical leakage; thus all current must flow between the steel discs, whose mutual spacing is adjustable from 0 to 10 cm. A substrate of cloth or other material for test can be placed on the bottom electrode, or on both electrodes (facing each other) if first moistened adhere to the disc surface. Figure 48 shows experimental data for linen substrates wetted with water and placed on either or both electrodes (discs). With no substrates on the discs, or with a dry substrate on the bottom disc, electric fields of several thousand volts/cm are applied to the discs. Only a very small current flows. But when the linen substrates are even slightly wetted with water, an enormous increase of three to four orders of magnitude is observed. Further, although the polarity of the wetted electrode (disc) has a minor effect, when both discs are wetted the current is larger than for either alone. A positive disc polarity works best, probably indicating that water ion species like $H^+(H_2O)_c$ are repelled away from a like-charged electrode in larger numbers than are negative

water ions. In these experiments, linen and other substrates saturated with water dried completely in a few minutes compared to an hour or more with no electric field applied. If a paddle of insulator material were passed between the discs with a current flowing, the current could be made to drop to the dry electrode value by blocking the entire area of the discs, or to some intermediate current depending on what fraction of the disc area was blocked. Thus the paddle was able to block completely the flow of charge carriers (water ions) from one disc electrode to the other.

We were concerned that the currents flowing from linen and other substrates might be artifacts due to corona discharges. For example, linen consists of fine fibres that, in a strong electric field, could stand on end to produce "points" from which large corona currents could flow. It did not seem likely that this would occur when the substrates were saturated with water (when the largest currents flowed), but to be certain we wetted other substrates with oil to seal any fibres to their surfaces. Figure 49 shows experimental data obtained when trials like those for water (Figure 48) were repeated for light oil, turpentine and water solutions of ethanol and acetone. It was found that all of these liquids produced large currents compared to dry electrode currents, but that water was most effective of all. The mechanism by which liquids other than water evaporate more rapidly in electric fields is not yet understood.

These experiments established that electrostatic drying could be employed with fabrics wetted with organic or inorganic liquids, and that greatly accelerated drying could be achieved compared to natural evaporation. Thus it should be possible to evaporatively decontaminate clothing wetted, for example, with nerve agent at greatly accelerated rates by using these techniques. It is also possible that decontamination of electrically-conductive surfaces could be achieved in this way. Further research is needed to explore these possibilities.

6.3 The Vapor Pressure of Water.

Asakawa²⁶ also observed that when a corona discharge occurred in a closed system containing water, the partial pressure of water vapor in the system increased significantly compared to the saturation vapor pressure of water at a given temperature. The author repeated Asakawa's experiments²⁴ and found, furthermore, that the vapor temperature did not increase upon application of corona discharge to the system; in fact, the vapor temperature often fell slightly. Thus, electrical heating was not the cause of the increase in vapor pressure. These results were also consistent with the observation that high-voltage electric fields increase the evaporation rate of liquid water (Figure 45). An increase in vapor pressure under corona conditions would certainly help to explain accelerated evaporation of water; the effect would be like that of raising the temperature to attain a higher saturation vapor pressure. In our experiments, water vapor partial pressure increased by as much as 74 percent, from 17.6 mm Hg to 30.6 mm Hg at 20°C, immediately upon application of 22 kV to an array of needle electrodes directly above the liquid water surface.

DeBoer³ has reminded us that water has a far lower vapor pressure than would be expected from classical theory for an ideal gas; one of the basic

tenets of this theory is that the molecular weight of an ideal substance is unchanging. From kinetic theory one can easily calculate how the vapor pressure of water should vary with its molecular weight. Thus, if especially under saturated conditions (100% RH, $s = 1$), extensive molecular clustering occurred in water vapor its effective molecular weight could considerably exceed 18. This would significantly reduce its saturation vapor pressure compared to that if it were a gas of single molecules. At the liquid water surface (liquid/vapor interface) that is so poorly understood, it indeed seems possible that water's effective molecular weight due to clustering might be much larger than 18 so as to explain its bizarre physical properties when compared to other substances.

The explanation of why the vapor pressure of water increases in the presence of corona discharges would then be straightforward. The corona would cause fragmentation of hydrogen bonds holding water clusters in the vapor together. The effective molecular weight of the vapor would fall precipitously toward 18 from a larger value in the previously-clustered vapor. This would cause an immediate increase in water vapor pressure, but without an increase in temperature. In fact, the vapor temperature could actually fall due to the fragmentation of the hydrogen bonds and absorption of latent heat of vaporization by the water species. Calculations show that, just at the onset of corona, electronvolts of energy are available for every neutral cluster even in water vapor, even if the vapor is almost completely clustered. Thus sufficient energy is available to dissociate many hydrogen bonds per cluster, leading to cluster dissociation throughout the vapor volume and to a sudden increase in vapor pressure, exactly as is observed.

7. DISCUSSION

This report has discussed many militarily-significant properties of atmospheric water vapor and its adsorbed surface layers. The physical nature of water both in its liquid and vapor phases has been examined, and several insights have been offered into the nature of the vapor interface with its liquid and with surfaces upon which molecular layers of water are adsorbed. The discussion serves to point out how little we really do know about this seemingly simple substance which comprises most of our bodies, and without which life on earth would be impossible. Its extensive hydrogen bonding causes it to behave more as a polymer than as a simple molecule under many diverse conditions; its effective molecular weight must be highly variable, although we cannot think of molecular weight here in the same sense that we do concerning chemically-bonded polymers and other substances. Water remains an enigma, the extent of which we are only recently beginning to perceive. Its molecules can almost be thought of as building blocks, readily able to hydrogen-bond to each other and to a hierarchy of other molecules, thus selectively engaging in such complex and fundamental interactions as those that build DNA and genetically code our life forms.

But for all its complexity, the manifestations of water in our environment are so commonplace that we assume we can easily deal with any problems they might cause us. Heating solves many problems because water's saturation vapor pressure and thus its relative humidity are so dependent

upon temperature. By using sufficient heat we can dry wet fabrics and eventually remove sticky adsorbed water layers from surfaces. But we are not so aware that by drying we are drastically altering the populations and size distributions of countless water clusters in water vapor or moist air, and that extensive molecular and ionic interactions occur during this seemingly simple act. In some applications, these interactions can have significant or even serious consequences. The mass of the water ion cluster of size ten, $H^+(H_2O)_{10}$, is 181. The mass of a molecule of agent GD is 182. Thus if we want to detect toxic GD vapor in moist atmospheric air using an ionization detector like CAM based on mass spectroscopic principles, the job becomes quite difficult in the presence of large populations of ion clusters of size ten. Figure 18 shows that the mean size of water ion cluster distributions at 23°C and 75% RH in clean air is about $c_{\mu} = 8$; if the RH were increased above 75% the mean cluster size would be closer to 10. But by heating the sampled air we can shift the cluster distribution far to the left, thus leaving few clusters of size ten in the sample while not affecting the GD molecules that are to be detected. Other C-agent molecules have other masses, corresponding to different sizes of water clusters. When we recall that other atmospheric gases such as nitrogen also can form complex water ions of many different masses, the problems of detecting specific toxic molecules in the air become still more apparent.

The IR and longer-wavelength transmission of the atmosphere is strongly affected by, and is often dictated by, the water vapor continuum absorption arising from huge populations of neutral water clusters in the vapor. Passive remote C-agent detectors, which depend upon natural IR radiation in the 7-13 μ m window region or in other spectral regions, are intended to give warning of toxic agents in the atmosphere at long ranges, so that protective measures can be taken. Operators assume that if they can see, e.g., a distance of ten kilometers, their remote sensors also will "see" at least this far. But this assumption is wrong under many conditions and, furthermore, the operator cannot be warned because infrared signals arriving at the detector are ambiguous. It is possible for toxic vapors to approach within a few hundred meters of the detector, without warning, while the operator assumes that because of clear visibility of the atmosphere that his warning radius is several kilometers.

The electrical activity of the atmosphere is greatly affected by, and is often dictated by, water vapor. High-voltage systems operating at higher humidities are troubled by water surface layers that cause electrical leakage and inefficient operation, if not actual damage to system components. Electronic circuitry is always at risk, especially in tropical climates. The ion content and electrical conductivity of moist air appear to be strongly affected by relative humidity, thus confounding problems of vapor decontamination by corona discharges, and even the filtration of fine particles that are usually trapped on filters by electrostatic forces in dry air.

Adsorbed water surface layers directly affect the adhesion of biological and radiological dusts to surfaces, and their subsequent decontamination, as functions of humidity which often exhibit hysteresis-like behavior. Drying of water and other liquids, probably including C-agents, is greatly accelerated in strong AC or DC electric fields.

Detectors using atmospheric sensors that depend upon surface effects are almost certain to be affected by adsorbed water layers that respond unpredictably to changes in humidity. Surface sensors are finding increased use in biological applications, and include optical sensors such as germanium probes used in infrared internal reflectance spectroscopy.

8. CONCLUSIONS AND RECOMMENDATIONS

The research results and discussion presented in this report lead to the conclusion that there are at least several areas for Primary Military Applications of present knowledge and new research results:

A. Point detectors based on ionization mass spectrometry principles, such as the Chemical Agent Monitor (CAM), in which large water ion clusters can "look" like C-agent molecules and thus confound detection.

B. Infrared remote sensors, particularly those utilizing passive radiation, whose warning range is strongly dependent upon the atmospheric water vapor continuum absorption with or without the operator's knowledge; many applications are probable as well in electromagnetic obscuration and countermeasures, generally.

C. Decontamination procedures and technologies, including:

(1) Surface adhesion vs. humidity and its effects on biological and radiological contamination and removal.

(2) Accelerated evaporation of contaminants on fabrics and other surfaces in large electric fields.

(3) Corona discharge:

(a) in vapor detoxification.

(b) in possible surface decontamination scenarios.

D. Surface effects and survivability:

(1) Humidity and electrical insulation.

(2) Hysteresis behavior of adsorbed water layers vs. humidity.

(3) Electrostatic modification of surfaces, e.g. in filtration of fine particulates.

(4) Production of ions directly from adsorbed surface water layers in electric fields.

These applications areas can be evaluated to determine how, and to what extent, present knowledge can be directly applied, and in which areas new research studies are required if significant payoffs are to be anticipated in CBR defense. As a minimum, the following problems are Recommended for Study:

A. A brief research study is needed to review all mass spectral data obtained during the CAM development; this will be a cooperative effort between research and development personnel. Its purposes will be (1) to

gather and analyze all available data on ion mass spectra, particularly water ion mass spectra, as functions of humidity, temperature and other parameters; (2) to understand what improvements were incorporated in CAM during development to improve its specificity for C-agent molecules in the presence of water ion clusters and other ions; (3) to update our knowledge so as to determine whether further improvements are possible in present or future-generation ionization detectors.

B. A brief research study is needed to review to state of development of remote infrared C-agent detection systems as regards their real vs. perceived operation in the presence of water vapor continuum absorption due to clusters in the atmosphere. The author, developing remote IR sensors more than 20 years ago, investigated atmospheric propagation problems that led to our present knowledge of molecular structure in water vapor; yet this knowledge has never been applied to the military systems from which it was acquired. The purposes of the study will be (1) to gather and analyze typical data from developmental remote IR systems under a variety of atmospheric conditions; (2) to coordinate research results with field operational observations and problems, if any; (3) to suggest ways to improve future systems and/or the unambiguity of their detection and warning capabilities.

C. A brief research study is needed to collate and analyze available data on molecular layer thicknesses on surfaces for water and other substances as functions of temperature and humidity. Its purposes will be (1) to study adhesive forces holding contamination on surfaces and their hysteresis-like behavior; (2) to optimize decontamination procedures, e.g., for biological and radiological dusts on surfaces vs. relative humidity.

D. A substantial research study is needed to investigate high-voltage effects on the accelerated evaporation and detoxification of liquids on surfaces and in airstreams. Its purposes will be (1) to study the feasibility of accelerated evaporative decontamination of clothing and other absorbent material in large electric fields; (2) to reconsider application of corona discharges to airstreams and to surfaces for decontamination in light of the role of adsorbed water surface layers, and water ions in moist air, on the efficiencies of such systems; (3) to measure water surface layer thicknesses on surfaces in high-voltage fields as functions of relative humidity and temperature, by using electrical conductivity techniques.

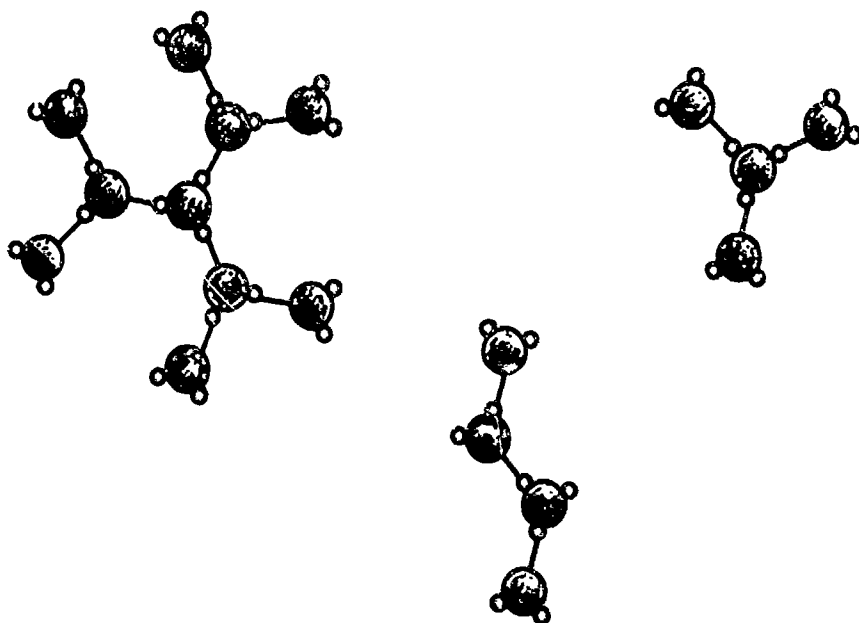
E. A substantial research effort is needed, preferably under ILIR funding, to complete important research on the structure of atmospheric water vapor using electrical measurements. Specific questions to be investigated will include: (1) the mechanism accounting for greatly enhanced rates of evaporation of water and other liquids from cloth and other substrates in large electric fields; (2) verification that the ion content and electrical conductivity of atmospheric moist air are strongly dependent upon relative humidity; (3) whether water ions are produced directly from adsorbed molecular layers of water on surfaces between which electric potentials exist; (4) why the vapor pressure of water is increased greatly in the presence of corona discharges, and the molecular mechanisms that are involved; (5) what can be learned from these studies concerning the precise nature of water and its vapor/liquid interface (the liquid surface).

LITERATURE CITED

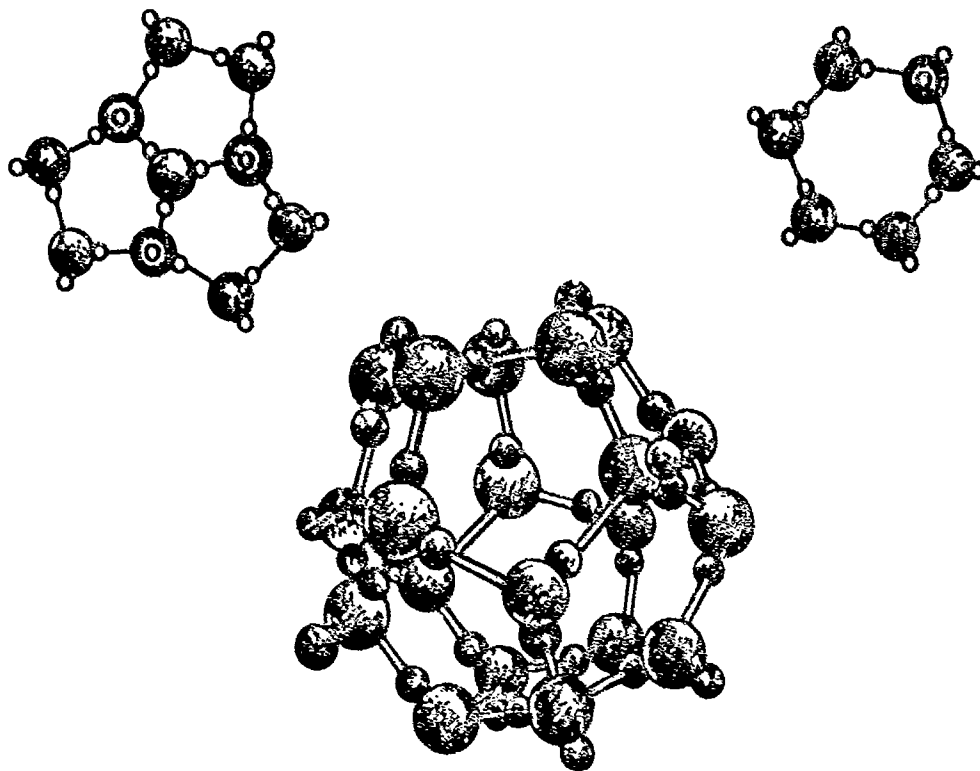
1. Frank, H.S., in Franks, F., ed., Water: A Comprehensive Treatise, Vol. 1, Plenum Press, New York, NY, 1972; pp. 515-543.
2. Luck, W.A.P., in Franks, F., ed., Water: A Comprehensive Treatise, Vol. 1, Plenum Press, New York, NY, 1972; pp. 209 ff.
3. deBoer, J.H., The Dynamical Character of Adsorption, Oxford Press, Clarendon, England, 1953, pp. 16 ff.
4. Abraham, F.F., Homogeneous Nucleation Theory, Academic Press, New York, NY, 1974.
5. Wilson, C.T.R., Philos. Trans. 189, 265 ff (1897).
6. Wilson, C.T.R., Philos. Trans. 192, 403 ff (1899).
7. Wilson, J.G., Principles of Cloud Chamber Technique, Cambridge University Press, England, 1951, pp. 1-29.
8. Croxton, C.A., Statistical Mechanics of the Liquid Surface, Wiley Interscience, New York, NY, 1980, pp. xi, 198-218.
9. Bignell, K.J., Quart. J. Roy. Meteorol. Soc. 96, 390-402 (1970).
10. Varanasi, P., Chou, S., and Penner, S.S., J. Quant. Spectrosc. Radiat. Transfer 8, 1537-1541 (1968).
11. Gimmetstad, G.G., and Gebbie, H.A., J. Atmos. Terres. Phys. 38, 525 ff (1976).
12. Wolynes, P.G., and Roberts, R.E., Appl. Opt. 17, 1484 (1978).
13. Carlon, H.R., Infrared Phys. 19, 49-64 (1979).
14. Carlon, H.R., J. Atmos. Sci. 36, 832-837 (1979).
15. Emery, R.J., Zavody, A.M., and Gebbie, H.A., J. Atmos. Terres. Phys. 42, 801 ff (1980).
16. Gebbie, H.A., Nature 296, 422-424 (1 April 1982).
17. Vernon, M.F., Krajnovich, D.J., Kwok, H.S., Lisy, J.M., Shen, Y.R., and Lee, Y.T., J. Chem. Phys. 77(1), 47 ff (1982).
18. Mark, T.D., and Castleman, A.W. Jr., Experimental Studies on Cluster Ions, Advances in Atomic and Molecular Physics, Vol. 20, Academic Press, New York, NY, 1985, pp. 65-172.
19. Carlon, H.R., J. Phys. D: Appl. Phys. 17, 1221-1228 (1984).

20. Israel, H., Atmospheric Electricity (Israel Program for Scientific Translations), Jerusalem, 1971, Vol. 1.
21. Carlon, H.R., and Harden, C.S., Appl. Opt. 19, 1776-1786 (1980).
22. Carlon, H.R., Infrared Phys. 22, 43-49 (1982).
23. Carlon, H.R., On the Ion Content of Moist Atmospheric Air and the Molecular Structure of Water Vapor Thus Inferred, CRDEC-TR-88088, U.S. Army Chemical Research, Development and Engineering Center, Aberdeen Proving Ground, MD 21010-5423, April 1988, UNCLASSIFIED report.
24. Carlon, H.R., U.S. Secretary of the Army Science and Engineering Fellowship, performed at the University of Manchester Institute of Science and Technology (UMIST), Manchester, England, UK, May 1986 to May 1987; research studies on atmospheric electricity and molecular structure in water vapor and moist air.
25. Chalmers, J.A., Atmospheric Electricity, Pergamon Press, London, 1967, pp. 86-88.
26. Asakawa, Y., Behavior of Fluids Under Electric Fields, in Wada, Y., Perlman, M.M. and Kokado, H., eds., Charge Storage, Charge Transport and Electrostatics With Their Applications, Elsevier Press, 1972, pp. 89-92.

EXAMPLES OF WATER CLUSTERS



OPEN STRUCTURE



CLOSED STRUCTURE

SOURCE: L.E. STODDARD, J.L. KASSNER

Figure 1. Examples of Water Clusters

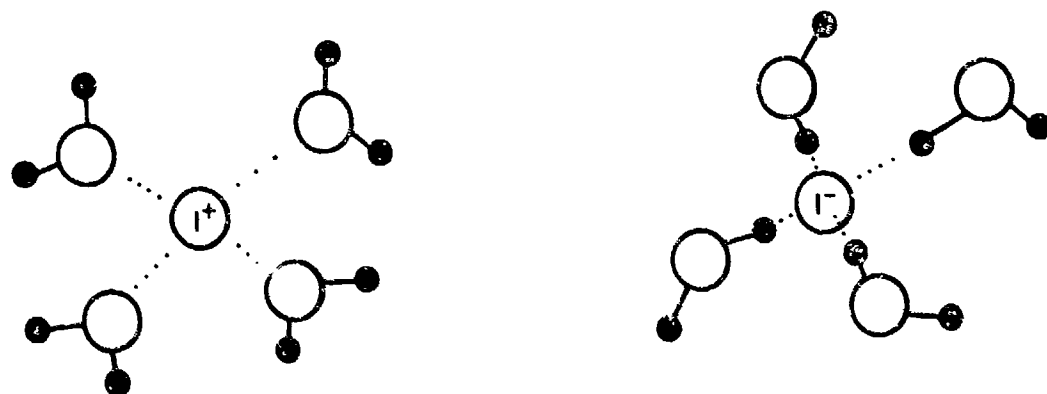


Figure 2. Water Molecules (Monomers) Clustering About Ions.

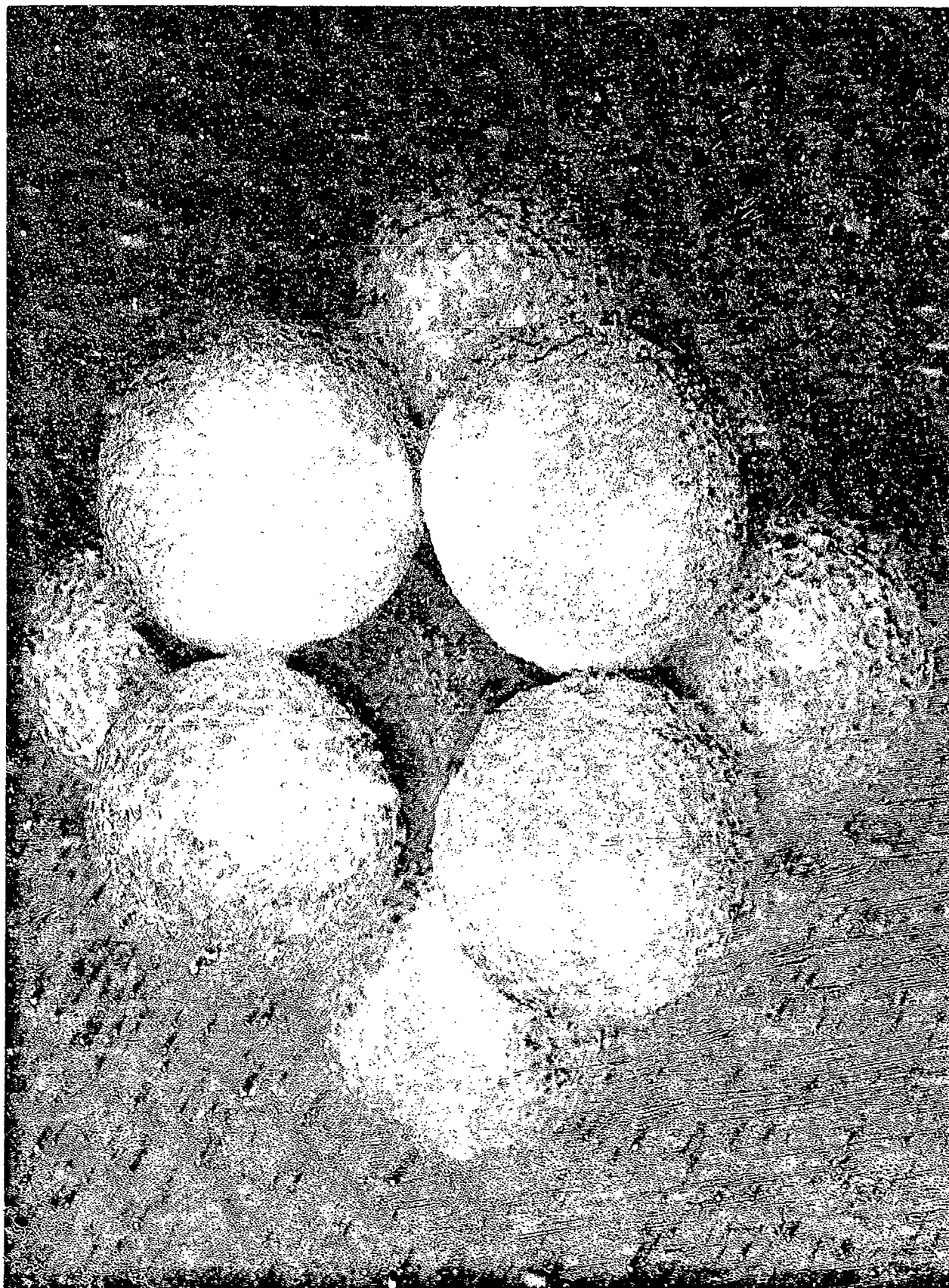


Figure 3. Model of a Water Ion (Center) "Swarmed" by Water Monomers.

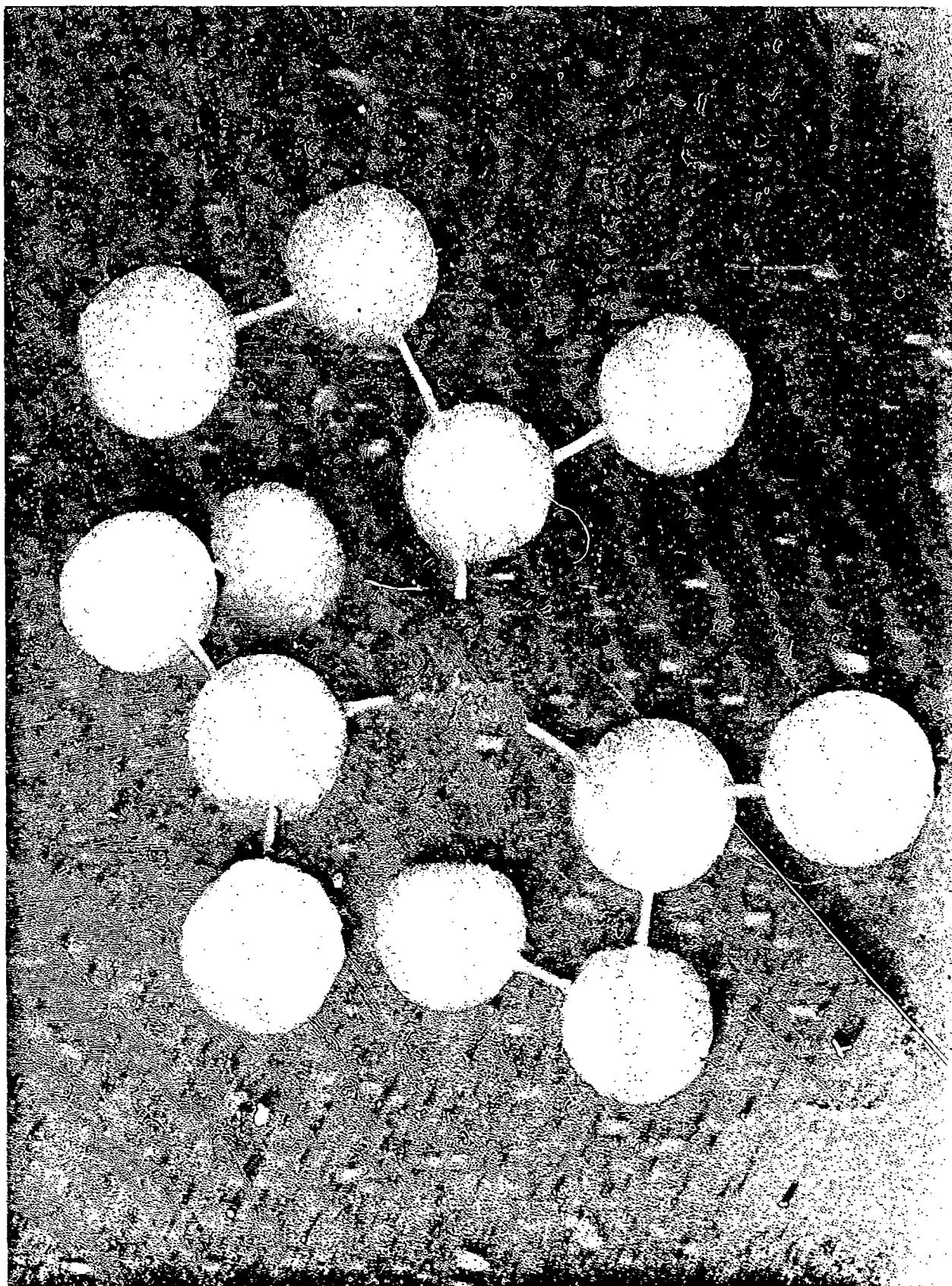


Figure 4. An Open-Chain Water Cluster of "Size" $c = 13$, e.g., $H^+(H_2O)_c$.

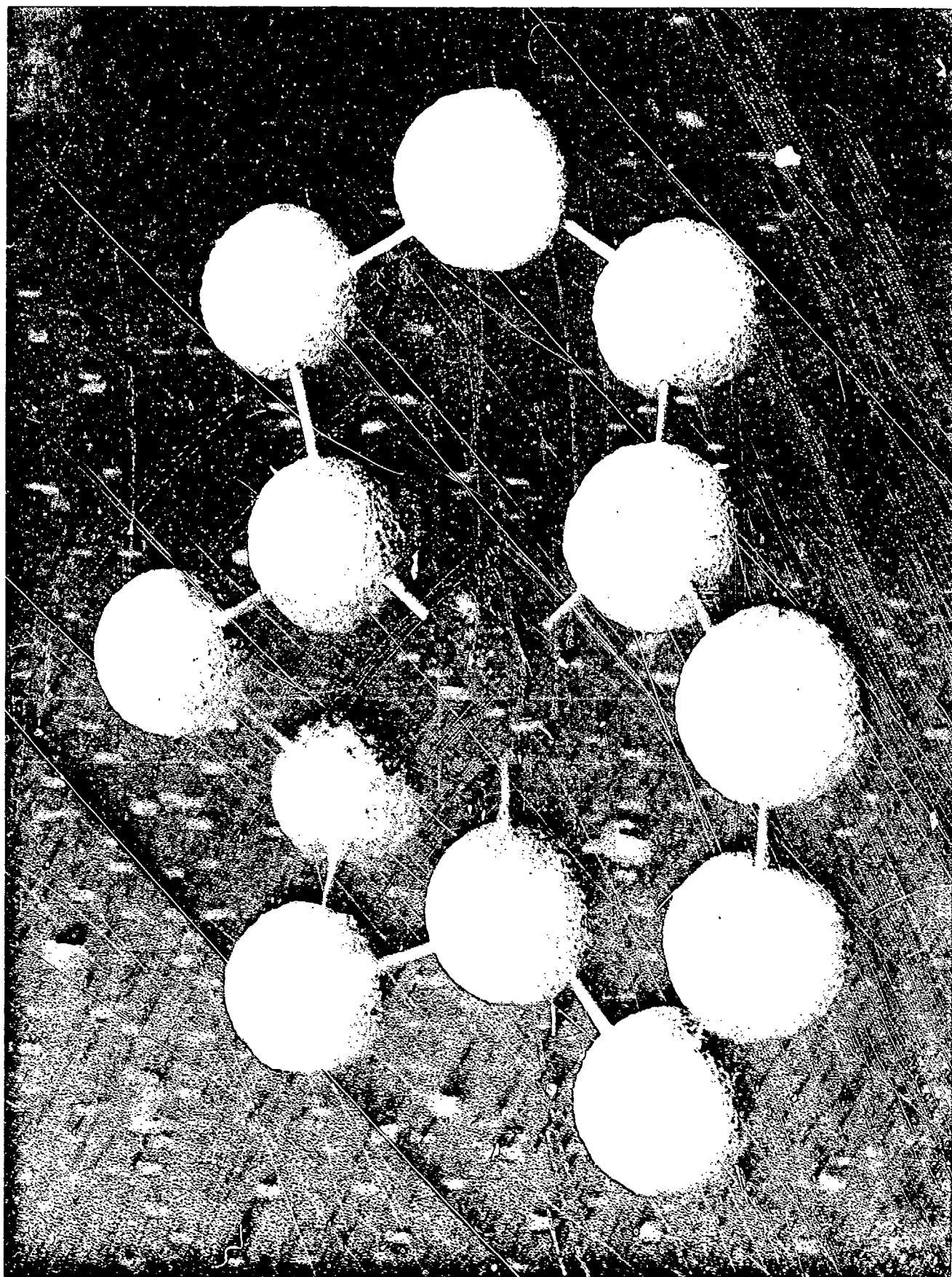


Figure 5. A Closed-Chain Water Cluster of Size 13.

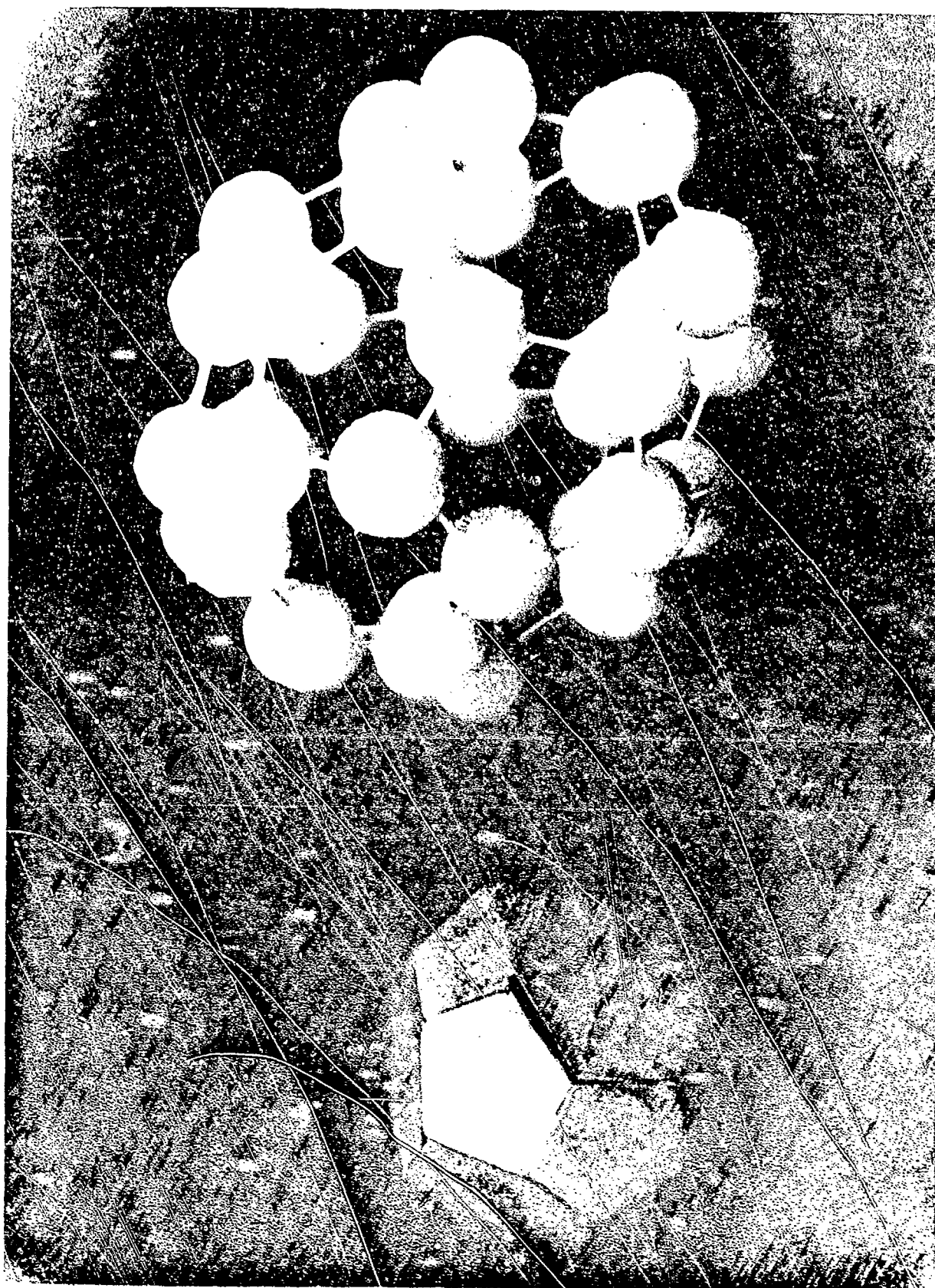


Figure 6. Models of a Closed-Structure, Clathrate-Like Large Water Cluster, With Monomers at the Apexes and Hydrogen Bonds Represented by the Edges.

DROPLET OR CLUSTER EQUILIBRIUM EQUATION

$$\frac{R\theta\delta}{M} \ln \frac{p}{p_0} = \left(\frac{2T}{a} + \frac{dT}{da} \right) + f(H) - \left(\frac{1}{\epsilon_1} - \frac{1}{\epsilon_2} \right) \frac{q^2}{8\pi a^4}$$

WHERE:

R = GAS CONSTANT, 8.314×10^7 ERGS/ $^{\circ}$ K-MOLE

θ = ABSOLUTE TEMPERATURE, $^{\circ}$ K.

δ = DENSITY OF THE DROPLET, G/CM³

M = MOLECULAR WEIGHT, G/MOLE.

p/p_0 = EQUILIBRIUM SATURATION OR SUPERSATURATION RATIO

T = SURFACE TENSION, DYNES/CM

a = DROPLET RADIUS IN CM

ϵ_1, ϵ_2 = DIELECTRIC CONSTANTS OF VAPOR AND CONDENSED LIQUID

q = ELECTRONIC CHARGE, 4.813×10^{-10} STATCOULOMB

$f(H)$ = A FUNCTION RELATING THE EFFECT OF HYDROGEN BONDS IN WATER CLUSTERS TO CLUSTER RADIUS OR SIZE. THIS TERM HAS ALWAYS BEEN IGNORED, AS J. G. WILSON STATES:

".... (THE EQUATION ABOVE)'....' IS CLEARLY INCOMPLETE WHEN, AS FOR WATER, STRONGLY POLAR MOLECULES FORM AN ORIENTED SURFACE LAYER. NO DETAILED TREATMENT OF THIS MODIFICATION HAS BEEN MADE."

- PRINCIPLES OF CLOUD CHAMBER TECHNIQUE, CAMBRIDGE (1951)

Figure 7. The Thomson/Kelvin Equation, With Explanation.

WATER CLUSTER AND DROPLET EQUILIBRIA

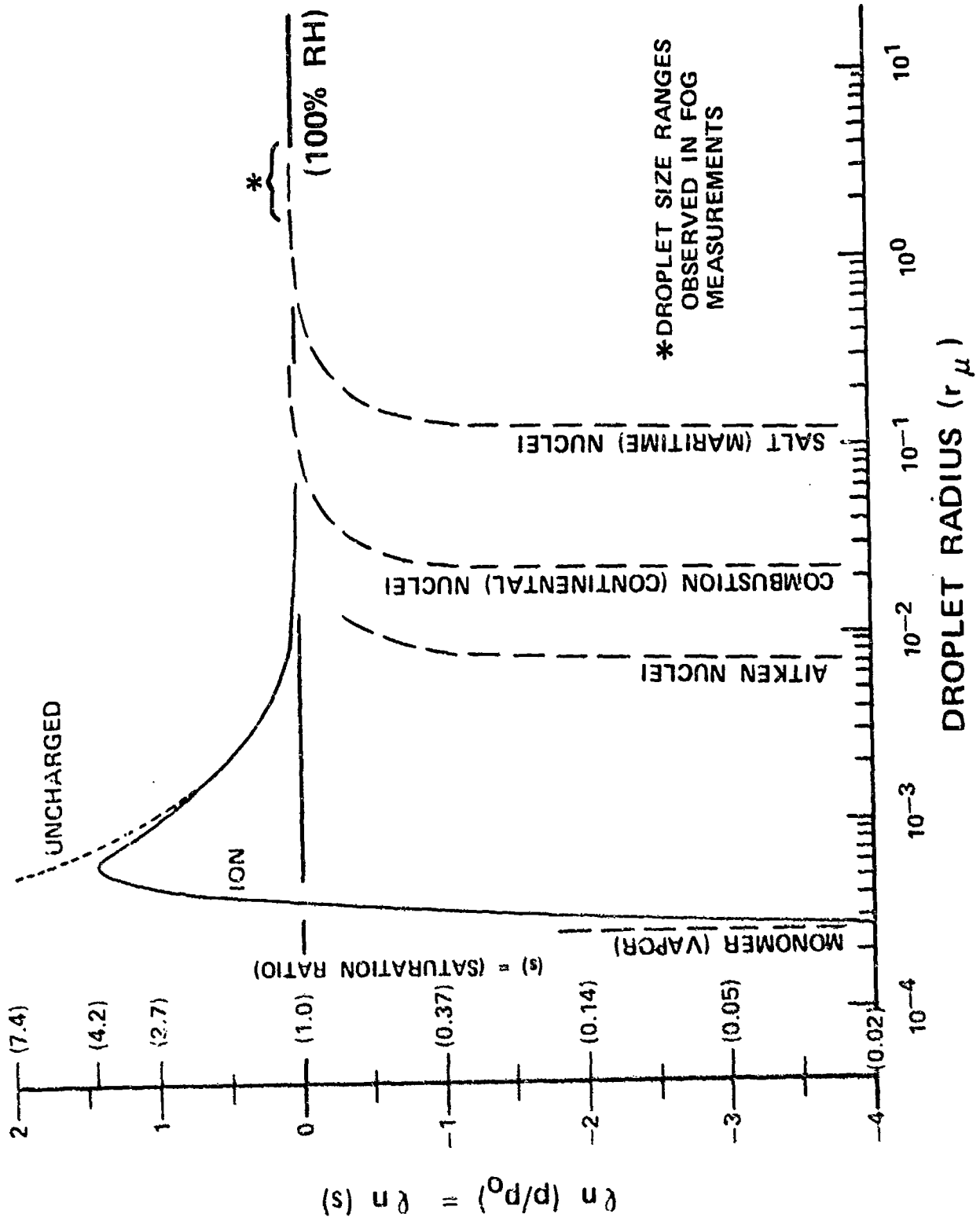


Figure 8. Water Cluster and Droplet Equilibrium Curves.

C.T.R. WILSON

ON THE NEUTRAL NUCLEI (WATER CLUSTERS) ACCOUNTING FOR "CLOUD-LIKE" CONDENSATION.

"... IT IS DIFFICULT TO ACCOUNT FOR THE IMMENSE NUMBER OF THESE NUCLEI, OTHERWISE THAN ON THE VIEW THAT THEY ACTUALLY ARE SIMPLY SMALL AGGREGATES OF WATER MOLECULES, SUCH AS MAY COME INTO EXISTENCE MOMENTARILY THROUGH ENCOUNTERS OF THE MOLECULES. ON THIS VIEW THE DIMENSIONS OF THE MOLECULES CANNOT BE SMALL COMPARED WITH 6×10^{-8} CENTIM.' . . ."

PHILOS. TRANS. (LONDON) V. 189, 265 (1897)

Figure 9. C.T.R. Wilson's Reasoning That the Known (Correct) Water Molecule Radius Was Too Small by a Factor of Three.

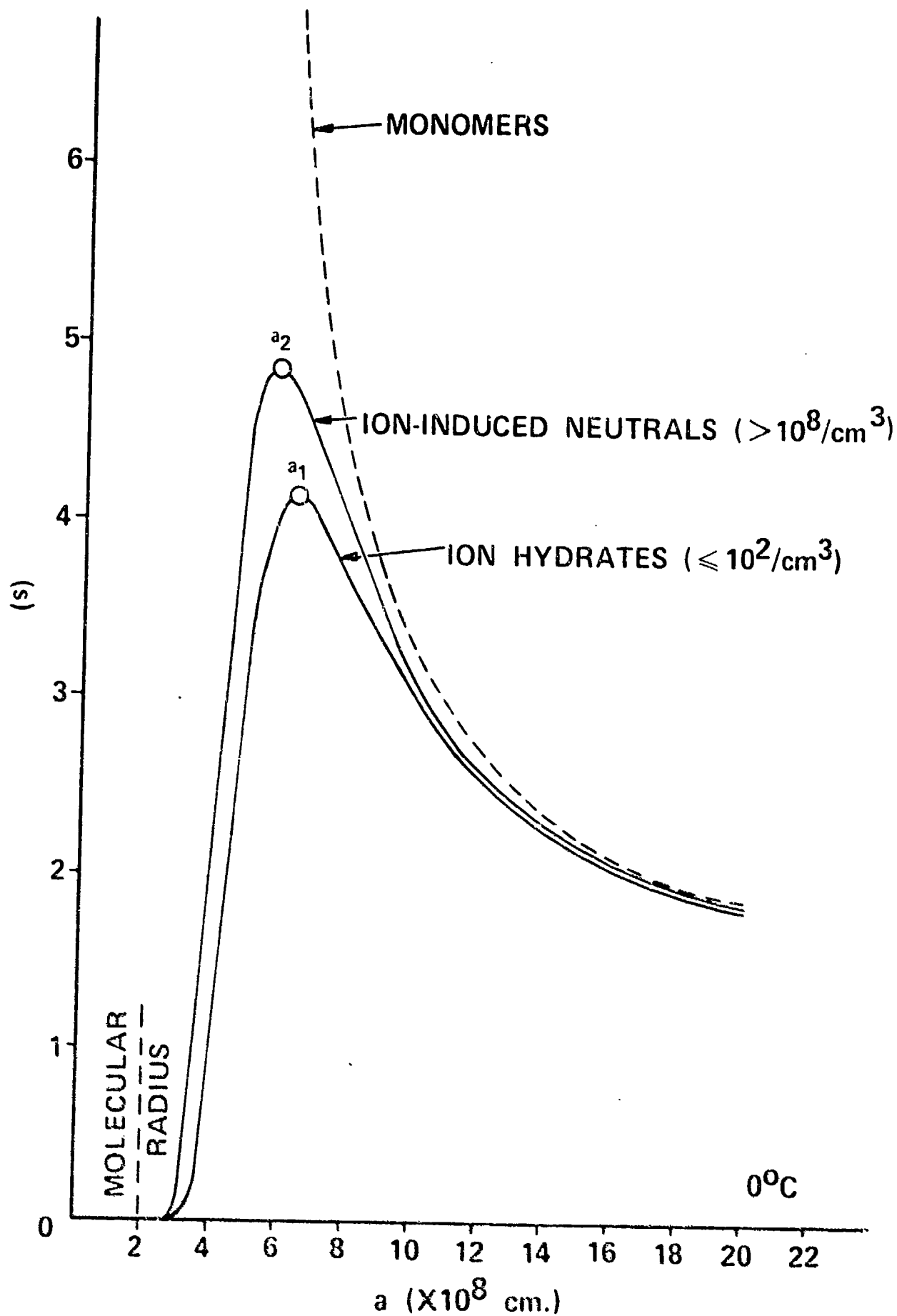
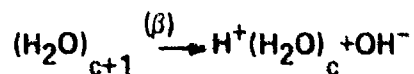


Figure 10. Cluster Equilibrium Curves Deduced by Including Hydrogen Bonding Effects in the Thomson/Kelvin Equation.

BASIC PREMISES

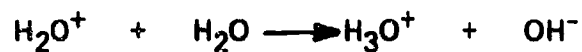
1. WATER VAPOR IN CONTACT WITH LIQUID WATER CONTAINS ELECTRICALLY-NEUTRAL WATER CLUSTERS THAT ARE PRODUCED BY EVAPORATION. TRUE EQUILIBRIUM EXISTS AT SATURATION.
2. THE CLUSTER POPULATIONS EXIST IN PEAKED STATISTICAL SIZE DISTRIBUTIONS WHERE THE NUMBER OF MONOMERS PER CLUSTER RANGES FROM TWO TO ABOUT 45 AND THE MEAN SIZE IS STATISTICALLY SIGNIFICANT. THE DISTRIBUTIONS AND POPULATIONS SHIFT WITH HUMIDITY AND TEMPERATURE, AND CAUSE CORRESPONDING CHANGES IN ELECTROMAGNETIC ABSORPTION SPECTRA OF THE VAPOR.
3. THE NEUTRAL CLUSTER POPULATIONS DISSOCIATE TO A SMALL EXTENT UNDER NATURAL RADIATION BY REACTIONS LIKE:



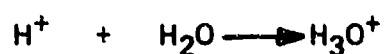
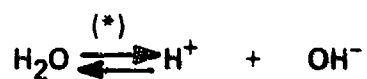
TO YIELD IONS THAT CAN BE MEASURED BY MASS SPECTROMETRY OR ELECTRICAL CONDUCTIVITY. THE YIELD CAN BE INCREASED BY USING SOFT RADIATION (LIKE β).

Figure 11. Basic Premises if Water Clusters Are Assumed to Form by Evaporation of Liquid Water or Droplets.

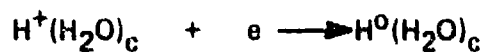
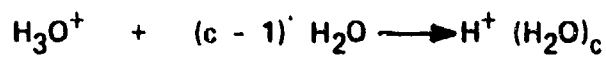
EXAMPLES OF CLUSTER-FORMING MECHANISMS:



OR:



FOLLOWED BY:



(*) = ENERGY SUPPLIED

Figure 12. Examples of Ion Mechanisms Leading to Ion-Induced, Neutral Cluster Formation in Water Vapor.

EXAMPLES OF CLUSTER-FORMING MECHANISMS

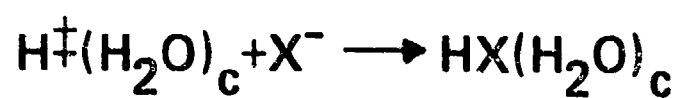
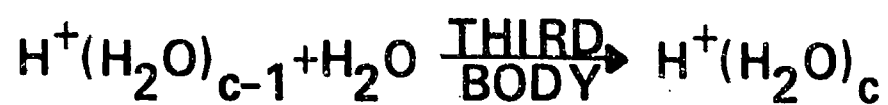
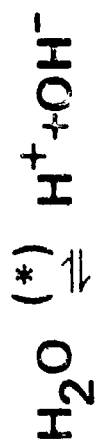


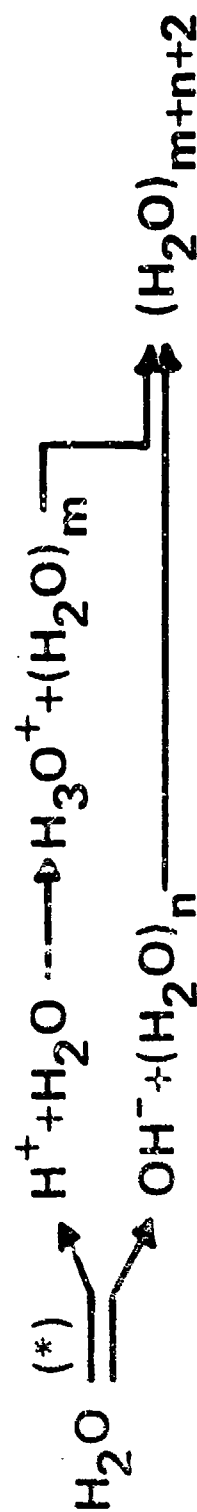
Figure 13. Further Example of Ion-Induced, Neutral Cluster Formation.

EXAMPLES OF CLUSTER-FORMING MECHANISMS



(*) = ENERGY ADDED

OR, POSSIBLY:



(NEUTRALS)

Figure 14. Other Examples of Cluster-Forming Mechanisms.

CONCEPTUALIZATION OF WATER CLUSTER EQUILIBRIA

Note: Species are shown in groups to aid conceptualization, rather than homogeneously spaced as in a true vapor

Factors affecting:
 — cluster population
 --- cluster size

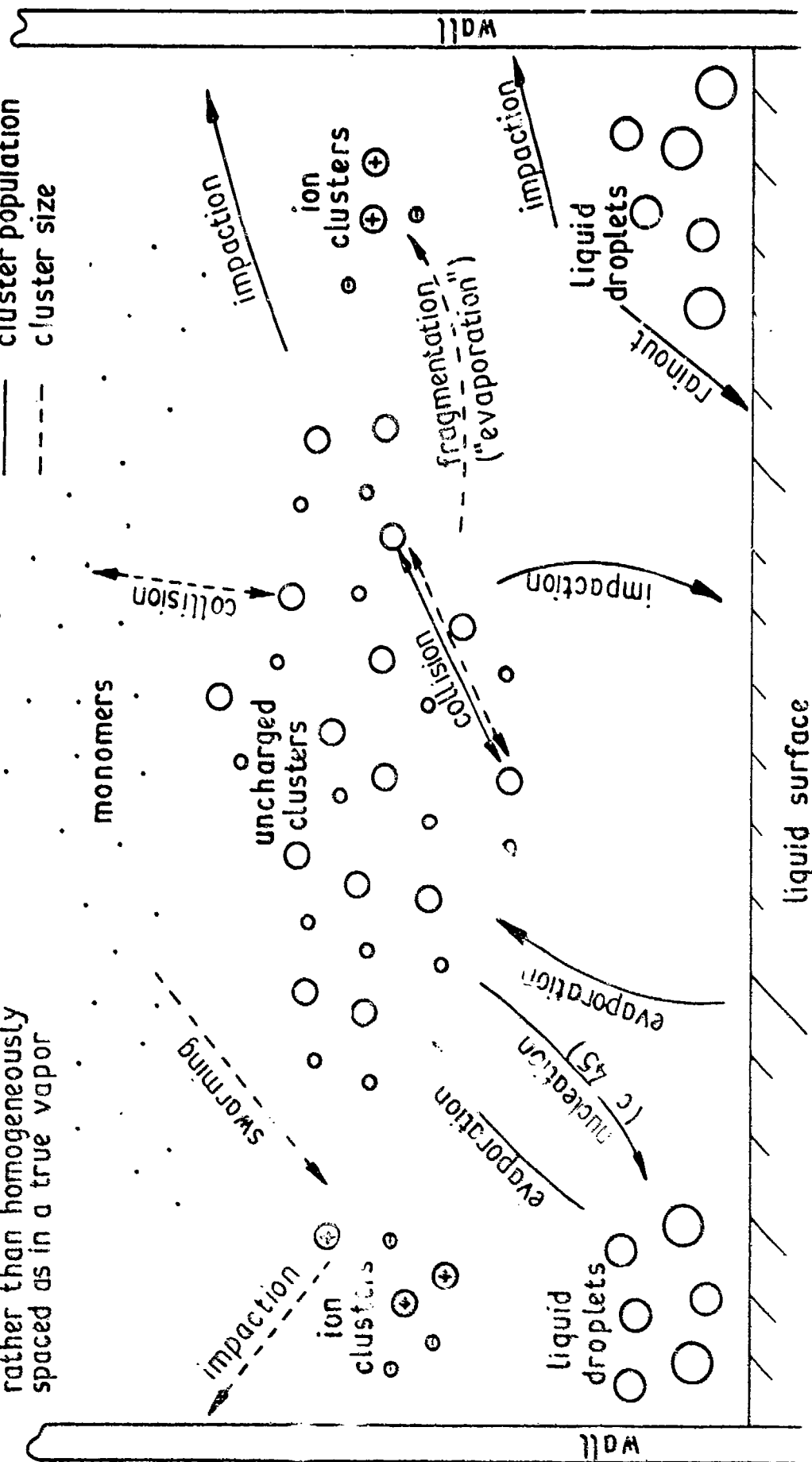


Figure 15. Conceptualization of Water Cluster Equilibria in Water Vapor.

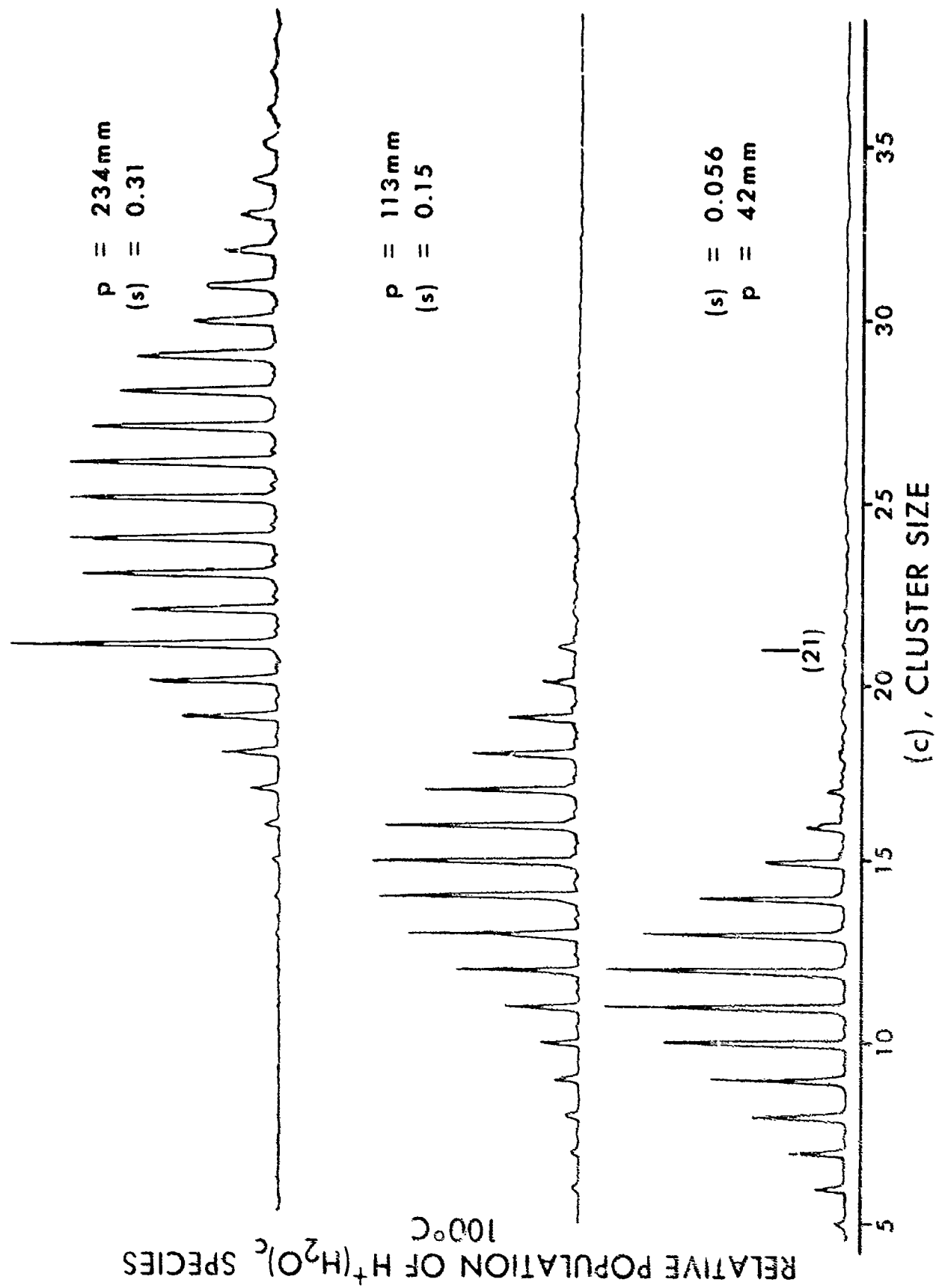


Figure 16. Ion Mass Spectra at 100°C for Several Saturation Ratios.

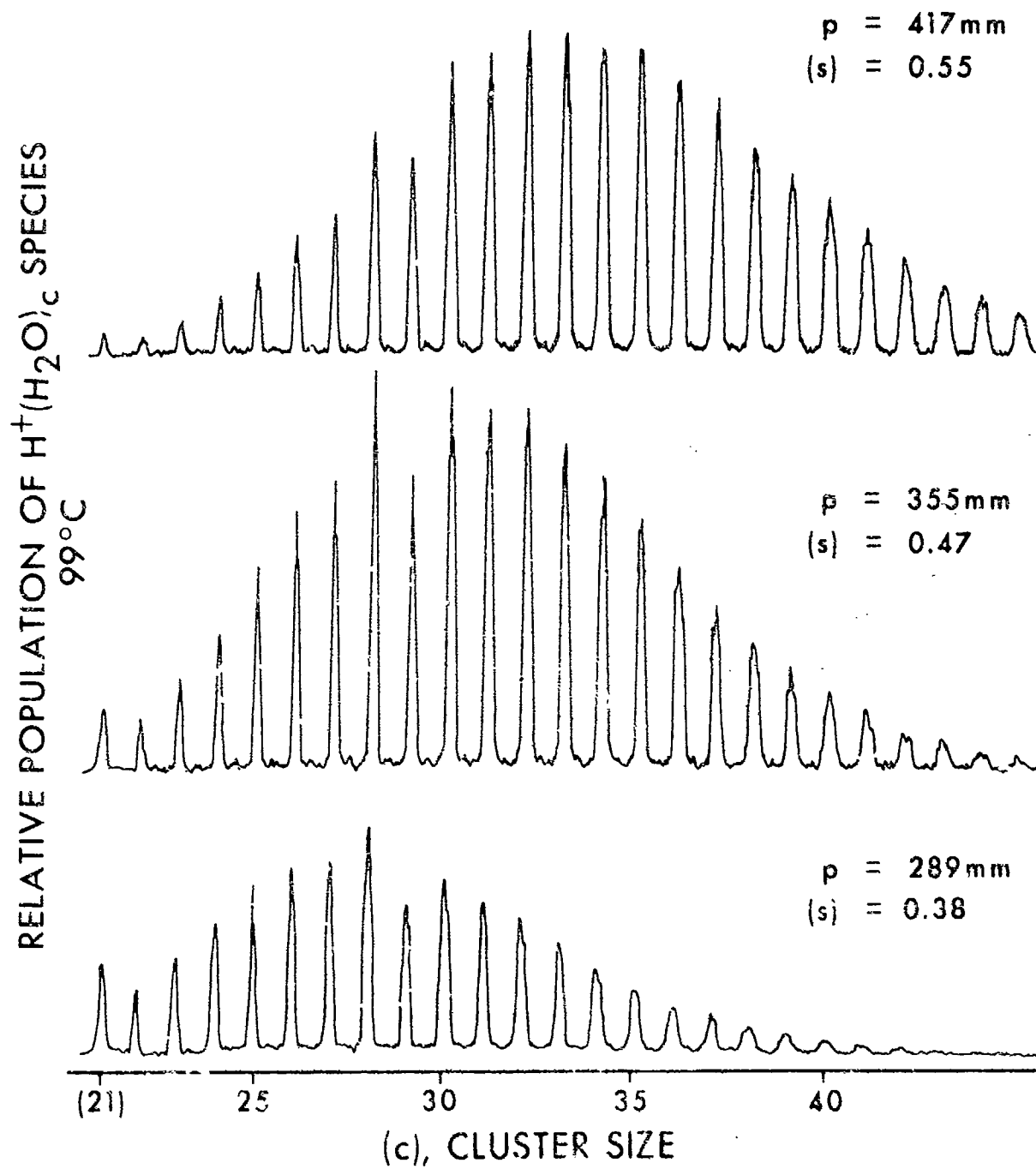


Figure 17. Ion Mass Spectra at 99°C for Several Saturation Ratios.

SPECTRUM OF 'CLEAN AIR' SHOWING REACTANT IONS $H^+ (H_2O)_c$

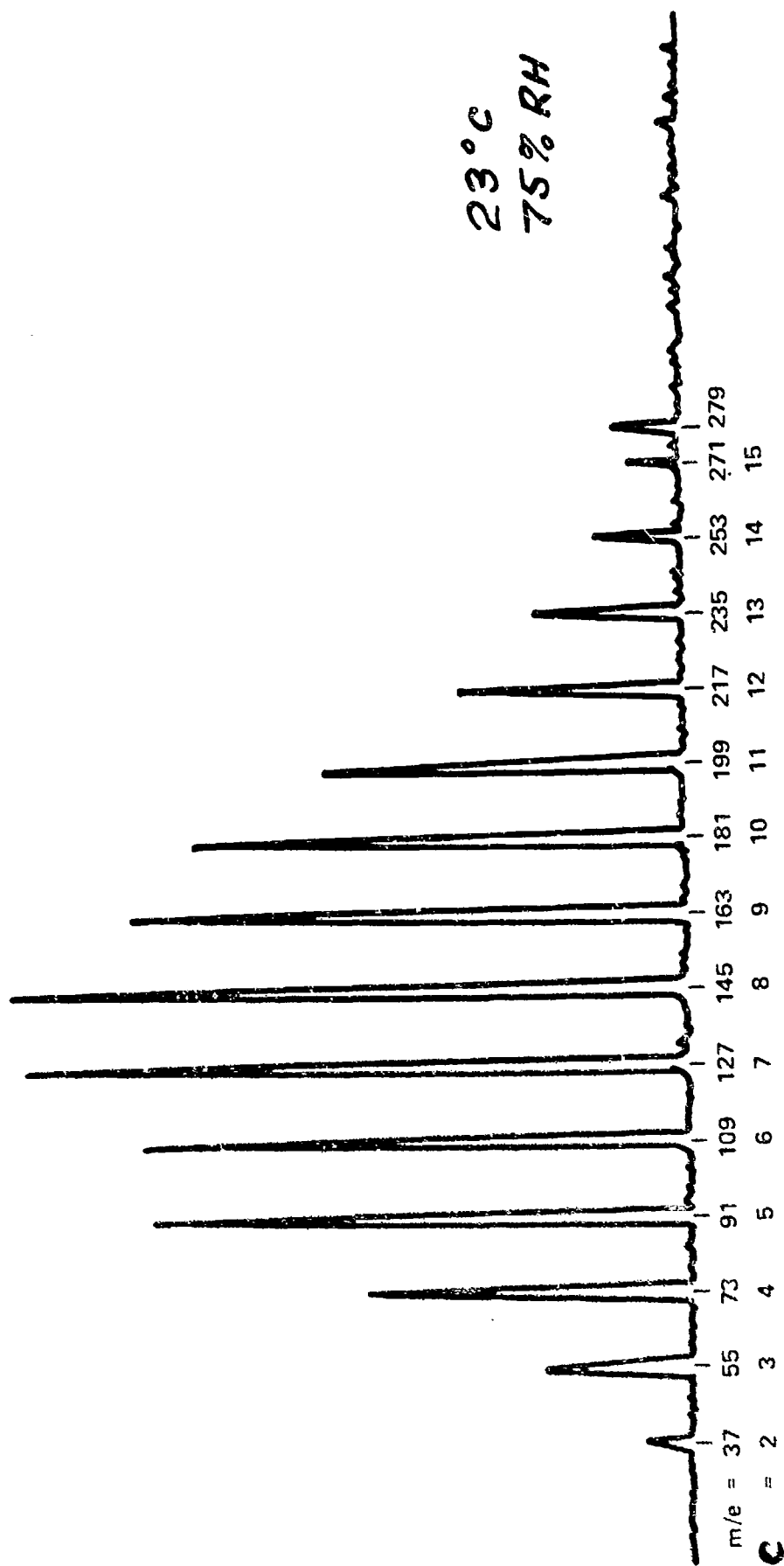


Figure 18. Ion Mass Spectrum of "Clean Air" at 23°C and 75% RH.

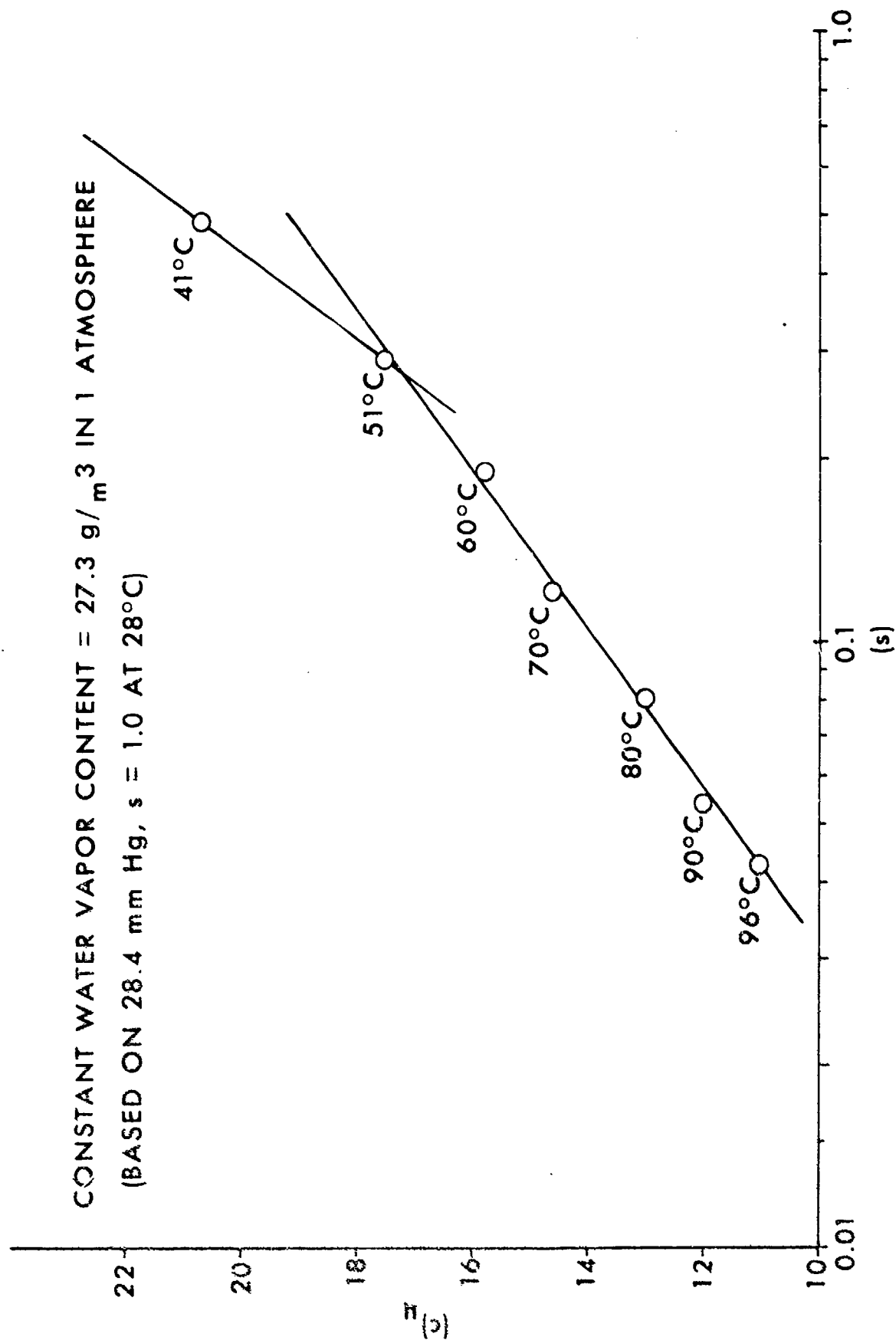


Figure 19. Effect of Heating Water Vapor Sample at Constant Partial Pressure from Saturation ($s = 1.0$) at 28°C to $s = 0.042$ at 96°C ; Corresponding Mean Size of the Cluster Distribution Falls from $\mu = .6$ to $\mu = 11$.

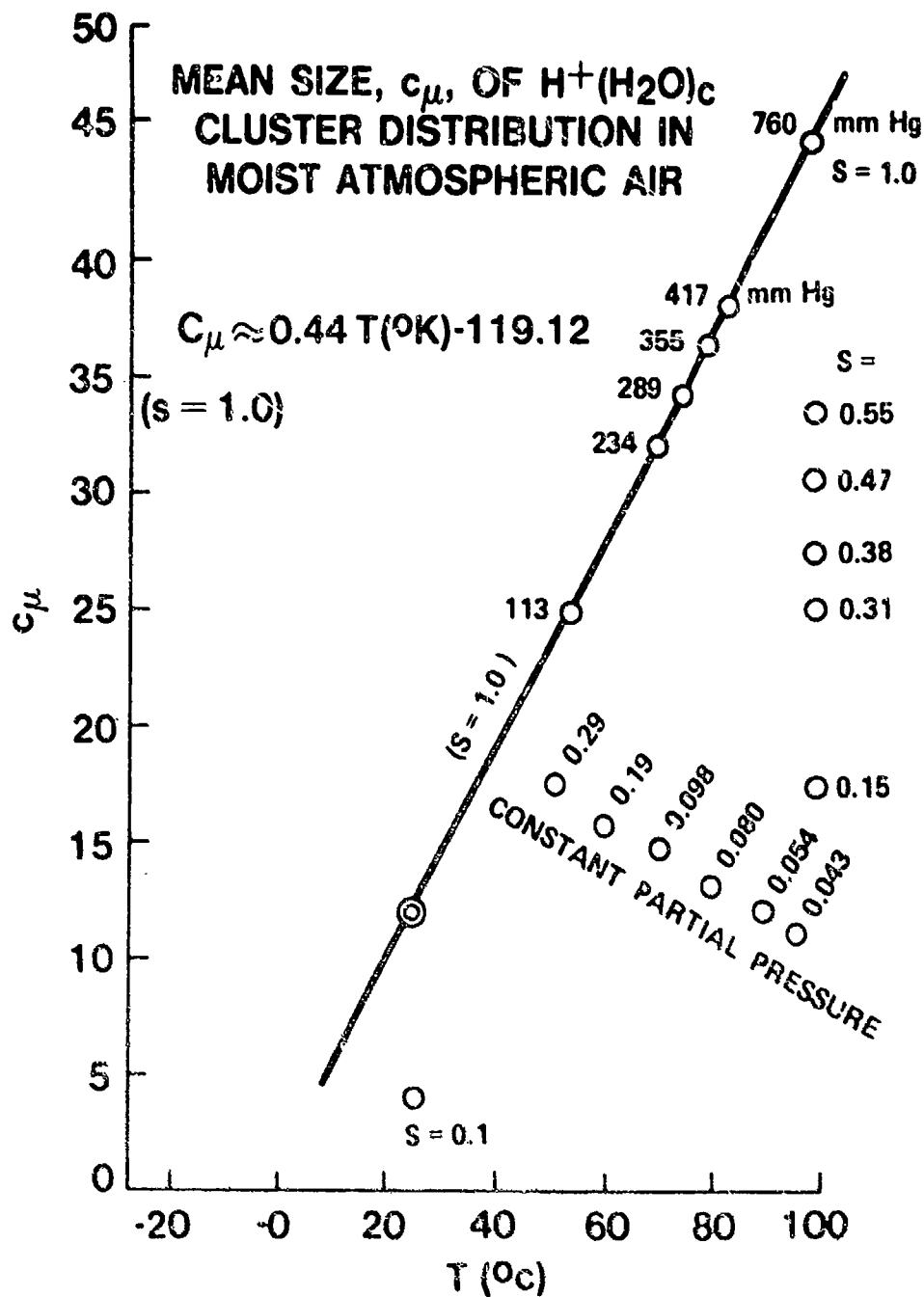


Figure 20. Mean Cluster Size, c_μ , of Water Ion Clusters $H^+(H_2O)_c$ in Moist Atmospheric Air, Based on Available Data Points Shown.

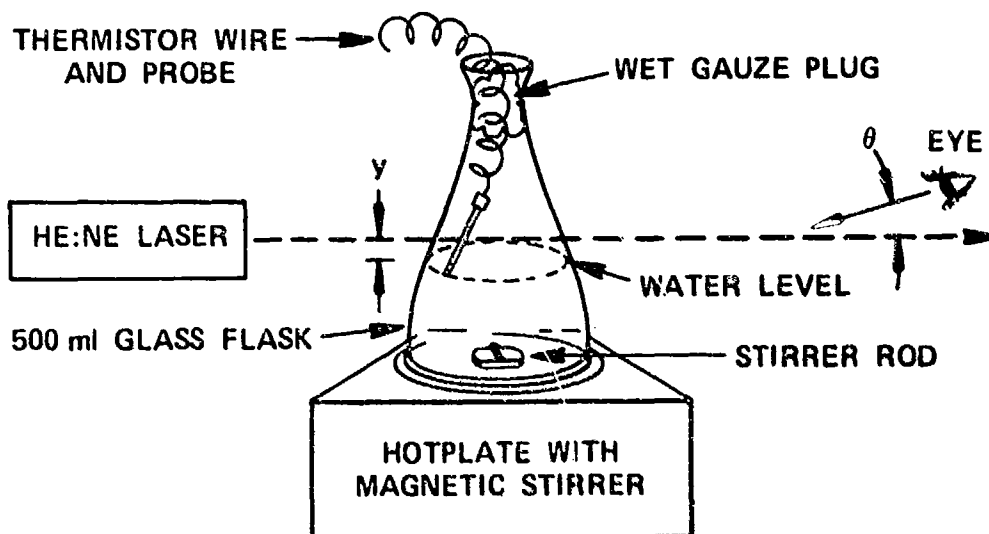


Figure 21. Droplet Nucleation Experiment in Which Nucleation Rate is Estimated by Light Scattered from He:Ne Laser Beam in Perfectly Clear Saturated Atmospheric Air, as a Function of Temperature (Ref. 19).

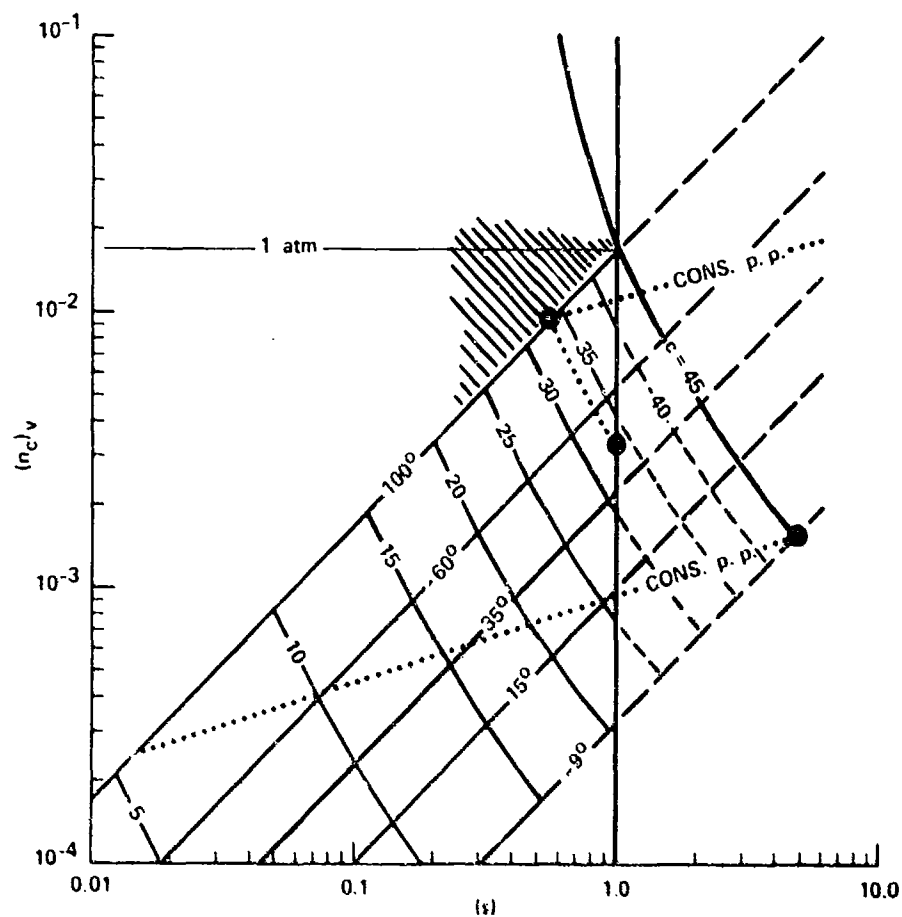


Figure 22. Schematic Diagram Showing How a Single "Critical" Water Cluster Size of $c = 45$ Can Account for All Droplet Nucleation in Water Vapor Over a Wide Range of Temperature and Saturation Ratio (See Text).

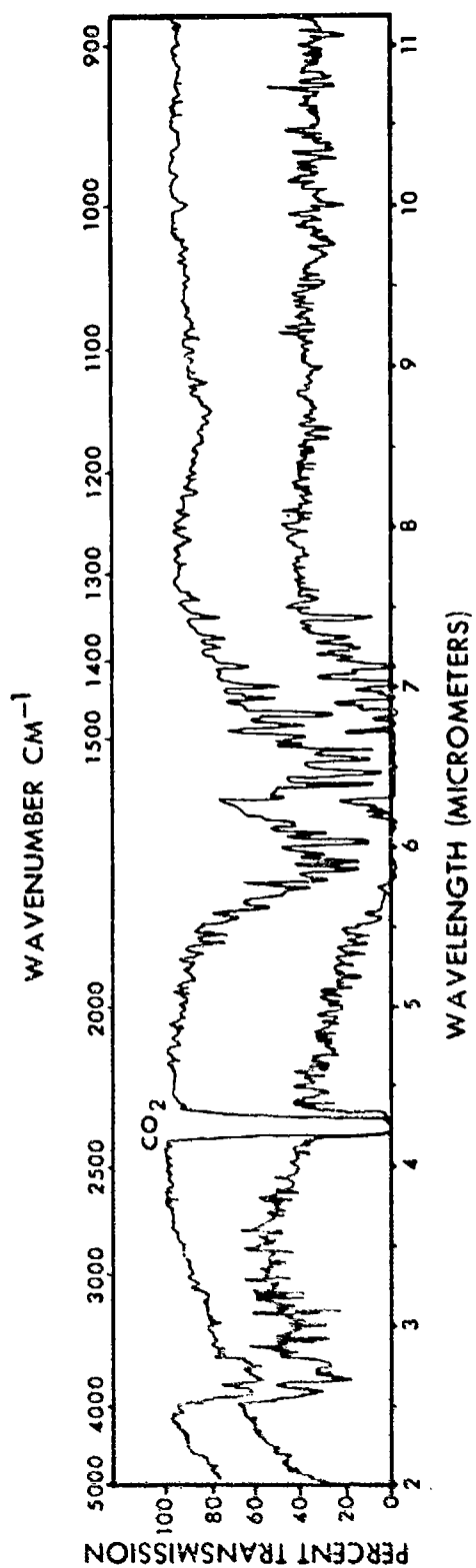


Figure 23. Infrared (IR) Transmission Spectrum of the Atmosphere for Two Different Optical Path Lengths.

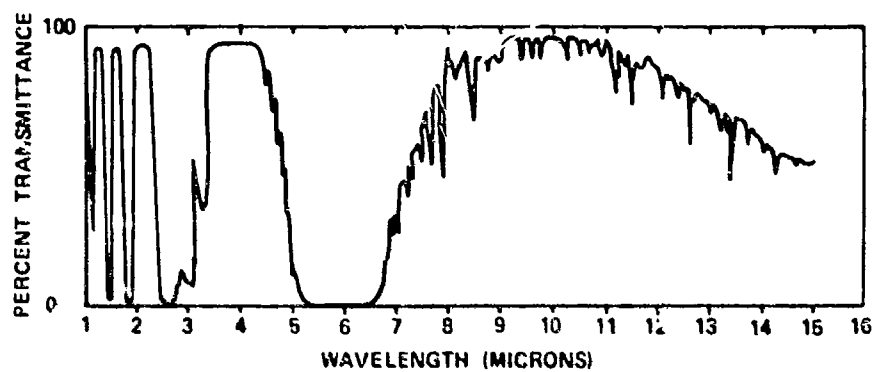


Figure 24. Infrared (IR) Transmission Spectrum of Water Vapor.

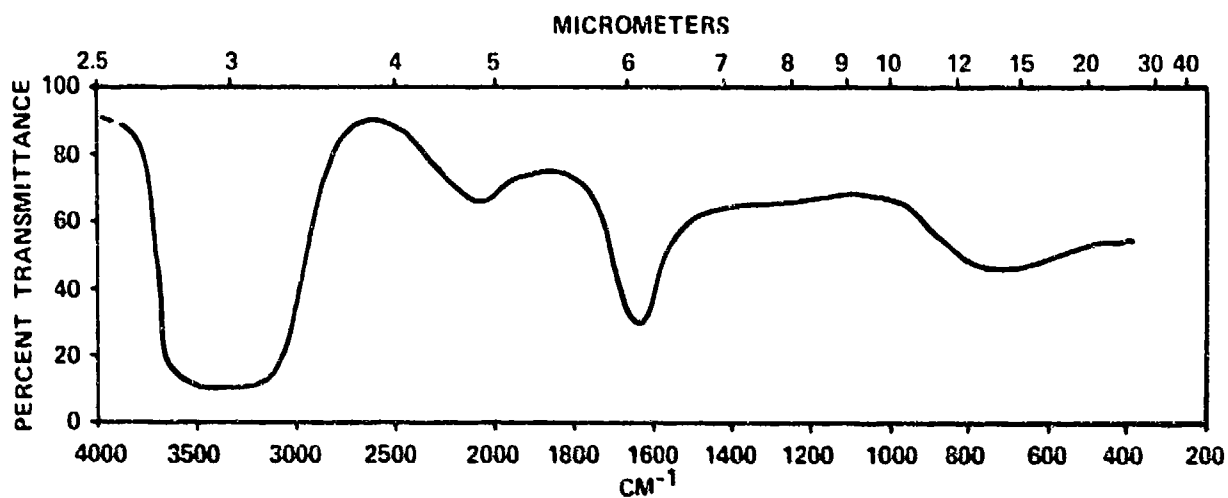


Figure 25. Infrared (IR) Transmission Spectrum of Water Film 10µm Thick.

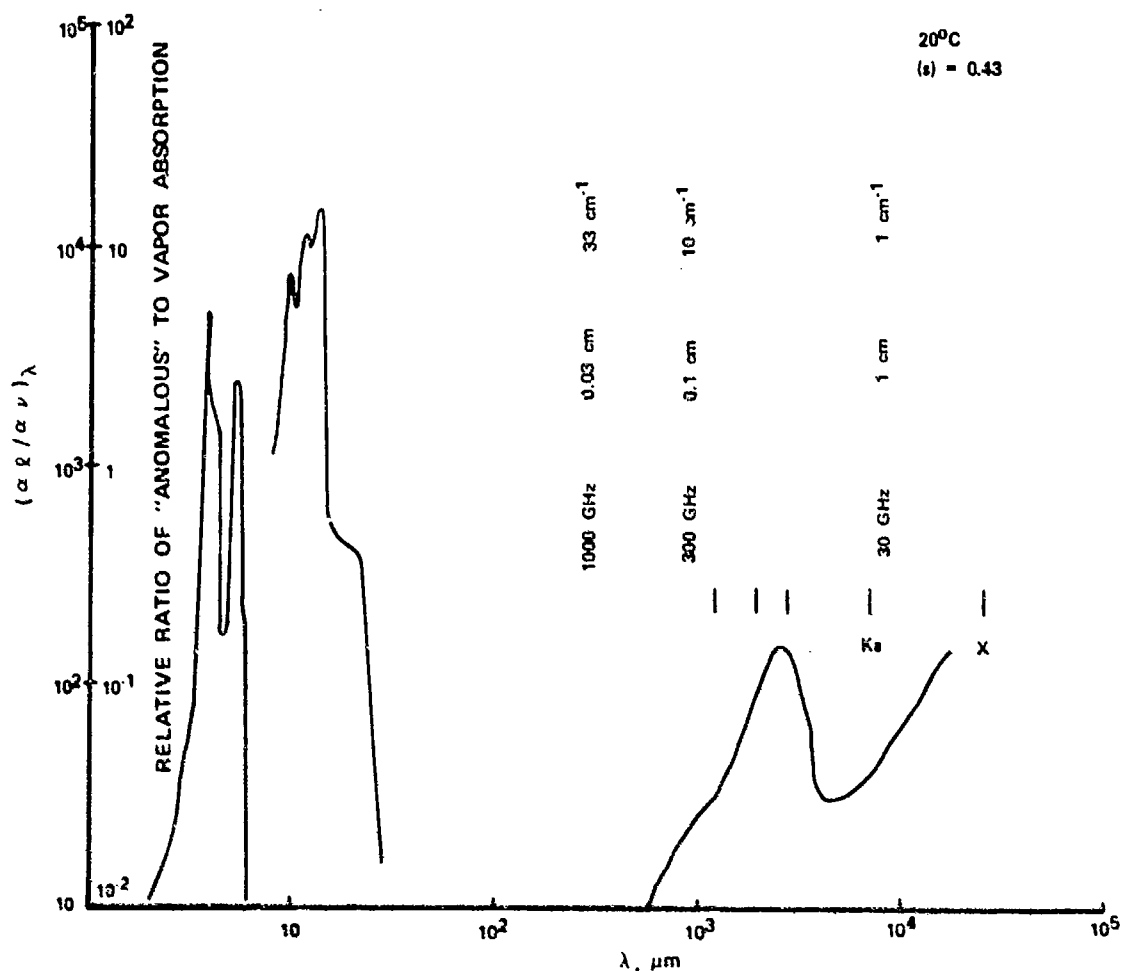


Figure 26. Ratio of Liquid Water to Vapor Absorption Coefficients vs. Wavelength from Infrared to Centimeter-Wavelengths; also Shown on Ordinate is Ratio of "Anomalous" or Continuum Absorption, Due to Water Clusters, to Absorption of All Water Monomers, Based on 10^{-3} Fraction of Cluster in Vapor at 20°C and $s = 0.43$ (43% RH); Ratios Are Much Larger for Very Humid Conditions, Especially if Droplets Are Present in the Vapor.

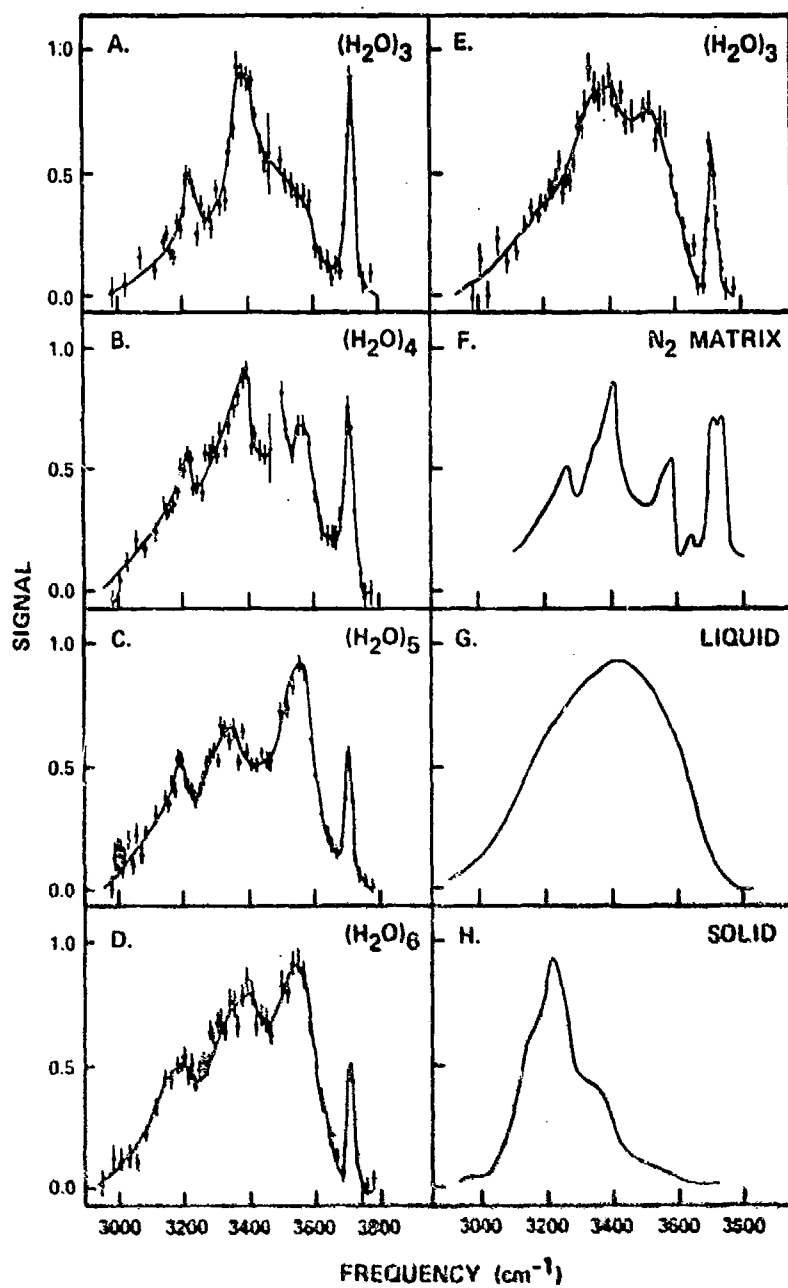


Figure 27. Infrared (IR) Spectra of Individual Neutral Water Clusters, by Size (Ref. 17); as Cluster Size Increases from $c = 3$ to 6, Cluster Spectra Increasingly Resemble the Liquid Water Spectrum Shown at G.



Figure 28. Experimental Set-Up for Simultaneous Measurement of IR Absorption and Ion Content (Electrical Conductivity) of Moist Atmospheric Air; Long-Path Optical Cell ("White cell") is Shown Connected by Hoses for Air Recirculation to Cabinet Containing Vapor Electrical Conductivity Cells.

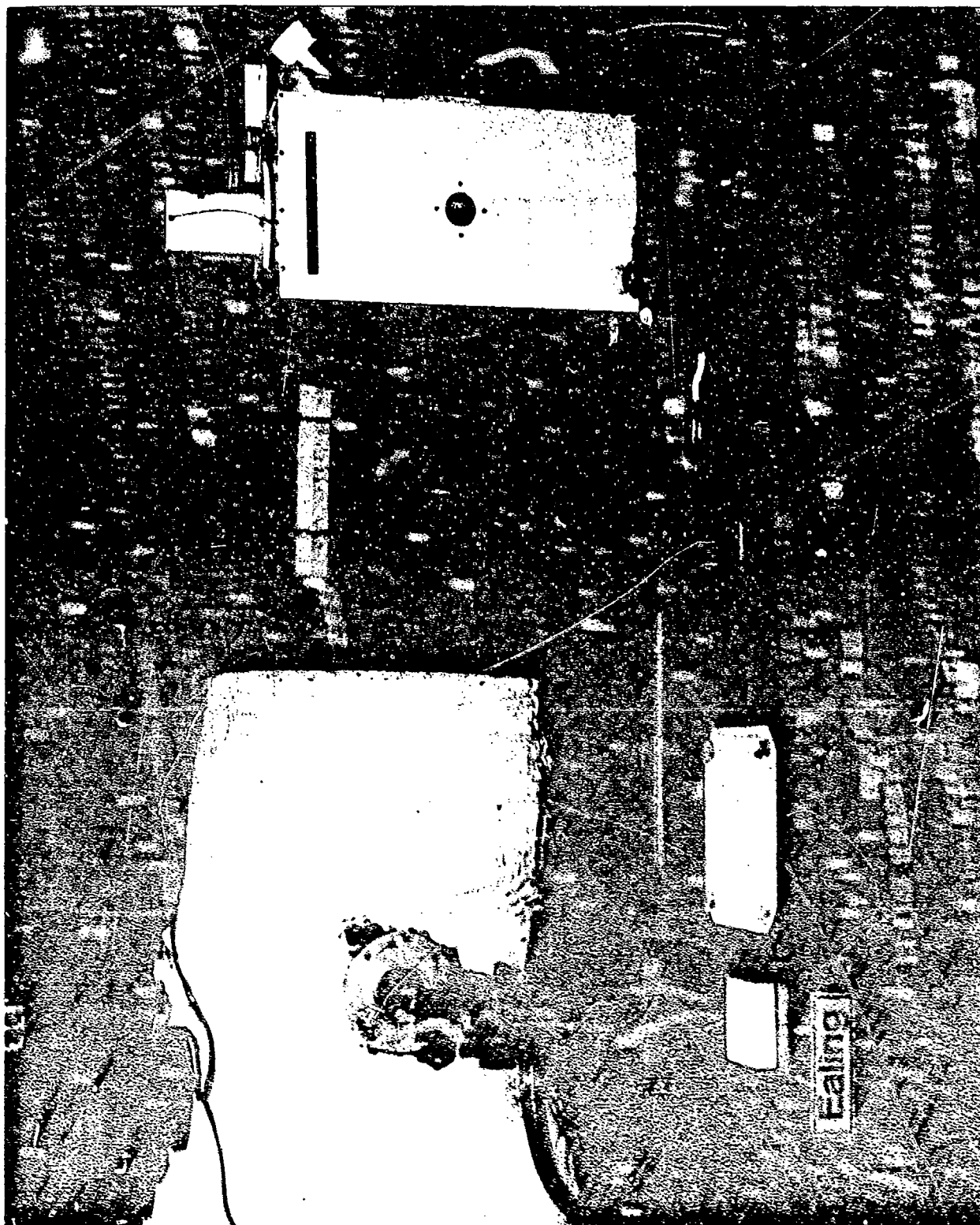
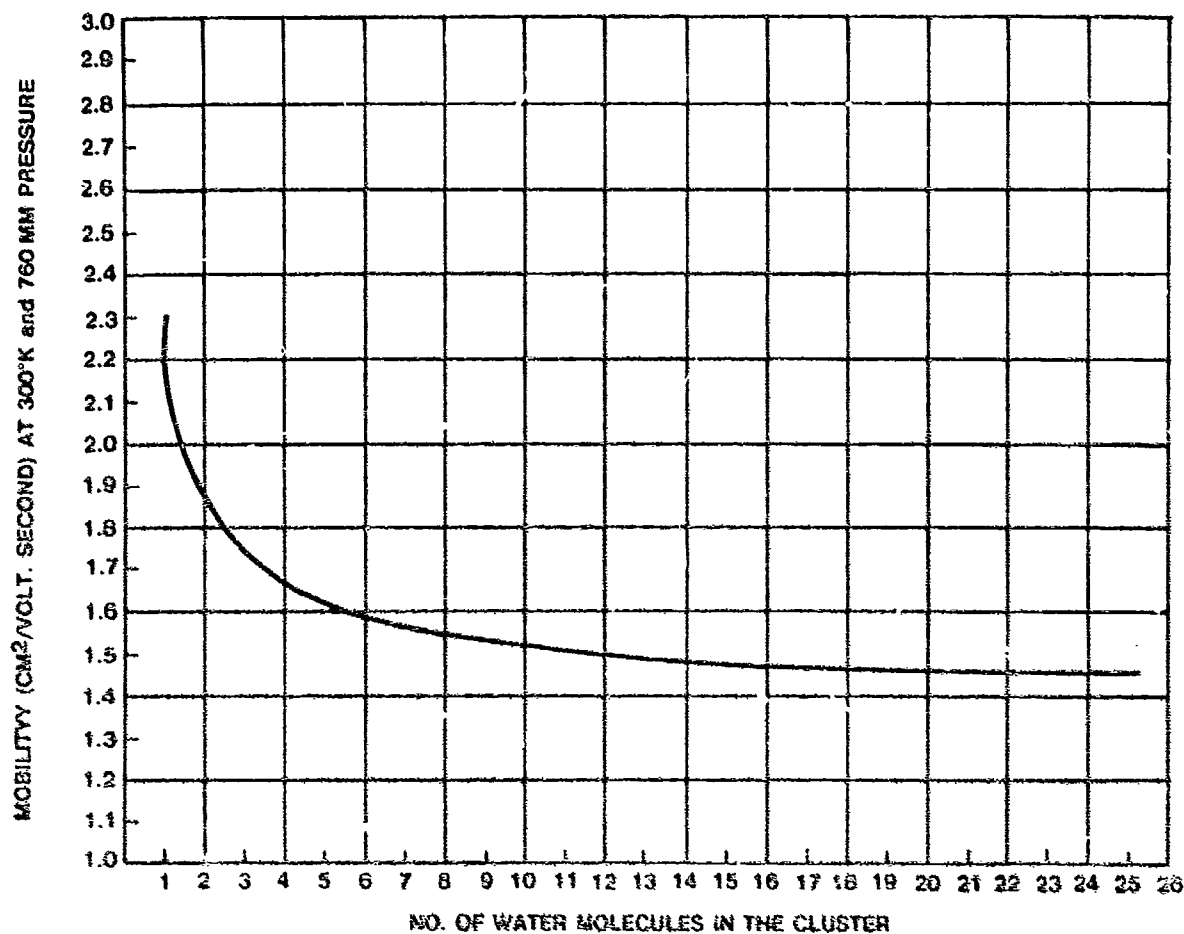


Figure 29. Close-Up of White cell, Showing Precision Optical Bench and IR Radiometer.



CALCULATED MOBILITIES OF WATER CLUSTER IONS IN NITROGEN FOR
DIFFERENT NUMBERS OF WATER MOLECULES IN THE CLUSTER.

GA 0029-01

Figure 30. Mobility of Singly-Charged Water Ions vs. Size, for Atmospheric Conditions.



Figure 31. An Early Pair of Vapor Electrical Conductivity Cells, Identical in Plate Spacing, Number (40), and Insulator Configuration; They Differ Only in Plate Area Thus Allowing Air Conductivity to Be Discerned Regardless of Any Leakage Currents Across the Insulators.

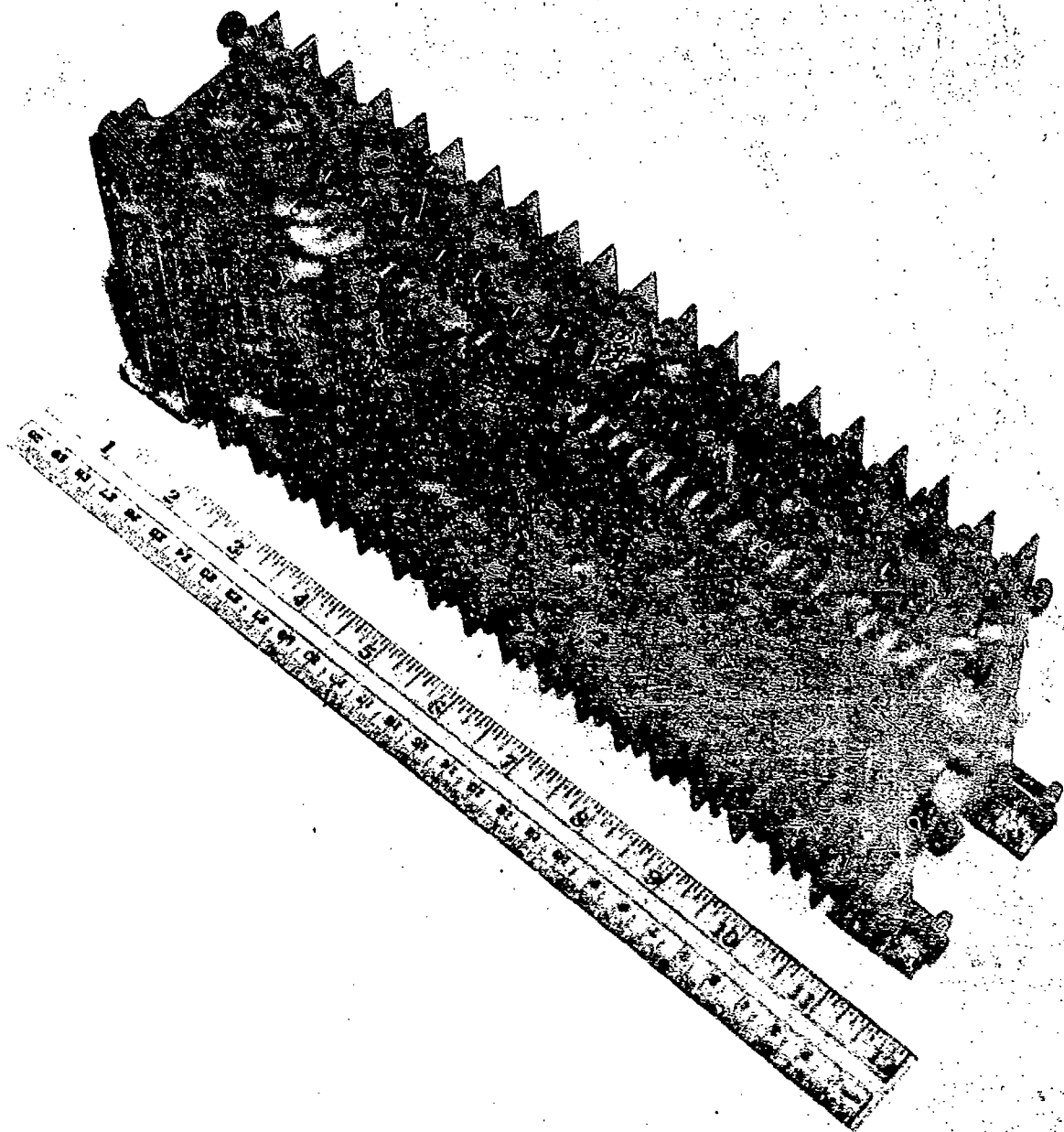


Figure 32. Improved Cell Design, Using Only Two Insulators and Lightweight (Aluminum) Plates; Also See Figure 33.

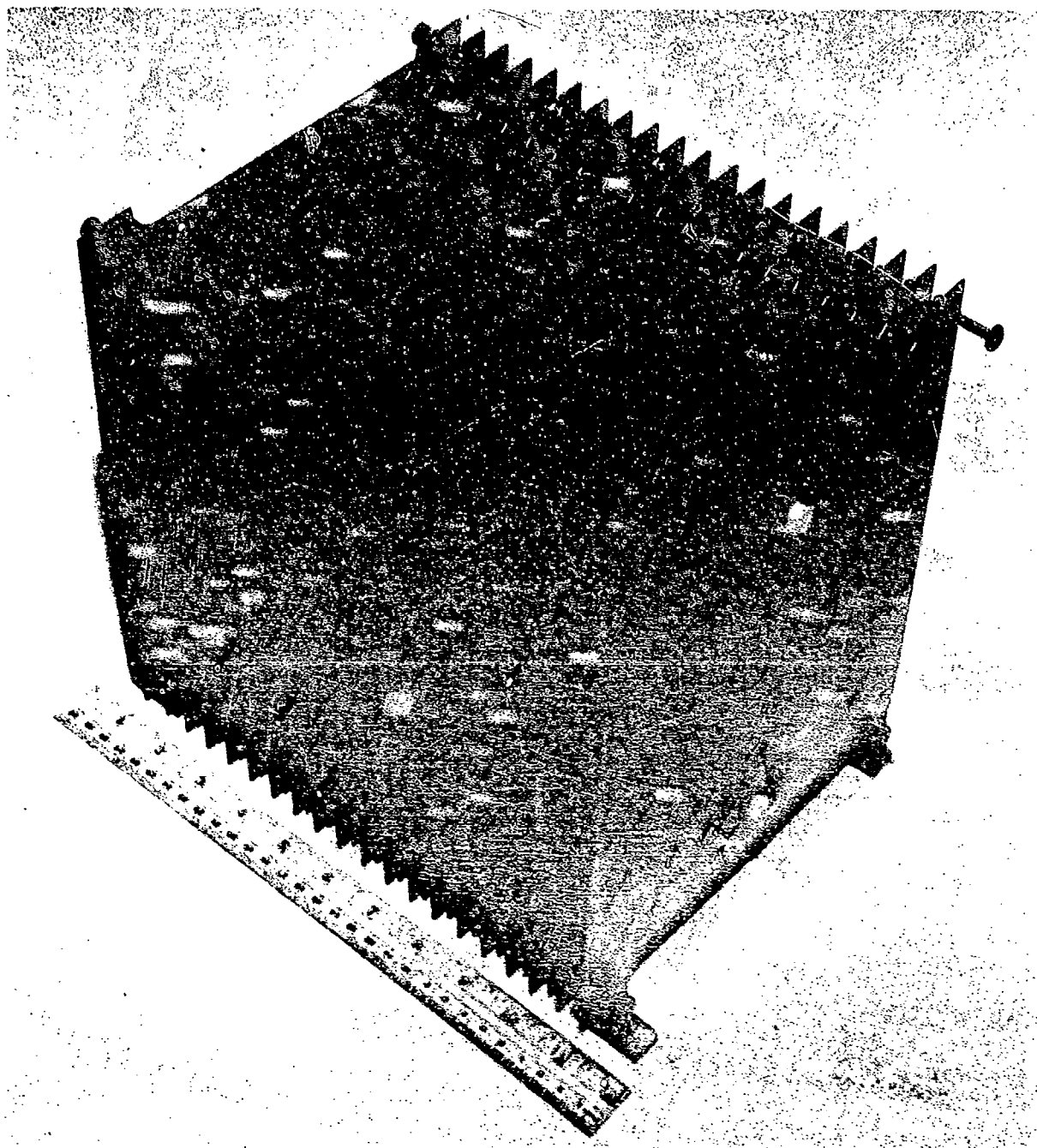


Figure 33. Improved Cell Design; Cell Differs From That in Figure 32 Only in Plate Area and Thus in Vapor Conductivity Sensitivity; Otherwise Cell Plate Spacing, Number (40), and Insulator Configurations Are Identical.

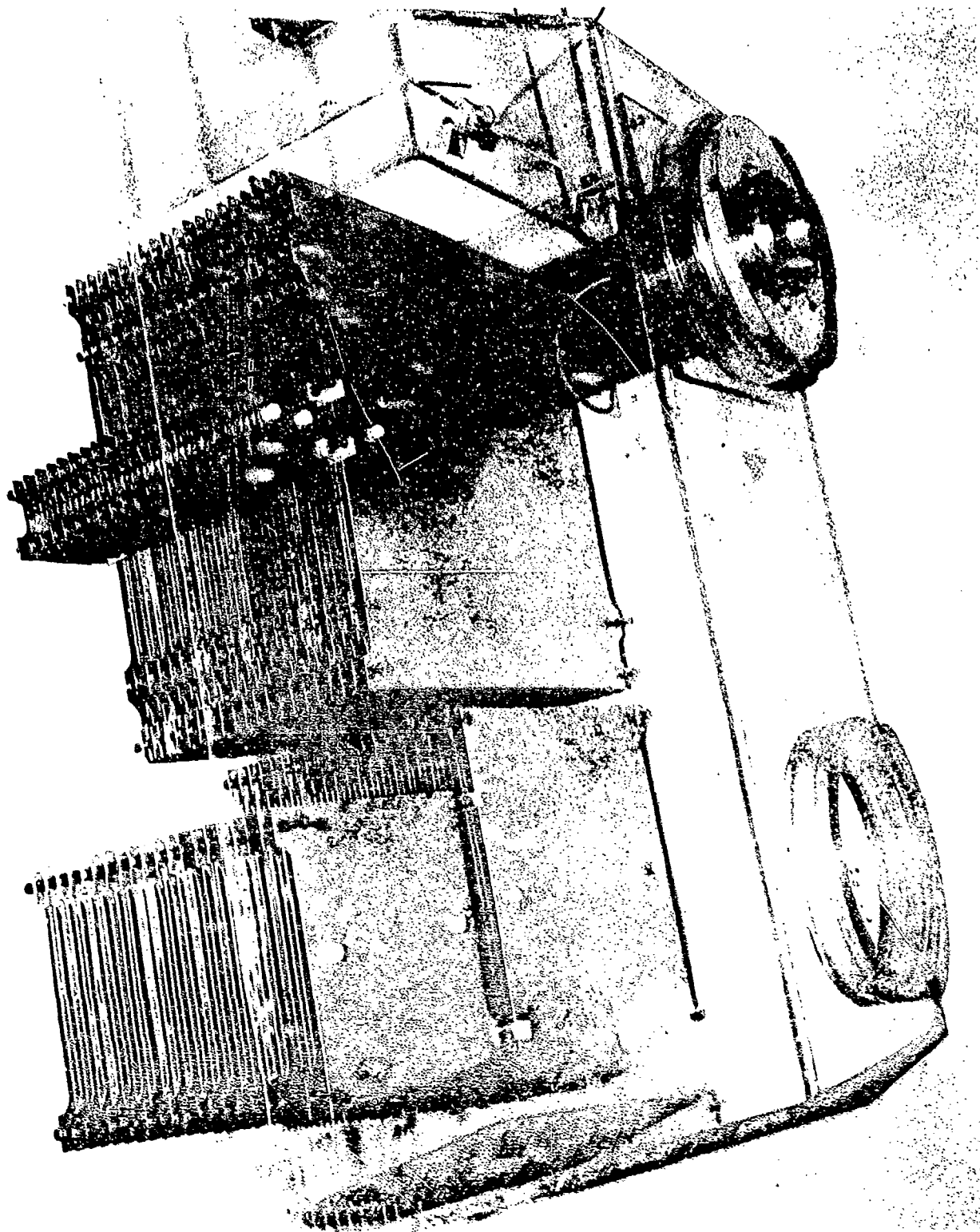


Figure 34. Family of Improved Cells Differing Only in Plate Area, in Cabinet Also Shown in Experimental Set-Up in Figure 28.

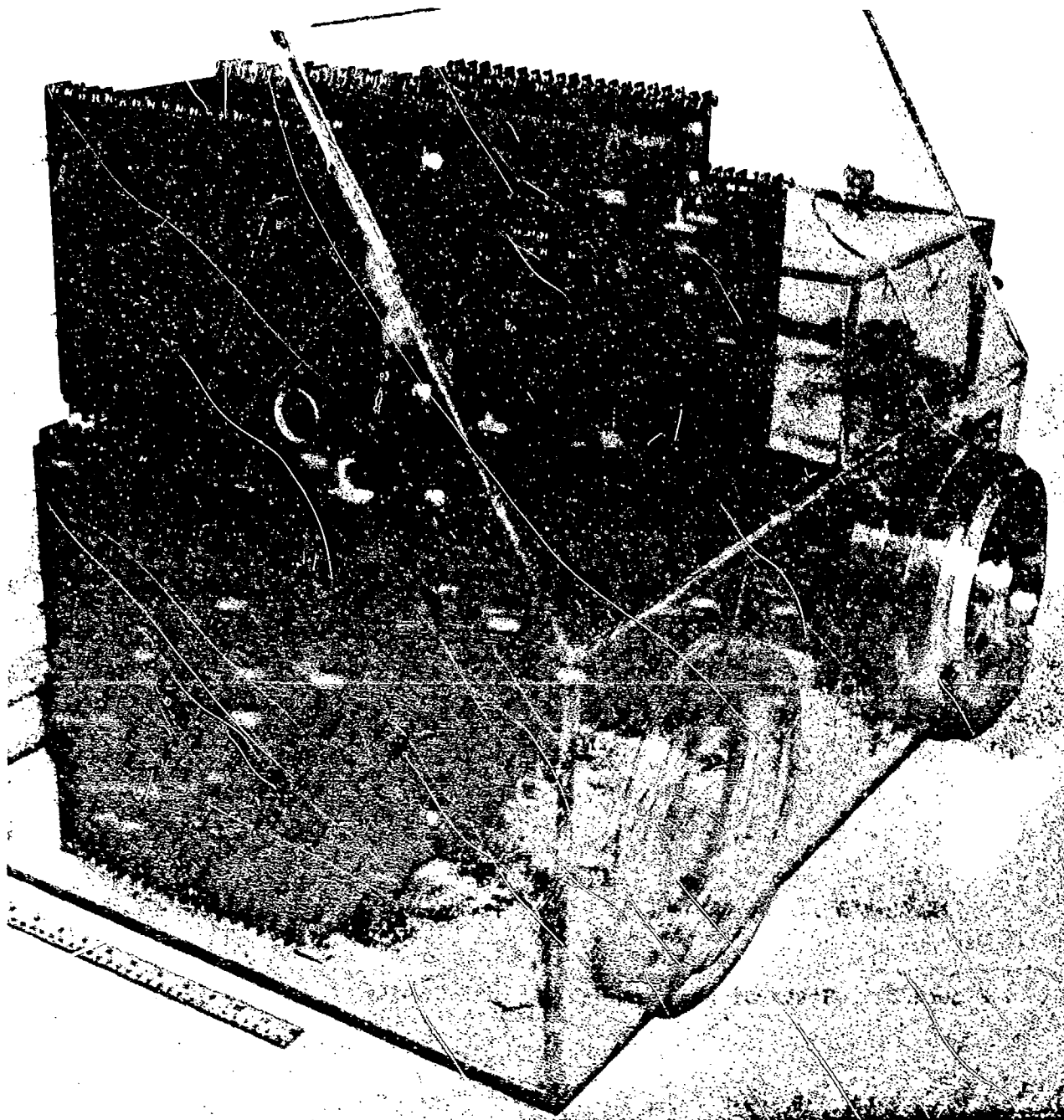


Figure 35. Oblique View of Family of Cells Shown in Test Cabinet in Figures 28 and 34.

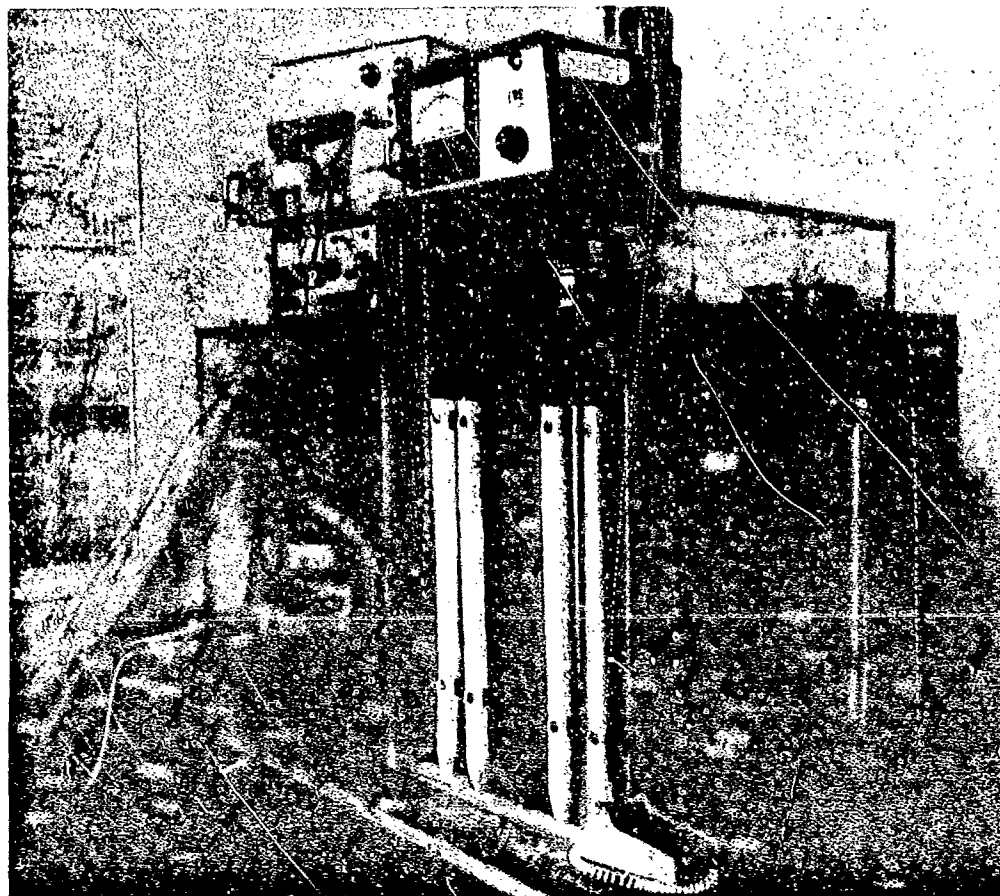


Figure 36. State-of-Art Cell Design With Insulators in Heated Chamber.

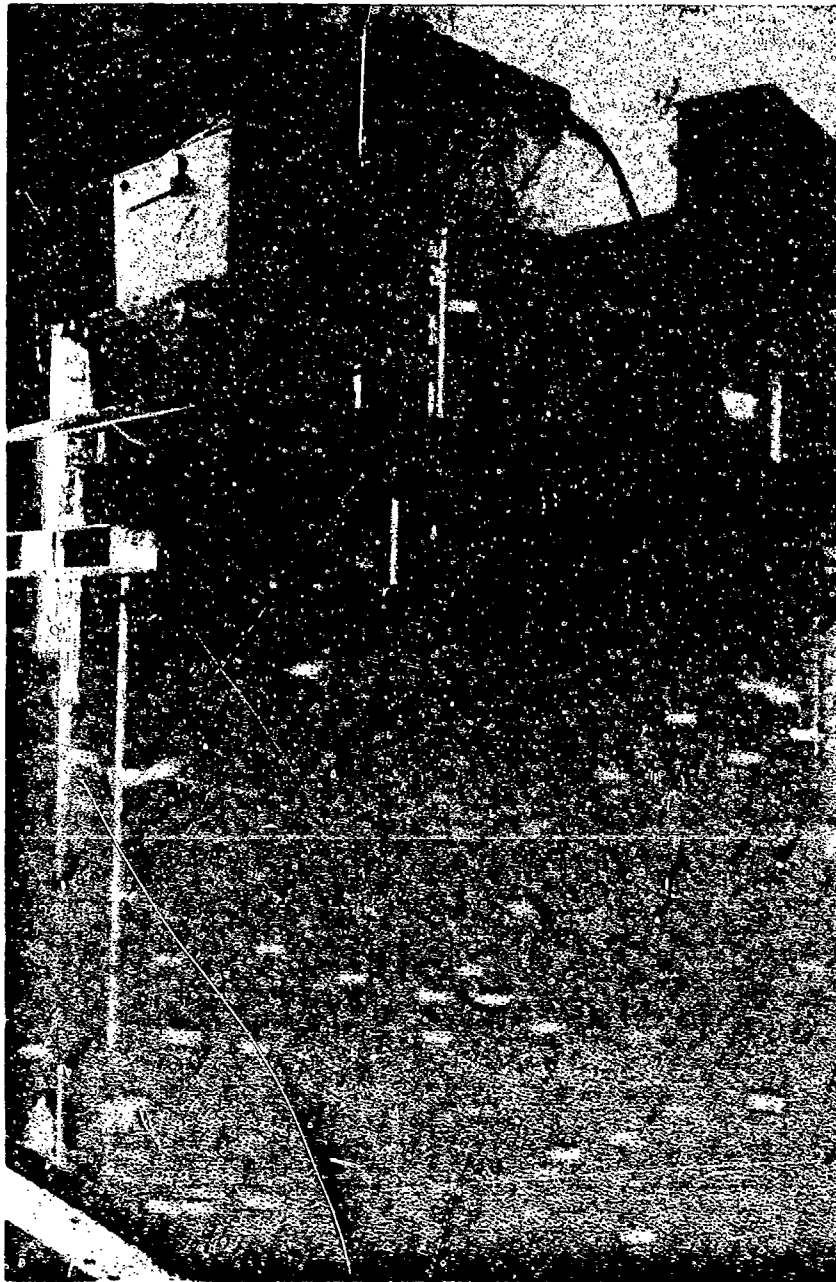


Figure 37. State-of-Art Cell Design Showing Detail of Insulators in Separate, Heated Chamber.

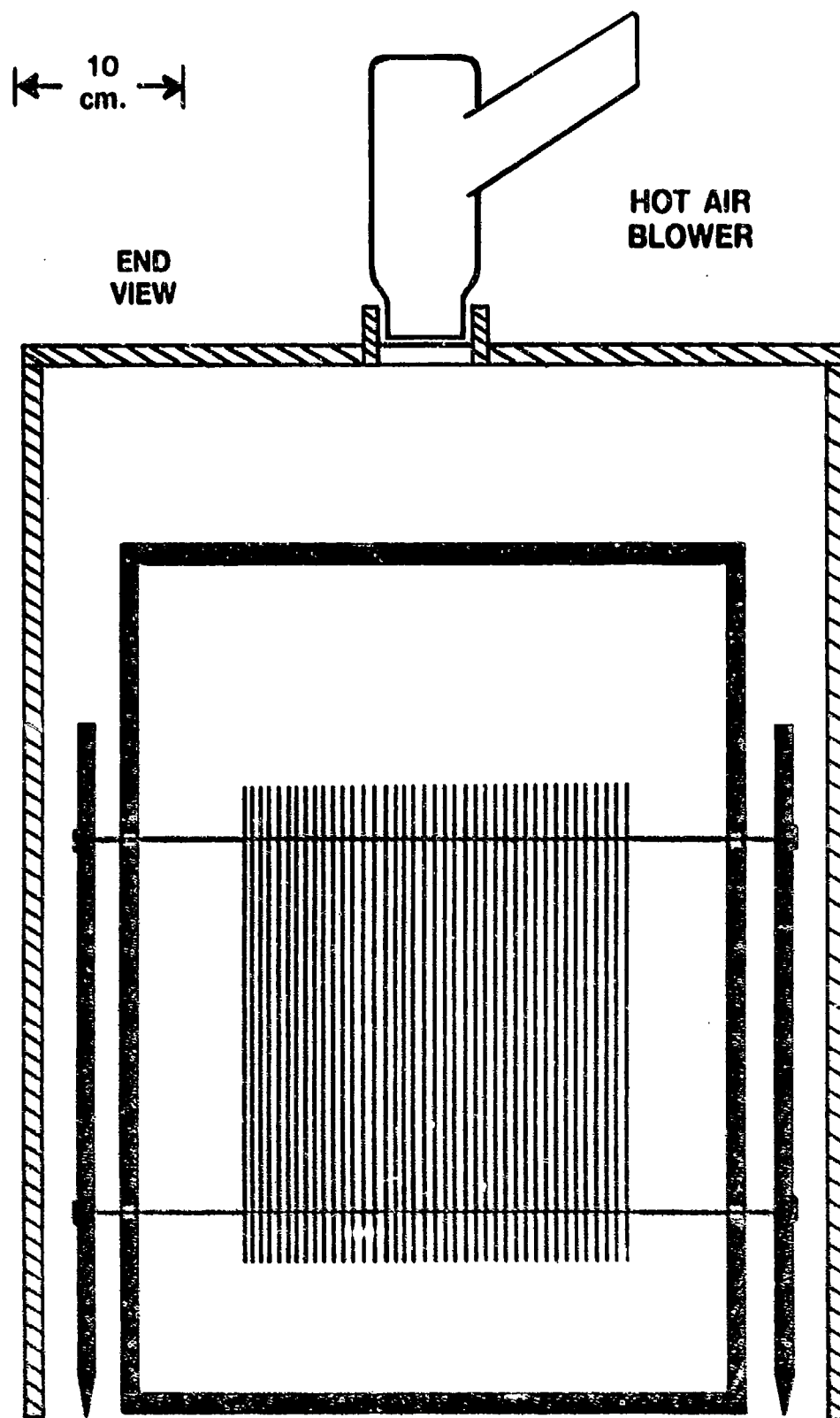
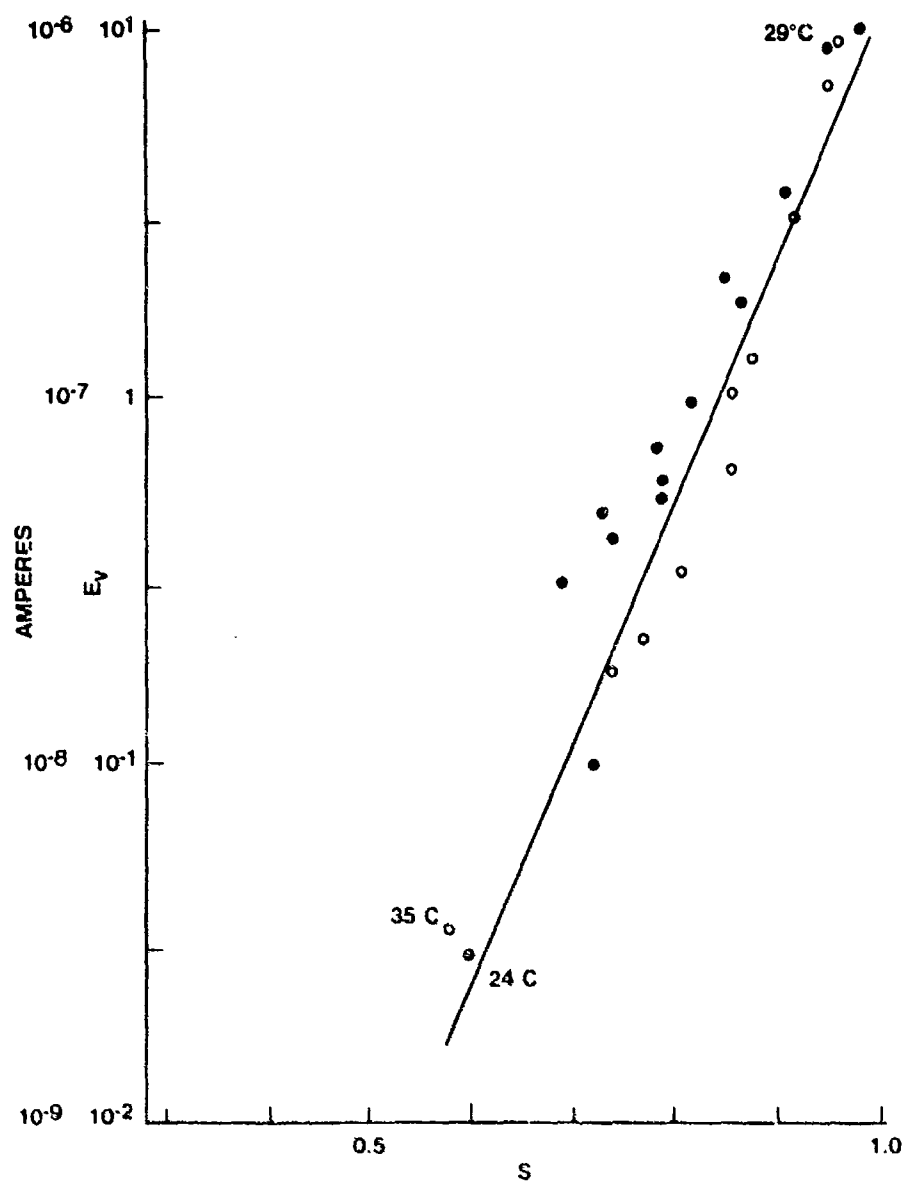


Figure 38. Schematic of State-of-Art Cell Shown in Figures 36 and 37; Heated Air Duct Containing Insulators is Shown, With Small Holes to Inner Test Chamber Through Which Pass Steel Rods Supporting Cell Plates Inside Chamber.



DB 0000-11

Figure 39. Data From State-of-Art Cell (Figures 36-38) Showing s^{13} Dependency of Cell (Vapor) Current vs. Saturation Ratio, for Humidification by Ultrasonic Nebulizer (Solid Points) and Drying Down (Hollow Points); Voltage Applied to Cell was 400 VDC.

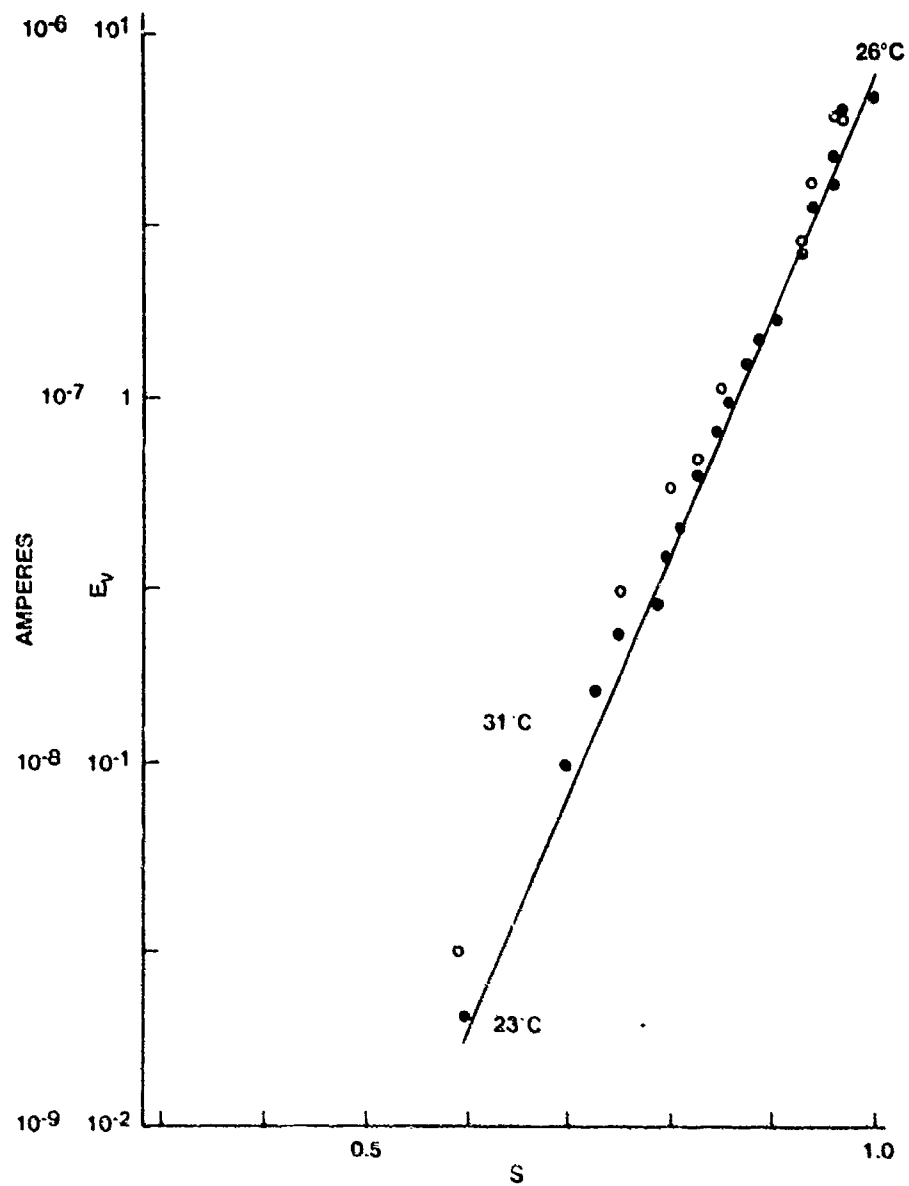


Figure 40. Data as in Figure 39 for Slightly Different Test Conditions.

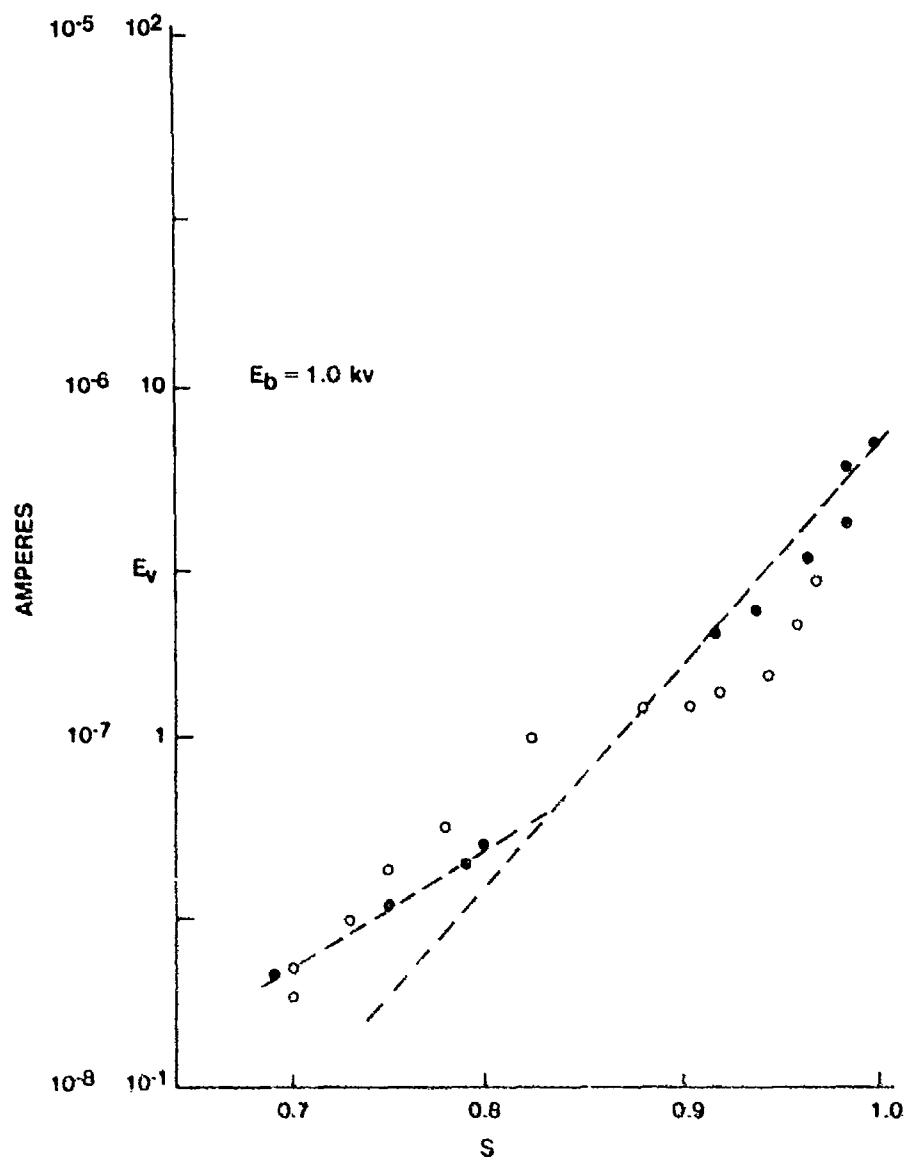


Figure 41. Data as in Figure 39, Except for 1000 VDC Voltage Applied to Cell, Showing s^7 and s^{13} Dependencies of Cell (Vapor) Current on Saturation Ratio During Humidification (Solid Points) and "Hysteresis" Effects During Drying-Down (Hollow Points).

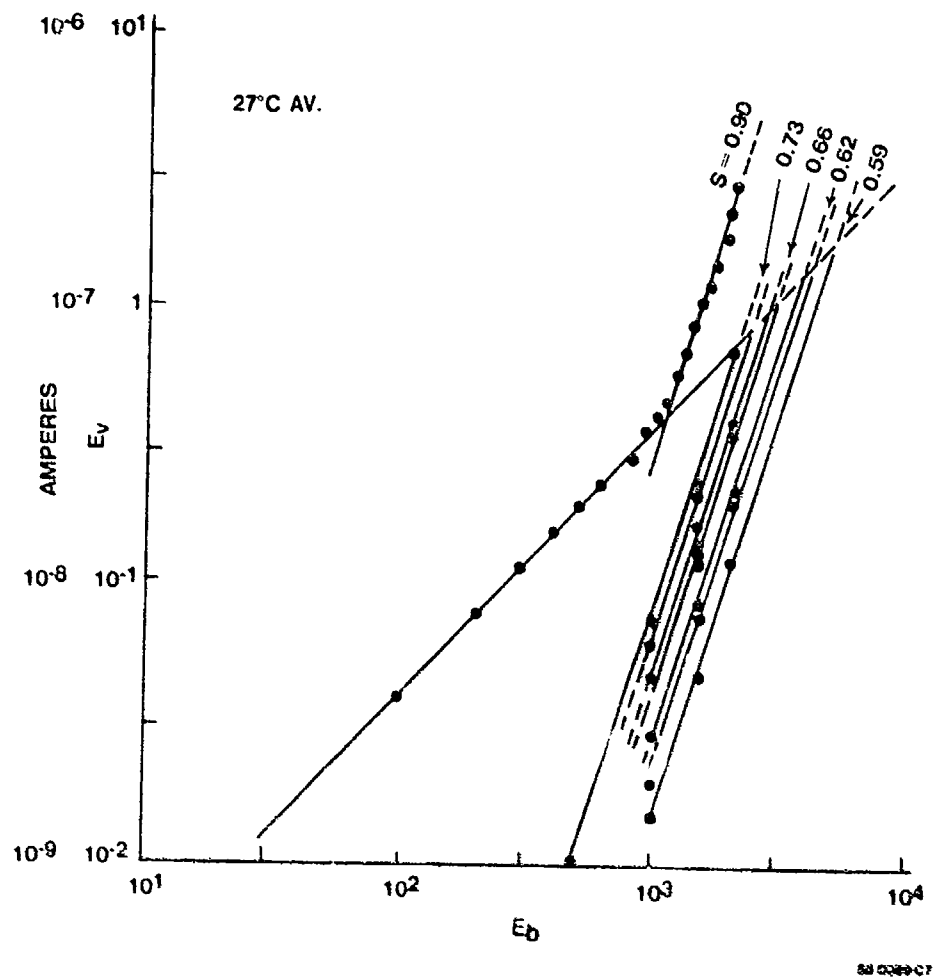


Figure 42. More Data From New cell (Figures 36-38), for a Range of DC Voltages (E_b) Applied to Cell at Average Temperature of 27°C; Saturation Ratios as Marked on the Curves; Note "Knee" in Top Curve.

ACCUMULATION OF WATER MONOLAYERS ON SURFACES vs % RELATIVE HUMIDITY

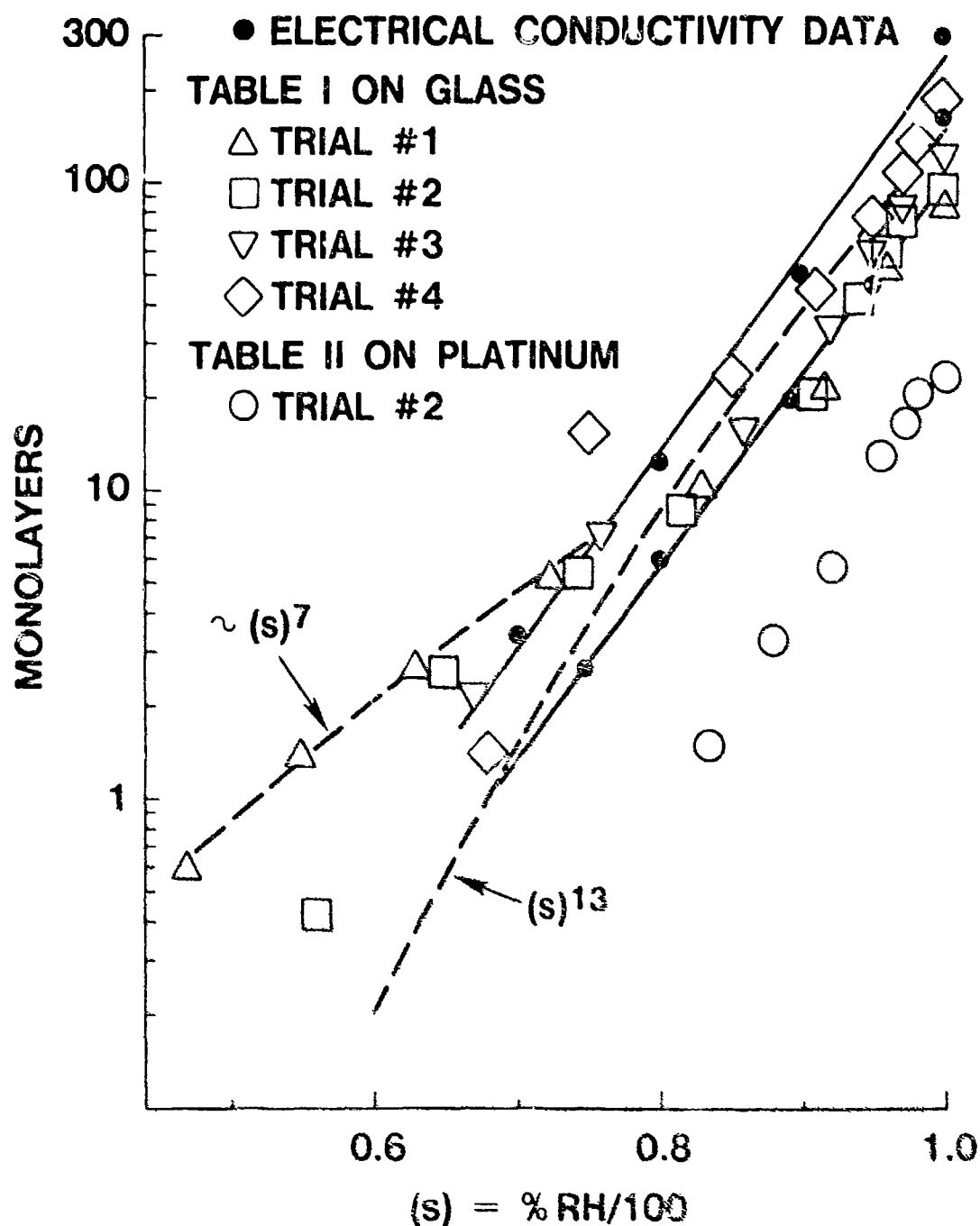


Figure 43. Accumulation of Water Monolayers on Surfaces, vs. Saturation Ratio, $s = (\%RH/100)$.

PARTICLE ADHESION DUE TO CAPILLARY CONDENSATION vs RELATIVE HUMIDITY

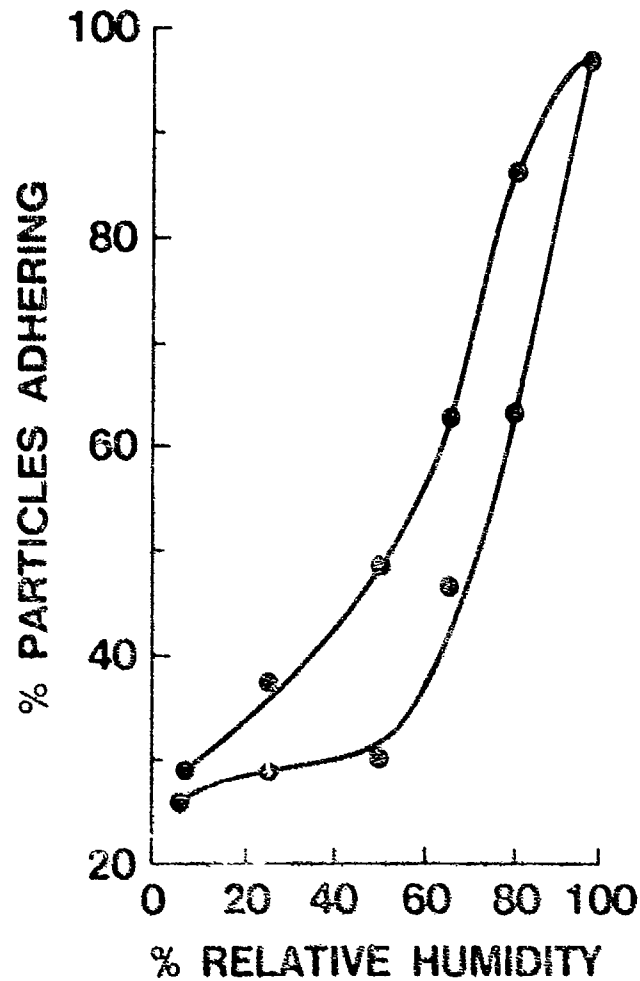
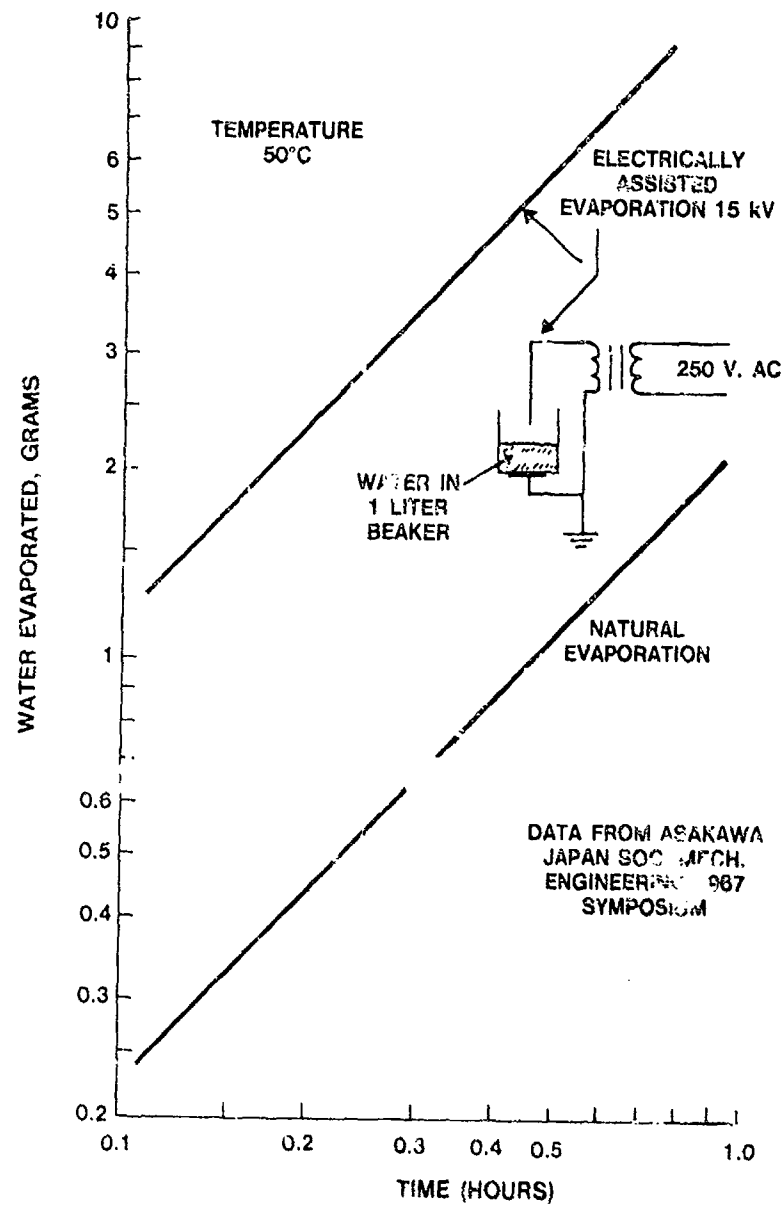


Figure 44. Hysteresis Effects in Surface Adhesion Force Due to Changes in Adsorbed Water Surface Layer With Relative Humidity.



DB 0089-09

Figure 45. Evaporation Rates of Water at 50°C From Metal Beaker, With and Without 15 kVAC Electric Field Applied to Assist Evaporation.

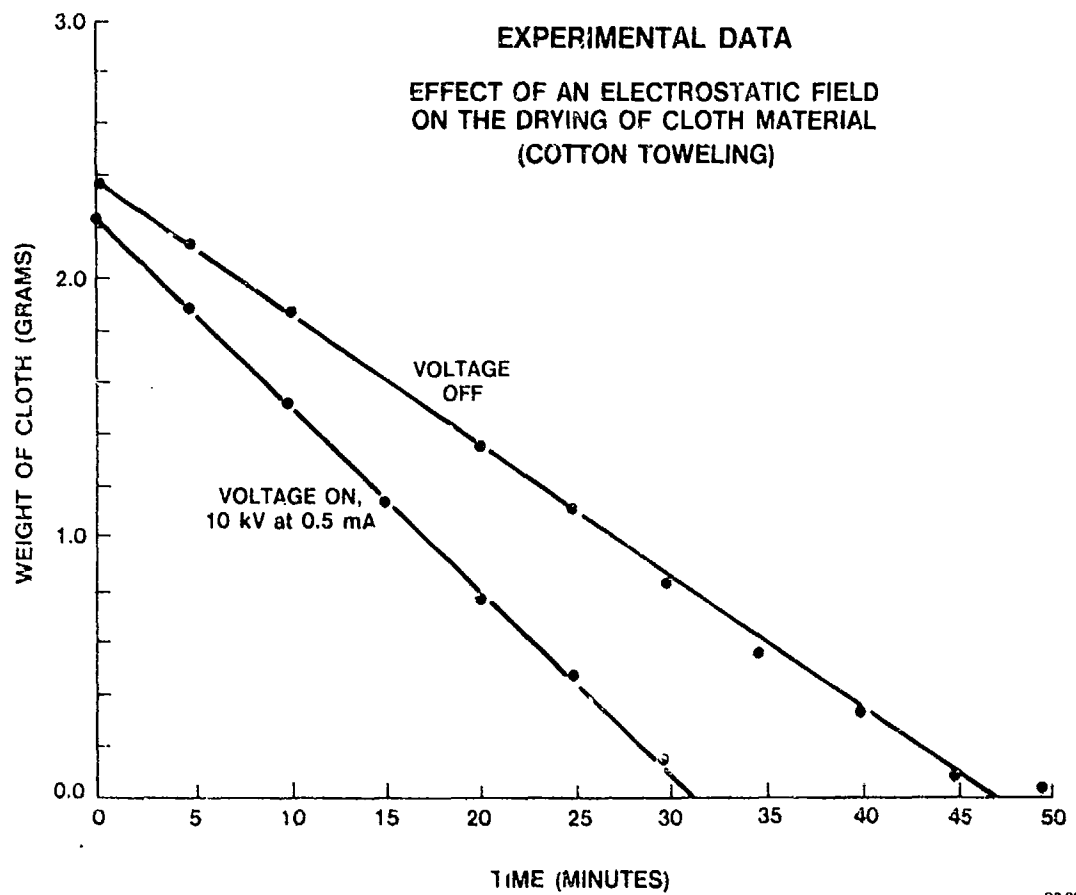


Figure 46. Drying Rates of Cotton Toweling With and Without 10 kVDC Electric Field Applied to Assist Operation.

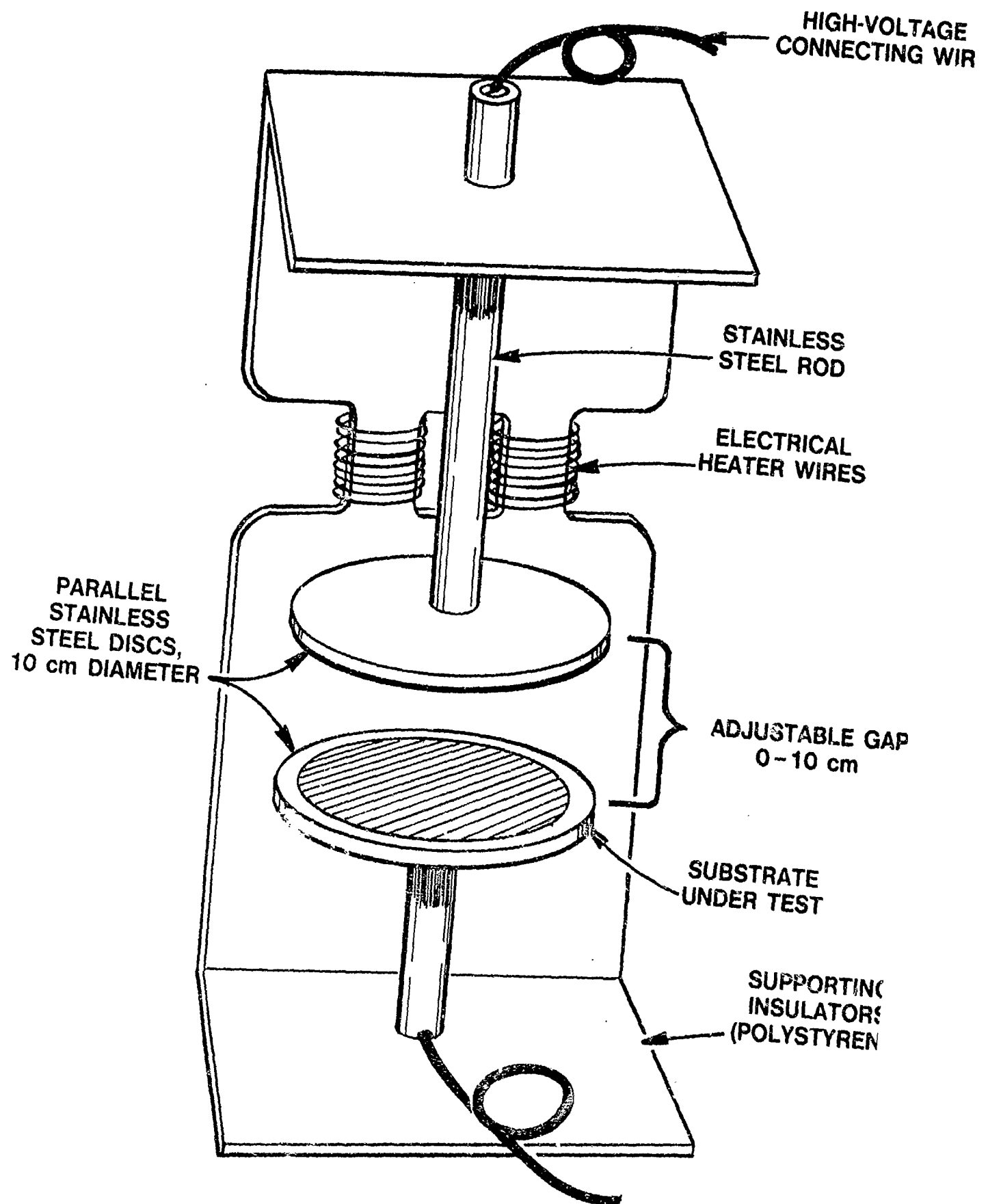
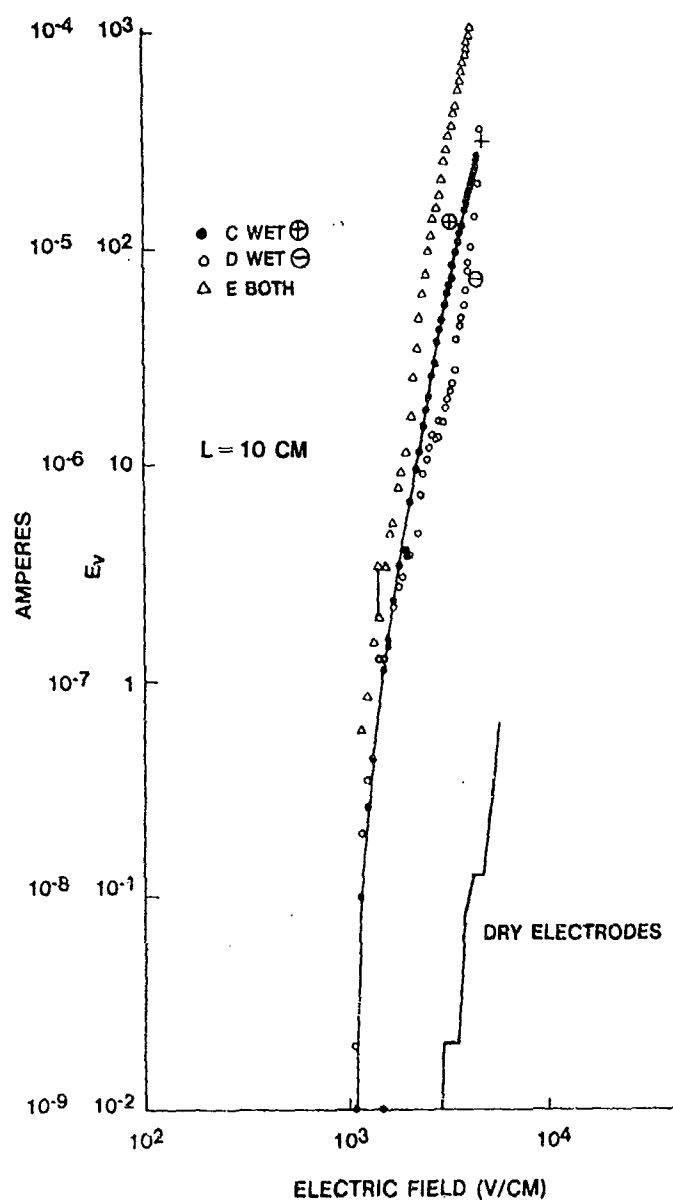


Figure 47. Author's Device to Demonstrate 10^3 - 10^4 Increase in Evaporation Rate From Linen and Other Wetted Substrates in High-Voltage Electric Fields.

LINEN WET WITH WATER (ON STAINLESS STEEL ELECTRODES)



DS 0089-15

Figure 48. Data from Author's Device (Figure 47) Using Linen Substrates on One or Both Disc Electrodes; Substrates Wetted with Water.

LINEN WET WITH LIQUIDS (ON STAINLESS STEEL ELECTRODES)

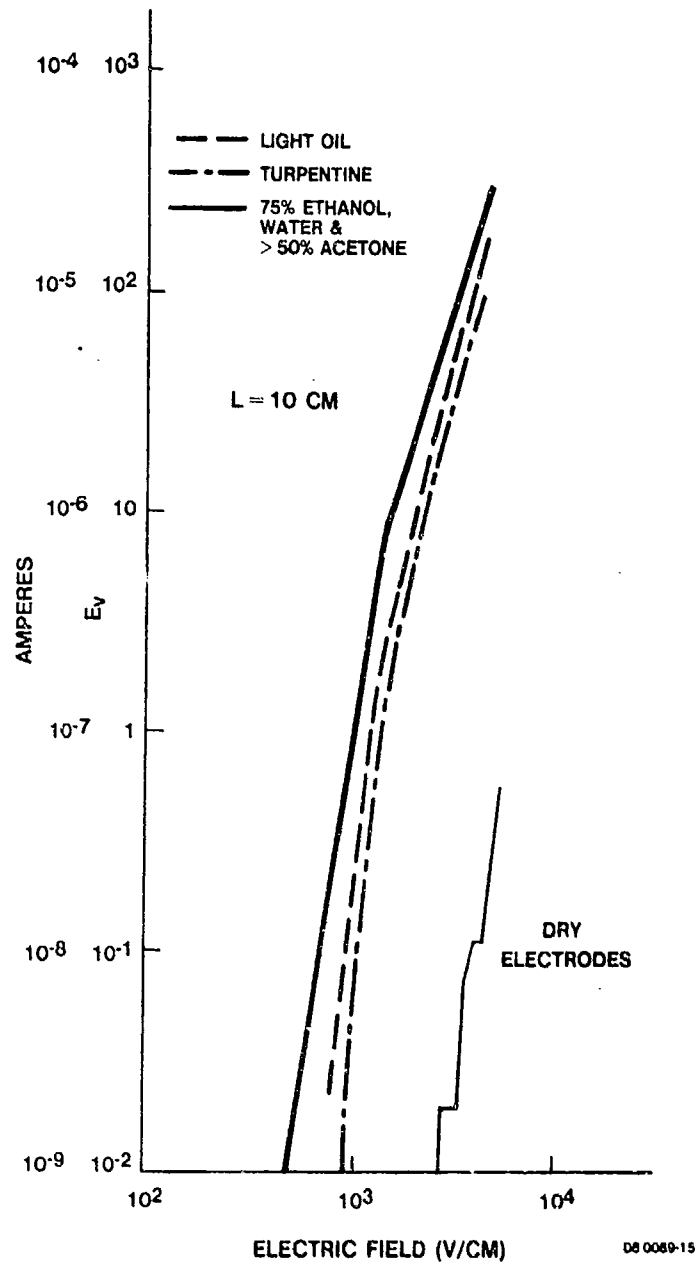


Figure 49. Data from Author's Device (Figure 47) Using Linen Substrates on One or Both Disc Electrodes; Substrates Wetted with Oil, Turpentine, or Water Solutions of Ethanol or Acetone.